THEORY OF THE ANOMALOUS HALL EFFECT IN THE INSULATING REGIME

A Dissertation

by

XIONGJUN LIU

Submitted to the Office of Graduate Studies of
Texas A&M University
in partial fulfillment of the requirements for the degree of

DOCTOR OF PHILOSOPHY

August 2011

Major Subject: Physics

THEORY OF THE ANOMALOUS HALL EFFECT IN THE INSULATING REGIME

A Dissertation

by

XIONGJUN LIU

Submitted to the Office of Graduate Studies of
Texas A&M University
in partial fulfillment of the requirements for the degree of

DOCTOR OF PHILOSOPHY

Approved by:

Chair of Committee,	Jairo Sinova
Committee Members,	Artem Abanov
	Tahir Cagin
	Igor Roshchin
Head of Department,	Edward Fry

August 2011

Major Subject: Physics

ABSTRACT

Theory of the Anomalous Hall Effect in the Insulating Regime. (August 2011)
Xiongjun Liu, B.S., Nankai University; M.S., Nankai University
Chair of Advisory Committee: Dr. Jairo Sinova

The Hall resistivity in ferromagnetic materials has an anomalous contribution proportional to the magnetization, which is defined as the anomalous Hall effect (AHE). Being a central topic in the study of ferromagnetic materials for many decades, the AHE was revived in recent years by generating many new understandings and phenomena, e.g. spin-Hall effect, topological insulators. The phase diagram of the AHE was shown recently to exhibit three distinct regions: a skew scattering region in the high conductivity regime, a scattering-independent normal metal regime, and an insulating regime. While the origin of the metallic regime scaling has been understood for many decades through the expected dependence of each contribution, the origin of the surprising scaling in the insulating regime was completely unexplained, leaving the primary challenge to the last step to understand fully the AHE.

In this dissertation work we developed a theory to study the AHE in the disordered insulating regime, whose scaling relation is observed to be $\sigma_{xy}^{AH} \propto \sigma_{xx}^{1.40\sim1.75}$ in a large range of materials. This scaling is qualitatively different from the ones observed in metals. In the metallic regime where $k_F l \gg 1$, the linear response theory predicts that σ_{xx} is proportional to the quasi-particle lifetime τ, while σ_{xy}^{AH} scales as $\alpha\tau + \beta\tau^0$, indicating that the upper limit of the scaling exponent is 1.0. Basing our theory on the phonon-assisted hopping mechanism and percolation theory, we derived a general formula for the anomalous Hall conductivity (AHC), and showed that the AHC scales with the longitudinal conductivity as $\sigma_{xy}^{AH} \sim \sigma_{xx}^{\gamma}$ with γ predicted to be $1.33 \leq \gamma \leq 1.76$, quantitatively in agreement with the experimental observations.

This scaling remains similar regardless of whether the hopping process is long range type (varible range hopping) or short range type (activation E3 hopping), or is influenced by interactions, i.e. Efros-Shklovskii (E-S) regime. Our theory completes the understanding of the AHE phase diagram in the insulating regime.

To my father: Donglin Liu

ACKNOWLEDGMENTS

First of all, I would like to express my sincere gratitude to my Ph.D. advisor, Prof. Jairo Sinova. I would say Jairo is one of the best persons I have ever met in my research career. Jairo's guidance was more than essential in completing my Ph.D. research. He introduced me into the world of condensed matter physics and suggested the study of the anomalous Hall effect in the insulating regime. He guided me with his way to face this topic — always thinking of physical problems emerged from experiments, which will benefit me in my whole research career. Besides the research guidance, Jairo has also trained me with great patience in the skills to express physics clearly and give excellent presentations. Jairo is a very friendly person. His easy-going character, humorous personality, and continuous encouragement on my research will stay in my memory.

I am also indebted to my Master Thesis advisor, Prof. Mo-Lin Ge. As a senior scientist of high attainments in physics and mathematics, Prof. Ge trained and helped me establish a good background in quantum physics, and enlighten me on how to apply mathematics to physical problems. Without his generous help during my study at Nankai University and also after I left Nankai, I would not be able to carry out my doctoral research so smoothly.

Special thanks to Prof. Chia-Ren Hu for his continuous help in my study and research at Texas A&M University. At any time, Prof. Hu Welcomed me to bring any physical question to his office and have a detailed discussion with him. I appreciate his great patience in explaining to me so many fundamental problems in condensed matter physics. I thank him enormously.

My thanks also go to Prof. Valery Pokrovsky and Prof. Artem Abanov. I studied advanced quantum mechanics from Prof. Pokrovsky's course and learned a lot from him. I was also greatly enlightened by his deep knowledge of physics when talking about research with him. I benefited a lot in the discussions with Prof. Abanov,

who always provided many stimulating comments on my research and helped a lot in my papers.

I must thank Xin Liu and Zhengxin Liu, who are not only my best friends, but also most important collaborators in my research. In these years, we discussed everything in research and made progress through concerted efforts. I am also indebted to Prof. Congjun Wu, Dr. Mario F. Borunda, Prof. C. H. Oh, and Prof. L.C. Kwek, who helped me a lot in my research. I also thank my friends Meng Gao, Shuai Yang and Kai Wang. It's my pleasure and luck to have met them in College Station and spent four years of wonderful time in this small and peaceful town.

Finally, I want to express sincere gratitude to my mom, who produced, educated me and has always supported me. My mom-in-law deserves my appreciation, who has helped my family a lot since my first kid was born in the last year. I wish to thank my wife from the bottom of my heart for her support with my research. I also thank my daughter, Vivian Liu, whose birth brings me good luck.

TABLE OF CONTENTS

Page

Page

LIST OF FIGURES

FIGURE Page

FIGURE Page

FIGURE Page

1. INTRODUCTION

1.1 A brief review of the AHE

Being a central topic in the study of Ferromagnetic materials for nearly one century, the anomalous Hall effect (AHE) is a fundamental phenomenon which reflects the complex spin-charge transport in the spin-orbit coupled ferromagnetic systems [2]. Two years after the discovery of the ordinary Hall effect (OHE) by Edwin H. Hall in the presence of an external magnetic field, he discovered that the Hall effect in the ferromagnetic iron was much larger than in the nonmagnetic conductors, which is now known as the AHE [1]. Different from the OHE, which is a consequence of the Lorentz force due to the magnetic field, the AHE has much deeper origins based on the topological and geometrical properties of the electronic band structure and disorder scatterings. While having been attracting theoretical and experimental efforts for a long time, complete theoretical understanding of the AHE is still not available [2].

Early experimental work in ferromagnets established an empirical relation between the total Hall resistivity and the magnetization M_z and external magnetic field B_z by

$$\rho_{xy} = R_0 B_z + R_S M_z. \tag{1.1}$$

The first term, characterized by the ordinary Hall coefficient R_0, describes the ordinary Hall effect (OHE), whereas the second term, characterized by the anomalous Hall coefficient R_S, represents the AHE. In experiment the anomalous Hall resistivity

This dissertation follows the style of Physical Review Letters.

(AHR) is usually observed to follow a power law form versus the longitudinal resistivity $\rho_{xy} \sim \rho_{xx}^{\beta}$, with ρ_{xx} varied by changing the temperature T or density of states (DOS) around Fermi surface. When transformed to the anomalous Hall conductivity (AHC), the scaling relation takes the form $\sigma_{xy} \approx \sigma_{xy}/\sigma_{xx}^2 \sim \sigma_{xx}^{2-\beta}$. Historically, the AHE is a highly debated issue. The anomalous Hall coefficient R_S is usually much larger than R_0. This indicates that the simple explanation in terms of the enhancement of B_z for the OHE due to the internal magnetic field in ferromagnets fails. Karplus and Luttinger (KL) initiated the theoretical interpretation of the AHE, by considering the spin-orbit (SO) interaction as a perturbation to the band structure in the ferromagnetic state [3]. KL showed the band electrons acquire an anomalous velocity perpendicular to both the magnetization and the applied electric field, which gives the additional contribution to the Hall effect. The anomalous velocity comes from the interband matrix element of the velocity operator, and is a consequence of the SO interaction which mixes the spin-up and spin-down bands. The KL theory is now known as the intrinsic contribution to the AHE. Similar to the OHE, the AHE requires the time reversal (TR) symmetry to be broken, which is attained in the presence of the non-zero magnetization.

The KL theory dealt with the metallic regime, but did not take into account the impurity scattering, which seemed to be a crucial defect in a solid state theory. Smit criticized this theory by considering the impurity scattering, and argued that the main contribution to the AHE was the third order asymmetric scattering (i.e. skew scattering) by impurities in the presence of SO coupling [4, 5]. The skew scattering mechanism predicts that the AHC is linear in the longitudinal one, i.e. $\sigma_{xy}^{AH-sk} \propto \sigma_{xx}$ ($\beta = 1$). Following this criticism, Luttinger developed a systematic theory of the AHE based on the perturbation expansion in terms of impurity scattering strength V and up to the zeroth order in the presence of SO coupling [6]. In this study Luttinger argued that the transverse current was mainly coming from two terms, with the first term inversely proportional to impurity concentration n, while

the second one independent of the disorder scattering. Therefore such two terms respectively correspond to the skew scattering and intrinsic mechanisms. According to the dependence of the two types of contributions on the impurity scattering, it is expected that in the dilute limit of the impurity density the AHE will be dominated by the skew scattering contribution. Furthermore, Berger proposed another mechanism, side jump contribution, for the AHE [7, 8]. He found that upon impurity scattering, the electron will undergo a transverse displacement relative to the momentum direction. The side jump mechanism leads to further confusion for the AHE theory, since although born out of the impurity scattering, the side jump contribution is surprisedly independent of the impurity density, giving rise to the same scaling relation between the AHC and the longitudinal conductivity as in the intrinsic mechanism $\sigma_{xy}^{AH} \propto \sigma_{xx}^{0}$ ($\beta = 2$). As a result, the side jump and KL intrinsic contributions are difficult to distinguish in experiment.

The understanding of the AHE in the metallic regime has greatly benefited from the Berry phase formalism revealed by Berry in 1984 [9]. According to Berry's picture, when the wave function adiabatically evolves along a close path in the parameter space, after the evolution the wave function will gain an additional geometric phase. The Berry phase can be calculated through the area integral of the Berry's curvature over the parameter space enclosed by the closed path. While the Berry phase formalism was widely employed to understand the topological nature of the quantum Hall effect (QHE) [10], it is interesting that the consideration of this concept to the AHE was much later [11–14]. With the Berry phase formalism, one can express the KL term in terms of the area integral of the Berry's curvature over the momentum $\mathbf{k}$ space below the Fermi level. A clear connection between the Berry phase and the anomalous velocity can be derived in the semiclassical transport theory [11,12]. This result indicates the intrinsic contribution of the AHE is a geometric effect in the multi-band SO coupled electronic system. Inheriting the geometric property from the intrinsic AHE, the AHC may have interesting topological property when the

system has a band gap and the Fermi energy lies in the gap. In this case the AHC is quantized in units of e^2/h and is characterized by the 1st Chern number C_1 defined in the first Brillouin zone (FBZ). Such an effect, now referred to a quantum anomalous Hall effect (QAHE), has attracted much attention in the theoretical studies [15–22], and may invoke the experimental efforts in this field of research in the near future.

The recent advances on AHE in the metallic regime are focused on the systematic studies in both theory and experiment. Based on these studies, the three regimes (i.e. the skew scattering, side jump and intrinsic contributions) have been confirmed in the different situations [2,23,24]: (i) ($\sigma_{xx} > 10^6$ $(\Omega\text{cm})^{-1}$) A high conductivity regime in which $\sigma_{xy}^{AH} \sim \sigma_{xx}$, dominated by skew scattering; and (ii) (10^4 $(\Omega\text{cm})^{-1} < \sigma_{xx} < 10^6$ $(\Omega\text{cm})^{-1}$) a scattering-independent regime: $\sigma_{xy}^{AH} \propto \sigma_{xx}^0$, which includes the intrinsic and side jump contributions. Furthermore, a systematic study employing different (Boltzmann, Kubo, and Keldysh) linear response theories has been performed to explore the different regimes of the AHE in the metallic regime [25–33]. Among these theories, the semiclassical Boltzmann equation (SBE) has the greatest physical transparency. To study the AHE, the modern version of SBE needs to be considered by taking into account the Berry curvature and coherent interband mixing due to SO coupling and disorder scattering. The quantum-mechanical treatments based on the Kubo and Keldysh formalisms provide more rigorous study of the metallic AHE. In the linear regime, the equivalence of the three formulations of transport theory are confirmed [2], which may enable a thorough understanding of the AHE in the metallic regime.

Relative to the metallic regime, the AHE in the disordered insulating regime was less studied in experiment although it has attracted more and more attention in recent years. Nevertheless, several groups have observed an approximate scaling relation between AHC and the longitudinal conductivity $\sigma_{xy}^{AH} \propto \sigma_{xx}^{\gamma}$ with $1.40 \leq \gamma \leq 1.75$ when the system is in the disordered insulating regime [34–46]. The early experiment on AHE in this regime was done in magnetite Fe_3O_4 [34], and the recent experimen-

tal observations of this scaling are reported in large range of materials including granular Fe/SiO_2 films, magnetite epitaxial thin films, dilute magnetic semiconductor (DMS) $Ga_{1-x}Mn_xAs$, and ferromagnetic semiconductor anatas $Ti_{1-x}Co_xO_{2-\delta}$. Specifically, the experiments in the insulating $Ga_{1-x}Mn_xAs$ samples and Fe nanocomposites observed the scaling exponent as $1.40 \leq \gamma \leq 1.60$ [35–37, 39, 42], while those in ferromagnetic oxides and magnetites mostly show the scaling exponent $1.50 \leq \gamma \leq 1.75$ [38, 40, 41, 43–46]. The AHE theory in the metallic regime is generally based on the perturbation expansion in terms of small parameter $1/(k_F l)$ in the typical metallic phase. Here k_F is the magnitude of the Fermi wave vector, and l is the length of mean free path. Hence, the observed scaling relation in the insulating regime cannot be explained by available microscopic theories of metals based on impurity scattering, since the condition $k_F l \gg 1$ is no longer satisfied for disordered insulators [2, 47]. The few previous studies of the AHE in the insulating regime focused on manganites and $Ga_{1-x}Mn_xAs$; while the manganites do not exhibit this scaling, the studies on insulating $Ga_{1-x}Mn_xAs$ did not show this scaling [48–50]. As a result, the understanding of the AHE in the insulating regime becomes the main challenge to understand the AHE phase diagram, and this is the main issue we study in the present dissertation.

1.2 Spin-orbit coupling

The SO coupling is the central ingredient in the AHE. In this section we point out different types of SO interaction. A familiar example for the SO coupling is the Pauli SO interaction in atomic physics, which is obtained by reducing the Dirac equation to the non-relativistic form in the presence of an external coulomb potential. The reduction can result in the coupling between the orbital and spin degree of freedom of the electron. However, since the SO coupling Hamiltonian for such case

$$H_{so} = \frac{e^2\hbar^2}{4m_0c^2}\vec{\sigma} \cdot (\nabla V \times \frac{\mathbf{P}}{m_0}) \tag{1.2}$$

depends inversely on the vacuum electron mass m_0 and light speed c, this effect is normally very weak for the non-relativistic momentum $\mathbf{P}$ of the electron. Here V is the coulomb potential and σ is the Pauli spin matrix. Actually, for the vacuum case the weak SO coupling is a result of the large energy gap between electrons and positrons ($\Delta E \sim 2m_0c^2 \sim 2.0$MeV). Such a situation, however, can be changed in the semiconductor quantum wells, whose band structure shows many similarities to the situation of free relativistic electrons. In the III-V semiconductor quantum wells, for example, the energy gap between conduction and valence band is of order 1eV or smaller [51], which makes it possible to obtain a relatively large SO coupling effect in the semiconductor materials.

The SO coupling in semiconductors can be studied with the $\mathbf{k}\cdot\mathbf{p}$ theory [52], which can be briefly introduced as follow. Note when we talk about here different types of SO coupling in semiconductors, we are referring to the effective coupling between the on-site total angular momentum and the Bloch momentum ($\mathbf{k}$). We shall see such SO coupling is a consequence of the $\mathbf{k}\cdot\mathbf{p}$ term and the SO interaction in Eq. (1.2). Eigenstates of a lattice system are described by Bloch wave functions [53]. Considering also the SO coupling term given in (1.2), one obtains the Schrödinger equation

$$\big[\frac{P^2}{2m_0} + V_0(\mathbf{r}) + \frac{e^2\hbar^2}{4m_0c^2}\vec{\sigma}\cdot(\nabla V_0 \times \frac{\mathbf{P}}{m_0})\big]\phi_{\nu\mathbf{k}}(\mathbf{r}) = E_{\nu\mathbf{k}}\phi_{\nu\mathbf{k}}(\mathbf{r}), \tag{1.3}$$

where the Bloch function $\phi_{\nu\mathbf{k}}(\mathbf{r}) = e^{\mathbf{k}\cdot\mathbf{r}}\mu_{\nu\mathbf{k}}$ with $\mu_{\nu\mathbf{k}}(\mathbf{r})$ the lattice periodic term and ν the band index. Taking off the plane-wave part of the Bloch wave function and rewriting the above Schrödinger equation on $\mu_{\nu\mathbf{k}}(\mathbf{r})$ we get

$$\big[\frac{P^2}{2m_0} + V_0(\mathbf{r}) + \frac{\hbar^2k^2}{2m_0} + \frac{\hbar}{m_0}\mathbf{k}\cdot\vec{\pi} + \frac{e^2\hbar^2}{4m_0c^2}\vec{\sigma}\cdot(\nabla V_0 \times \frac{\mathbf{P}}{m_0})\big]|\mu_{\nu\mathbf{k}}(\mathbf{r})\rangle = E_{\nu\mathbf{k}}|\mu_{\nu\mathbf{k}}(\mathbf{r})\rangle, \tag{1.4}$$

where $\vec{\pi}$ is defined by

$$\vec{\pi} = \mathbf{P} + \frac{\hbar}{4m_0c^2}\sigma \times \nabla V_0. \tag{1.5}$$

In the presence of SO coupling, the spin quantum number σ is generally not conserved. In the $\mathbf{k}\cdot\mathbf{p}$ theory, one shall diagonalize the Hamiltonian (1.4) by neglecting the SO coupling term to obtain the eigen states $|\nu\mathbf{k}\rangle$, and then treat the SO coupling as a perturbation [52, 54]. The eigenstates $|\nu\mathbf{k}\rangle$ satisfy

$$\big[\frac{P^2}{2m_0} + V_0(\mathbf{r}) + \frac{\hbar^2k^2}{2m_0} + \frac{\hbar}{m}\mathbf{k}\cdot\mathbf{P}\big]|\nu\mathbf{k}\rangle = E_{\nu\mathbf{0}}|\nu\mathbf{k}\rangle. \tag{1.6}$$

The eigenstates $|\nu\mathbf{k}\rangle$ are usually solved with the wave-vectors around a high symmetry point (typically the band edge). For direct band gap semiconductors such high symmetry point is $\mathbf{k} = 0$ [54]. In the basis of $|\nu\mathbf{k} = 0\rangle$, we obtain the eigenstates $|\mu_{n\mathbf{k}}(\mathbf{r})\rangle$ with SO coupling by

$$|\mu_{n\mathbf{k}}(\mathbf{r})\rangle = \sum_{\nu'\sigma'} C^n_{\nu'\sigma'}(\mathbf{k})|\nu'\sigma'\mathbf{k} = 0\rangle. \tag{1.7}$$

Note in the state $|\nu\sigma\mathbf{k} = 0\rangle$ the spin is conserved. The coefficient $C^{\nu}_{\nu'\sigma}(\mathbf{k})$ can be obtained by substituting above formula into Eq. (1.4). For this we obtain

$$\sum_{\nu'\sigma'}\big[(E_{\nu'\mathbf{0}} + \frac{\hbar^2k^2}{2m_0})\delta_{\nu\nu'}\delta_{\sigma\sigma'} + \frac{\hbar}{m_0}\mathbf{k}\cdot\mathbf{P}^{\sigma\sigma'}_{\nu\nu'} + \Delta^{\sigma\sigma'}_{\nu\nu'}\big]C^n_{\nu'\sigma'}(\mathbf{k}) = E_{n\mathbf{k}}C^n_{\nu\sigma}(\mathbf{k}), \tag{1.8}$$

where $\mathbf{P}^{\sigma\sigma'}_{\nu\nu'}$ and $\Delta^{\sigma\sigma'}_{\nu\nu'}$ are respectively defined through

$$\mathbf{P}^{\sigma\sigma'}_{\nu\nu'} = \langle\nu\sigma\mathbf{k}|\vec{\pi}|\mathbf{k}\sigma'\nu'\rangle, \tag{1.9}$$

$$\Delta^{\sigma\sigma'}_{\nu\nu'} = \frac{\hbar}{4m_0^2c^2}\langle\nu\sigma\mathbf{k}|\vec{\sigma}\cdot(\nabla V_0 \times \mathbf{P})|\mathbf{k}\sigma'\nu'\rangle. \tag{1.10}$$

In the calculation one usually neglects the SO coupling term in the term $\mathbf{P}^{\sigma\sigma'}_{\nu\nu'}$ and thus $\vec{\pi} = \mathbf{P}$ and $\mathbf{P}^{\sigma\sigma'}_{\nu\nu'} = \delta_{\sigma\sigma'}\mathbf{P}_{\nu\nu'}$. Due to the odd parity of $\mathbf{P}$, the term $\mathbf{P}^{\sigma\sigma'}_{\nu\nu'}$ couples only states with opposite parity. The SO coupling term $\Delta^{\sigma\sigma'}_{\nu\nu'}$ leads to a splitting of the degenerate energy levels $E_{n\mathbf{k}}$ even at $\mathbf{k} = 0$. For the III-V type semiconductors (e.g. GaAs) with zinc blende structure, each unit cell includes 2 atoms, filled with 8 electrons. As a result, at least s orbital (with $l = 0$) and p orbital (with $l = 1$) must be take into account to calculate the band structure. Considering that zinc blende structure has two sublattices, the summation in Eq. (1.8) covers $2 \times (2 + 6) = 16$ orbitals. Without SO coupling, the p-orbitals at the valence band edge of a III-V type semiconductor (e.g. GaAs) are sixfold degenerate. The SO interaction $\Delta^{\sigma\sigma'}_{\nu\nu'}$ splits the sixfold degenerate states into a fourfold degenerate subspace, with total angular momentum $j = 3/2$ for the heavy hole and light hole states (Γ^v_8) and $j = 1/2$ for the SO split-off states (Γ^7_v).

Solving the Eq. (1.8) one can obtain the exact dispersion relation. Neglecting SO coupling and calculating up to second order of $\mathbf{P}$ by means of perturbation theory we obtain [52]

$$E_\nu(\mathbf{k}) = E_\nu(0) + \frac{\hbar k^2}{2m^*_\nu}, \tag{1.11}$$

where the effective mass is given by

$$\frac{1}{m^*_\nu} = \frac{1}{m_0} + \frac{1}{m_0^2}\sum_{\nu'} \frac{P^2_{\nu\nu'}}{E_\nu(0) - E_{\nu'}(0)}. \tag{1.12}$$

The effective mass gives the kinetic energy of the Bloch electrons around the band edge. To study different types of effective SO coupling for Bloch electrons belonging to different bands, one may consider only a few adjacent bands, and then the $\mathbf{k} \cdot \mathbf{p}$ interaction and SO coupling are fully taken into account only for these bands, whereas the contributions of the remote bands are considered by means of Löwdin perturbation theory [52]. For example, by taking into account the s ($j = 1/2$)

conduction bands, p ($j = 3/2$ and $j = 1/2$, respectively) valence bands, one may obtain the 8-band Kane model and the 8-band Kohn-Luttinger Model considering different approximations. The former (the Kane model) is very helpful to describe the conduction band physics by further reducing the 8-band Kane model to the conduction band with the Löwdin perturbation theory, while from the later one can study the Luttinger SO interaction for the $j = 3/2$ valence band holes [52, 54].

Now we present the specific results for different types of the SO coupling in typical semiconductor system. For the conduction band electrons, we have two types of SO couplings known by the Dresselhaus terms [55] and Rashba terms [56], respectively. The former SO coupling Hamiltonian is due to the bulk-inversion asymmetry:

$$H_D^{so} = \frac{\gamma}{\hbar^3}\big(\sigma_x P_x(P_y^2 - P_z^2) + \sigma_y P_y(P_z^2 - P_x^2) + \sigma_z P_z(P_x^2 - P_y^2)\big), \tag{1.13}$$

which is trilinear in the momentum. For the sufficiently low temperatures, and considering a very narrow quantum well grown along the [001] direction, one can approximately neglect the nonlinear terms of P_x and P_y and replace P_z^2 by $\langle P_z^2\rangle$. Thus H_D^{so} can be recast into

$$H_D^{so} = -\frac{\alpha}{\hbar}(\sigma_x P_x - \sigma_y P_y), \tag{1.14}$$

with $\alpha = \gamma\langle P_z^2\rangle$. On the other hand, the Rashba Hamiltonian is due to the structure inversion asymmetry and is of the form

$$H_R^{so} = -\frac{\lambda}{\hbar}(\sigma_x P_y - \sigma_y P_x). \tag{1.15}$$

The typical values of the Dresselhaus coefficient and Rashba coefficient are about $\alpha \sim 10^{-11}$eVm and $\lambda \leq 10^{-11}$eVm for GaAs quantum well. The SO coupling Hamiltonian can be equivalently understood with the picture that the electrons experience a non-Abelian gauge field for the orbital motion. For example, the gauge potential for

the Rashba model (1.15) reads $A_x = \frac{\lambda}{\hbar}\sigma_y, A_y = -\frac{\lambda}{\hbar}\sigma_x$, which is associated with a spin-dependent magnetic field along the z direction:

$$\mathcal{B} = \frac{e\lambda^2}{\hbar^2 c}\sigma_z \hat{e}_z. \tag{1.16}$$

Semiclassically, from this result one can judge that electrons with spin pointing to $+z$ direction experience an effective B field in $+z$ direction, while electrons with spin pointing to $-z$ direction experience an effective B field in $-z$ direction. As a result, if we apply an electric field in the $+x$ direction, the electrons in the $+z$ directional spin-polarization will move in the $-y$ direction, while the electrons in the $-z$ direction spin-polarization will move in the $+y$ direction due to the effective Lorentz force, leading to a pure spin current in the y direction. This phenomenon is known as the spin Hall effect (SHE) in the 2D Rashba system [57]. To have a nonzero anomalous Hall current, a Zeeman term is needed to break the TR symmetry.

For the valence-band hole systems around Γ point, the effective Hamiltonian are known as the Luttinger model [58]

$$H_L^{so} = \frac{\hbar^2}{2m}\big((\gamma_1 + \frac{5}{2}\gamma_2)k^2 - 2\gamma_2(\mathbf{k}\cdot\mathbf{S})^2\big), \tag{1.17}$$

where $\mathbf{S}$ is the spin-3/2 operator, and $\gamma_{1,2}$ are Luttinger parameters. A more general Luttinger Hamiltonian may include the term $\hat{p}_x^2 J_x^2 + \hat{p}_y^2 J_y^2 + \hat{p}_z^2 J_z^2$, which breaks the spherical symmetry [58]. It was obtained by S. Murakami et al that the above Hamiltonian describes a spin-dependent monopole field in the k-space after diagonalizing the term $\gamma_2(\mathbf{k}\cdot\mathbf{S})^2$ by a $\mathbf{k}$-dependent unitary transformation $U(\mathbf{k})$, which makes the electrons with spin-up polarizations and spin-up polarizations move in the opposite directions [59] when an external electric field is present. Thus the effective Lorentz force again accounts for a transverse pure spin current obtained in the Luttinger model when electrons are accelerated by external electric field (see more general discussion in the next section).

1.3 Berry phase

An intuitive picture for the Berry phase can be obtained by comparing the parallel translation of a vector in the curved space with the evolution of wave function in the quantum parameter space, as shown in the Fig. 1.1. Consider a vector $\vec{V}$ translating along the geodesic lines (orthodrome) which consist of a closed path on the two dimensional (2D) spherical surface (Fig. 1.1 (a)). After the translation and when the vector return to the starting point, we can see it generally differs from the initial case with an angle $\vec{V}_i \to \vec{V}_f$. Namely, a finite angle results between the initial vector and the final one. This effect is a consequence of the nonzero curvature of the spherical surface.

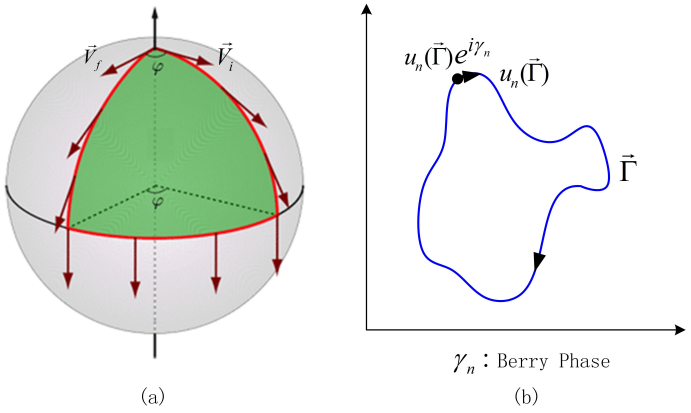

Fig. 1.1. (a) A vector $\vec{V}$ translates along the geodesic lines on the 2D spherical surface. (b) Adiabatic evolution of the wave function $u_n(\vec{\Gamma}_0)$ in parameter space acquires a geometric phase.

When we turn to the quantum mechanic system, the real space is replaced with the parameter space, and the vector is replaced with the wave function. Consider a quantum system with the Hamiltonian $H(\vec{\Gamma})$ depending on the parameter $\vec{\Gamma}$. At any point of the parameter space we may (partially) diagonalize $H(\mathbf{\Gamma})$ and obtain the eigenfunction $u_n(\vec{\Gamma})$, which is a function of the parameter $\vec{\Gamma}$. Then consider an adiabatic evolution along a closed path in the parameter space (Fig. 1.1 (b)).

Similar to the situation in the real space, after the evolution the final eigenfunction differs from the original one by a phase factor $u_n(\vec{\Gamma}_0) \to u_n(\vec{\Gamma}_0)e^{i\gamma_n}$. The phase γ_n is referred to the Berry phase [9] corresponding to the eigenfunction $u_n(\vec{\Gamma}_0)$, which has geometric significance. Mathematically, this phase can be calculated by

$$\begin{aligned} \gamma_n &= \frac{1}{\hbar}\oint \vec{\mathcal{A}}_n \cdot d\vec{\Gamma}, \\ &= \frac{1}{\hbar}\int \vec{\Omega}_n \cdot d^2\vec{\Gamma}, \end{aligned} \tag{1.18}$$

where $\vec{\mathcal{A}}_n = i\hbar\langle u_n(\vec{\Gamma})|\nabla_{\vec{\Gamma}}|u_n(\vec{\Gamma})\rangle$ is the U(1) Berry's connection, and $\vec{\Omega}_n = \nabla_{\vec{\Gamma}} \times \vec{\mathcal{A}}_n$ is the Berry's curvature. In the following we shall respectively discuss the Berry phase in the real space and momentum space.

1.3.1 Berry phase in the real space

In this subsection we present a general discussion for the Berry phase in the real space. Consider a quantum system which is characterized by a N-dimensional Hilbert space [60]. For example, we consider a spin-S system with $S = (N-1)/2$. The basis of the Hilbert space is described by $u = (u_{-S}, u_{-S+1}, ..., u_S)^T$. The total Hamiltonian reads $H = \mathbf{P}^2/2m^* + H_I[\mathbf{S}(\mathbf{r})]$, where the effective mass m^* is assumed to be the same for all $|u_k\rangle$ states. The off-diagonal part of the Hamiltonian $H_I[\mathbf{S}(\mathbf{r})]$ is a function of the spin $\mathbf{S}(\mathbf{r})$ which couples to the local parameters, i.e. the spatial position $\mathbf{r}$. The evolution of the present system is governed by

$$i\hbar\frac{\partial u(\mathbf{r})}{\partial t} = [\frac{\mathbf{P}^2}{2m^*} + V(\mathbf{r})]u(\mathbf{r}) + H_I[\mathbf{S}(\mathbf{r})]u(\mathbf{r}), \tag{1.19}$$

where $V(\mathbf{r})$ is the external potential and it is assumed to be diagonal. The diagonalization of $H_I[\mathbf{S}(\mathbf{r})]$ can be done through a local unitary transformation $U(\mathbf{r})$, $u = U(\mathbf{r})\chi(\mathbf{r})$, $H_I^d = U^\dagger H_I U$, where $\chi(\mathbf{r}) = (\chi_{-S}, \chi_{-S+1}, ..., \chi_S)$ is the diagonalized basis and on this basis H_I^d is diagonal. The diagonal elements $(H_I^d)_{kk} = \mathcal{E}_k$ repre-

sents the eigenvalue of χ_k. Note that the specific form of the unitary transformation $U(\mathbf{r})$ shall be solely determined by the off-diagonal Hamiltonian $H_I[\mathbf{S}(\mathbf{r})]$. Under the transformation by $U(\mathbf{r})$ we straightforwardly find the original Hamiltonian can be rewritten into

$$H \to U^\dagger H U = \frac{1}{2m^*}\left[i\hbar\nabla + \mathcal{A}(\mathbf{r})\right]^2 + V(\mathbf{r}) + H_I^d[S_z(\mathbf{r})], \tag{1.20}$$

where we have introduced the gauge potential

$$\mathcal{A}(\mathbf{r}) = i\hbar U^\dagger(\mathbf{r})\nabla_{\mathbf{r}} U(\mathbf{r}). \tag{1.21}$$

Since $U(\mathbf{r})$ considered here is a local unitary transformation on the N-dimensional Hilbert space, it is a $N \times N$ parameter-dependent matrix. As a result, the gauge potential defined based on Eq. (1.21) is generally non-Abelian and of the SU(N) symmetry. The non-Abelian gauge field is associated with the non-Abelian curvature which is defined by

$$\mathcal{F}_{\mu\nu} = \partial_\mu \mathcal{A}_\nu - \partial_\nu \mathcal{A}_\mu - i\frac{e}{c}[\mathcal{A}_\mu, \mathcal{A}_\nu], \tag{1.22}$$

with which the effective magnetic field is given by $\mathcal{B}_j = 1/2\epsilon_{jkl}F_{kl}$. One should keep in mind that to this step we do not apply the adiabatic condition in the equation of motion. The gauge field defined in eq. (1.21) is a pure gauge and it is easy to verify that $\mathcal{F}_{\mu\nu} = 0$. It is noteworthy that the non-Abelian pure gauge may have nontrivial significance by resulting in a phase to the wave function Φ:

$$\Phi(\mathbf{r}, t) \to \mathcal{P}e^{\frac{i}{\hbar}\int \mathcal{A}\cdot d\mathbf{l}}\Phi(\mathbf{r}, t), \tag{1.23}$$

where $\mathcal{P}$ is the operator of chronological ordering. The above phase factor is known as Wilson loop integral [61]. This phase factor can be non-zero even for a pure gauge,

since for the non-Abelian gauge field we have $\nabla \times \mathcal{A} \neq \mathcal{B} = 0$. To find the possible observable physics for this phase factor is an interesting issue in gauge field theory.

For the condensed matter system we are interested in the U(1) Abelian gauge potential which can be reduced from the the original SU(N) field $\mathcal{A}(\mathbf{r})$ by introducing the adiabatic condition [62]. The resulted U(1) adiabatic gauge potential is then generally associated with a non-zero curvature $F_{\mu\nu} \neq 0$. Specifically, we shall consider the case in the following that the system is non-degenerate, i.e. $\mathcal{E}_j \neq \mathcal{E}_k$ for $j \neq k$ $(j, k = -S, -S+1, ...S)$. When each eigenstate is separated from others by a sufficiently large difference in the eigenvalues, the coupling between each two states, say χ_j and χ_k, induced by the off-diagonal element $\mathcal{A}_{jk}(\mathbf{r})$ satisfies $|\frac{\mathbf{P}\cdot\mathcal{A}_{jk}}{m(\mathcal{E}_j-\mathcal{E}_k)}| \sim |\frac{\mathbf{v}_F\cdot\mathcal{A}_{jk}}{\mathcal{E}_j-\mathcal{E}_k}| \ll 1$, where v_F is the Fermi velocity. In this way, the adiabatic condition is satisfied and the transition between different states in eq.(1.20) can be ignored. The non-Abelian gauge field $\mathcal{A}$ is reduced from SU(N) symmetry to N independent U(1) Abelian gauge fields with

$$\mathcal{A}_j(\mathbf{r}) = i\hbar\langle\chi_j|\nabla_{\mathbf{r}}|\chi_j\rangle, \quad j = -S, -S+1, ...S, \tag{1.24}$$

and the corresponding scalar potential after applying the adiabatic condition $\phi_j(\mathbf{r}) = \frac{1}{2m}\sum_{k\neq j}\mathcal{A}_{jk}\cdot\mathcal{A}_{kj}$. In the dynamical equation of evolution (1.20), all components of the column vector χ become decoupled to each other and the evolution of χ_j is according to the effective Hamiltonian

$$H_j(\mathbf{r}) = \frac{1}{2m^*}\left[i\hbar\nabla + \mathcal{A}_j(\mathbf{r})\right]^2 + V_j'(\mathbf{r}), \tag{1.25}$$

with $V_j'(\mathbf{r}) = V(\mathbf{r}) + \phi_j + \mathcal{E}_j$. The curvature of U(1) gauge fields is given by $\mathcal{F}_{\mu\nu}^{(j)} = \partial_\mu A_\nu^{(j)} - \partial_\nu A_\mu^{(j)}$, which is generally non-zero. Consider a closed path in the real **r**-

space, after the adiabatic evolution along such path the eigenstate $\chi_j(\mathbf{r})$ acquires a Berry phase γ_j given by

$$\begin{aligned}\gamma_j &= i\oint \langle\chi_j|\nabla_{\mathbf{r}}|\chi_j\rangle\cdot d\mathbf{r}, \\ &= 2i\int dr_1\int dr_2\langle\partial_{r_1}\chi_j|\partial_{r_2}\chi_j\rangle. \end{aligned} \tag{1.26}$$

The effective Hamiltonian (1.25) describes that the particle in the state $|\chi_j\rangle$ experiences an effective magnetic field. Therefore, when an external electric field is applied, the accelerated particle will be exerted with an effective Lorentz force and be deflected to the transverse direction. This leads to the (anomalous) Hall effect.

For the spin-1/2 case, one may consider a simple example described by the following Hamiltonian

$$H = \frac{\mathbf{P}^2}{2m^*} + V(\mathbf{r}) + \mathbf{M}(\mathbf{r})\cdot\sigma, \tag{1.27}$$

where $\mathbf{M}(\mathbf{r}) = M_0\mathbf{n}(\mathbf{r})$ represents a chiral textured distribution of the Ferromagnetic magnetization. When the direction of the magnetization varies slowly in the space, one can diagonalize the Hamiltonian at each spatial point to obtain two bands, with the eigenvalues of them given by $\mathcal{E}_\pm = \hbar^2k^2/2m \pm M_0$. According to Eq. (1.24) one finds straightforwardly

$$\mathcal{A}^\mu_\pm(\mathbf{r}) = \pm\frac{1}{2}\frac{n_x\partial_\mu n_y - n_y\partial_\mu n_x}{1+n_z}. \tag{1.28}$$

The associated Berry curvature reads

$$\mathcal{B}^\mu_\pm = \pm\frac{1}{2}\epsilon^{\mu\nu\lambda}\epsilon^{ijk}n_i\partial_\nu n_j\partial_\lambda n_k. \tag{1.29}$$

An interesting situation is that considering a topological defect in a 2D ferromagnet when $\mathbf{n}(\mathbf{r})$ points to up direction at a point inside a region of the 2D plane but gradu-

ally relaxes to the down direction at the boundary of this region, one can see the area integral of the Berry curvature $\mathcal{B}_{\pm}$ yields an integer, which corresponds to the number of the Skyrmion excitations in the ferromagnetic material. It can be expected the AHE due to the textured magnetization in ferromagnet diminishes when temperature decreases, since Skyrmion excitations are suppressed at low temperature.

1.3.2 Berry phase in the **k** space

The Berry phase in the momentum space can be studied in the similar way [60]. Again, consider a spin-S system with SO coupling described by the Hamiltonian $H_{so}(\mathbf{S}, \mathbf{k})$. The quantum system is then a N-dimensional ($N = 2S+1$) Hilbert space with the basis $u = (u_{-S}, u_{-S+1}, ..., u_S)^T$. The total Hamiltonian can be obtained by

$$H = \frac{\mathbf{P}^2}{2m^*} + H_{so}(\mathbf{S}, \mathbf{k}) + V(\mathbf{r}), \tag{1.30}$$

where $V(\mathbf{r})$ includes the applied external fields such as the electric field. Similarly we diagonalize the SO coupling Hamiltonian by a unitary transformation in the **k** space: $u = U(\mathbf{k})\chi(\mathbf{k})$ and then $H_I^d = U^\dagger(\mathbf{k})H_I U(\mathbf{k})$, with $\chi(\mathbf{k}) = (\chi_{-S}, \chi_{-S+1}, ..., \chi_S)$. Note the position operator has the form $\mathbf{r} = i\hbar\partial_{\mathbf{k}}$ in the momentum space. Under this transformation we obtain the total Hamiltonian in the form

$$H \to U^\dagger(\mathbf{k})HU(\mathbf{k}) = \frac{\hbar^2 k^2}{2m^*} + H_I^d(S_z, k) + V(i\hbar\partial_{\mathbf{k}} + \mathcal{A}_{\mathbf{k}}), \tag{1.31}$$

where the gauge potential

$$\mathcal{A}(\mathbf{k}) = i\hbar U^\dagger(\mathbf{k})\nabla_{\mathbf{k}} U(\mathbf{k}) \tag{1.32}$$

By a similar procedure we consider the adiabatic condition which is generally valid when the difference in the eigenvalues of each pair of eigenstate is is large enough. For the present system the criteria $|\frac{\langle\chi_j|V(i\hbar\partial_{\mathbf{k}}+\mathcal{A}_{\mathbf{k}})|\chi_k\rangle}{\mathcal{E}_j-\mathcal{E}_k}| \ll 1$ (with $j \neq k$) ensures the

adiabatic condition. However, it is noteworthy that here the specific expression of the adiabatic condition depends on the form of the potential $V(\mathbf{r})$ which determines the coupling between each two states χ_j and χ_k. In this way, the non-Abelian gauge field $\mathcal{A}$ is reduced from SU(N) symmetry to N independent U(1) Abelian gauge fields with

$$\mathcal{A}_j(\mathbf{k}) = i\hbar\langle\chi_j|\nabla_{\mathbf{k}}|\chi_j\rangle, \quad j = -S, -S+1, ...S. \tag{1.33}$$

The evolution of $\chi_j(\mathbf{k})$ in the momentum space is according to the effective Hamiltonian $H_j(\mathbf{k}) = \frac{\hbar^2k^2}{2m^*} + \{H_I^d(S_z,k)\}_{jj} + V[i\hbar\partial_{\mathbf{k}} + \mathcal{A}_j(\mathbf{k})]$. Consider a closed path in the momentum $\mathbf{k}$-space, the Berry phase γ_j corresponding to such closed path evolution of the eigenstate $\chi_j(\mathbf{r})$ is given by

$$\gamma_j = 2i\int dk_x \int dk_y \langle\partial_{k_x}\chi_j(\mathbf{k})|\partial_{k_y}\chi_j(\mathbf{k})\rangle. \tag{1.34}$$

Similar to the result in the real space, when an electric field is applied, the particles experience an effective Lorentz force in the $\mathbf{k}$ space, which may give rise to the AHE. Below we consider the Rashba model as an example for the Berry phase effect in the momentum space, which is responsible for the intrinsic contribution to the AHE (the KL mechanism). The Hamiltonian reads

$$H = \frac{p^2}{2m^*} - \frac{\lambda}{\hbar}(\sigma_x p_y - \sigma_y p_x) + M_0\sigma_z, \tag{1.35}$$

where λ is the Rashba SO coupling constant, and M_0 is the magnetization in the perpendicular z direction. The AHC can be calculated in the linear response formula

$$\sigma_{xy}^{AH} = \frac{e\hbar}{V}\lim_{\omega\to 0}\sum_{\mathbf{k},s\neq s'}(f_{\mathbf{k},s'} - f_{\mathbf{k},s})\frac{\mathrm{Im}[\langle\mu_{\mathbf{k},s'}|\hat{j}_y^e|\mu_{\mathbf{k},s}\rangle\langle\mu_{\mathbf{k},s}|\hat{v}_x|\mu_{\mathbf{k},s'}\rangle]}{(E_{\mathbf{k},s} - E_{\mathbf{k},s'})(E_{\mathbf{k},s} - E_{\mathbf{k},s'} - \hbar\omega + i\eta)}, \tag{1.36}$$

with the charge current operator $\hat{j}_y^e = e\hat{v}_y$. The eigenstates $|\mu_{\mathbf{k},+}\rangle = [\cos\frac{\theta}{2}e^{i\phi}, \sin\frac{\theta}{2}]^T$ and $|\mu_{\mathbf{k},-}\rangle = [-\sin\frac{\theta}{2}e^{i\phi}, \cos\frac{\theta}{2}]^T$ with the eigenvalues $E_\pm = \hbar^2k^2/2m^* \pm \sqrt{M_0^2 + \lambda^2k^2}$, where $\theta = \tan^{-1}[M_0/(\lambda k)]$. Note that the velocity operator can also be written as $\hat{v}_y = [y, H]/i\hbar$. Substituting this result into above formula we can cancel out the denominator and then obtain

$$\begin{aligned} \sigma_{xy}^{AH} &= \frac{e^2}{i\hbar V}\sum_{\mathbf{k},s'\neq s}(f_{\mathbf{k},s} - f_{\mathbf{k},s'})\langle\mu_{\mathbf{k},s'}|\hat{x}|\mu_{\mathbf{k},s}\rangle\langle\mu_{\mathbf{k},s}|\hat{y}|\mu_{\mathbf{k},s'}\rangle, \\ &= -2\frac{ie^2}{\hbar V}\sum_{\mathbf{k},s} f(E_{\mathbf{k},s})\langle\frac{\partial\mu_{\mathbf{k},s}}{\partial_{k_y}}|\frac{\partial\mu_{\mathbf{k},s}}{\partial_{k_x}}\rangle. \end{aligned} \tag{1.37}$$

In the continuous limit we make replacement $\frac{1}{V}\sum_{\mathbf{k}} \to \int d^2\mathbf{k}/(2\pi)^2$, and can then rewrite the above formula as

$$\sigma_{xy}^{AH} = -\frac{e^2}{(2\pi)^2\hbar}\sum_s \oint_{C_F} d\mathbf{k}\cdot\langle\mu_{\mathbf{k},s}|i\frac{\partial}{\partial_{\mathbf{k}}}|\mu_{\mathbf{k},s}\rangle f(E_{\mathbf{k},s}). \tag{1.38}$$

Here C_F represents the contour of the Fermi surface. The integrand in above equation is just the Berry connection in the momentum space $\mathcal{A}_s(\mathbf{k}) = \langle\mu_{\mathbf{k},s}|i\frac{\partial}{\partial_{\mathbf{k}}}|\mu_{\mathbf{k},s}\rangle$, associated with the Berry curvature $\mathcal{B}_z^\pm = \partial_{k_x}\mathcal{A}_{k_y}^\pm - \partial_{k_y}\mathcal{A}_{k_x}^\pm$. Note that the Berry curvature for the two bands $\mathcal{B}_+$ and $\mathcal{B}_-$ are opposite, and their contribution to the conductivity is opposite. In the spin Hall system where $M_0 = 0$ the Berry curvature $\mathcal{B}_\pm = 0$ at $r = \sqrt{x^2+y^2} > 0$, but is infinite at $r = 0$. In this way, the gauge field $\mathcal{A}_\pm(\mathbf{k})$ represents a constant flux in the z axis. Since the effective magnetic fluxes are the same for the two bands in magnitude, while opposite in direction, the intrinsic charge Hall conductivity is exactly canceled out by the contribution of the two bands. This is reasonable, since the spin Hall system possesses TR symmetry, while a nonzero charge Hall conductance requires the TR symmetry to be broken.

We go back to the anomalous Hall system with $M_0 > 0$. For the case $-M_0 < \varepsilon_F < M_0$, only the lower band is occupied at the zero temperature, and then at the zero temperature we can rewrite the Eq. (1.38) as

$$\sigma_{xy}^{AH} = -\frac{e^2}{(2\pi)^2\hbar}\int dk_x dk_y \mathcal{B}_-(\mathbf{k}). \tag{1.39}$$

The above integral goes over the momentum space $k \leq k_F$. To see clearly the geometric property of the AHC, we denote the unit vector field by

$$\mathbf{n}(\mathbf{k}) = \bigg(-\frac{\lambda k_y}{d(\mathbf{k})}, \quad \frac{\lambda k_x}{d(\mathbf{k})}, \quad \frac{M_0}{d(\mathbf{k})} \bigg), \tag{1.40}$$

with $d(\mathbf{k}) = \sqrt{\lambda^2(k_x^2 + k_y^2) + M_0^2}$. One can verify that $\mathcal{B}_- = -\frac{\hat{e}_z}{2}\mathbf{n} \cdot \frac{\partial \mathbf{n}}{\partial k_x} \times \frac{\partial \mathbf{n}}{\partial k_y}$. The AHC then reads

$$\sigma_{xy}^{AH} = \frac{e^2}{h}\int \frac{dk_x dk_y}{4\pi}\mathbf{n} \cdot \frac{\partial \mathbf{n}}{\partial k_x} \times \frac{\partial \mathbf{n}}{\partial k_y} = \frac{e^2}{h}C_1, \tag{1.41}$$

where $C_1 = \Omega_C/4\pi$, with $\Omega_C = \int d^2\mathbf{k}\mathbf{n} \cdot \frac{\partial \mathbf{n}}{\partial k_x} \times \frac{\partial \mathbf{n}}{\partial k_y}$ the solid angle on the spherical surface S^2 enclosed by the contour that is the mapping of the Fermi line. As a result, the property of the AHC is fully determined by the mapping between the $\mathbf{k}$-space below the Fermi energy and the S^2. In the "usual" anomalous Hall effect where the parameters λ and M_0 are constants, such a mapping only covers part of the S^2, and then C_1 cannot be integers, say, the AHC is not quantized. However, when we consider a similar SO coupling Hamiltonian in the $2+1$ dimension multi-band insulating system, the coefficients λ and M_0 will be replaced with periodic functions of momentum $\mathbf{k}$, and the contribution to the AHC is obtained by the mapping of the whole first Brillouin zone (FBZ) to S^2. Since the geometry of the FBZ is a close surface (torus), a mapping degree is constructed between the FBZ and S^2 spherical surface. In this way the integral in Eq. (1.41) yields an integer, i.e. $C_1 \in \mathbb{Z}$, which

corresponds to the first Chern number. This is the basic idea for the realization of integer quantum Hall effect without Landau levels or QAHE [15–21].

Before moving to the end of this section we would like to clarify a confusing issue regarding to the relation between adiabatic condition and the AHE. In the discussion of the Berry phase we introduced the adiabatic condition with which the original $SU(N)$ unitary transformation is reduced to $U(1)$ case and then the Berry phase can be calculated. The adiabatic condition specifies the criteria of the adiabatic evolution with which the wave function can acquire a geometric phase. However, it seems that in the calculation of the AHC with Kubo formula (1.36) the adiabatic condition is not considered. From the first line in Eq. (1.37) we see the contribution to AHC arises from the off-diagonal elements in the gauge potential, while it is interesting the final result is exactly determined by the U(1) Abelian Berry's connection of the occupied electronic band. This indicates the linear response regime may have a close relation to the adiabatic condition. Actually, the linear response approximation requires that $|\frac{\langle\chi_j|e\mathbf{E}\cdot\mathbf{r}|\chi_k\rangle}{\mathcal{E}_j-\mathcal{E}_k}| = |\frac{e\mathbf{E}\cdot\mathcal{A}_{jk}(\mathbf{k})}{\mathcal{E}_j-\mathcal{E}_k}| \ll 1$ (with $j \neq k$), which is exactly the adiabatic condition (note the electric potential reads $V = e\mathbf{E}\cdot\mathbf{r}$). This condition can be understood that in the linear response regime the electrons are slowly accelerated in the weak electric field, which actually corresponds to the adiabatic evolution.

1.4 Outlook

In this dissertation, we present a theoretical approach to study the AHE when the system is in the disordered insulating regime and thus the hopping transport prevails. The AHC is obtained as a function of the longitudinal conductivity, which can be varied by changing temperature or density of states around fermi energy. Specifically, we calculate the lower and upper limits for the AHC in different extreme situations, from which we show the AHC scales the longitudinal conductivity as $\sigma_{xy}^{AH} \sim \sigma_{xx}^{\gamma}$ with γ predicted to be $1.38 \leq \gamma \leq 1.76$, quantitatively in agreement with

the experimental discoveries. Our result provides the understanding of the AHE in the hopping conduction regime.

The dissertation manuscript is organized as follows. In section 2, we briefly review the experimental studies in the disordered insulating regimes, with which we point out the challenging issues in the understanding of the insulating regime. The AHE theory in the metallic regime is discussed with the semiclassical Boltzmann equation (SBE) method in section 3. The intrinsic, side jump, and skew scattering contributions are introduced systematically in this section. Then in the section 4 we begin to study the theory of the insulating regime, with the hopping conduction mechanism being discussed in detail. Section 5 is devoted to studying the configuration averaging of the AHC in the random disordered insulating system. The percolation theory is introduced in this section. In section 6 we calculate analytically the lower and upper limits for the AHC, from which we obtain the correct scaling relation between AHC and the longitudinal conductivity. Several different situations for the AHC are considered. In the final section we present conclusions and further discussions regarding to AHE in the insulating regime.

2. EXPERIMENTAL STUDIES OF THE AHE

2.1 The insulating regime

In this section we briefly review the experimental results of the AHE in the disordered insulating regime. This review includes an early experiment done in Fe_3O_4 films, and the recent experimental observations in granular Fe/SiO_2 films, magnetite epitaxial thin films, ferromagnetic semiconductor anatas $Ti_{1-x}Co_xO_{2-\delta}$, and DMS $Ga_{1-x}Mn_xAs$.

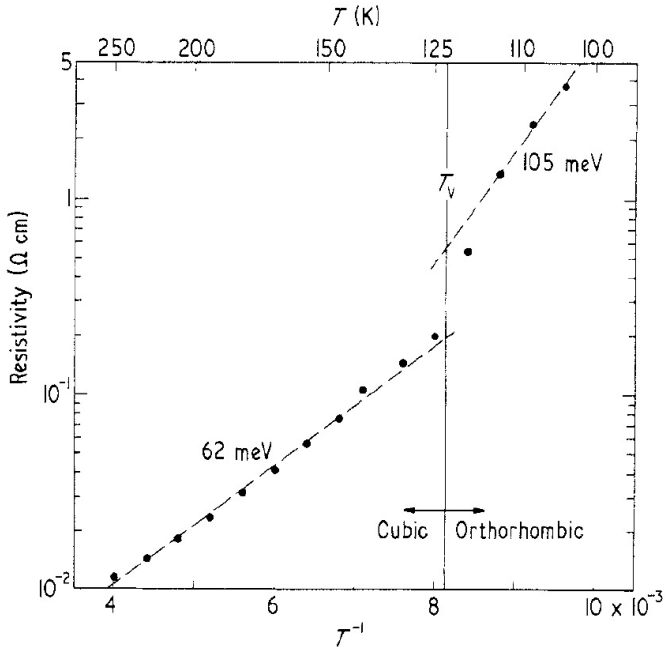

Fig. 2.1. The resistivity of 2500 Å Fe_3O_4 on Corning 0211 glass as a function of temperature ($1/T$). The Verwey transition at T_v is clearly indicated but the change in the resistivity is not as large as in bulk samples [34].

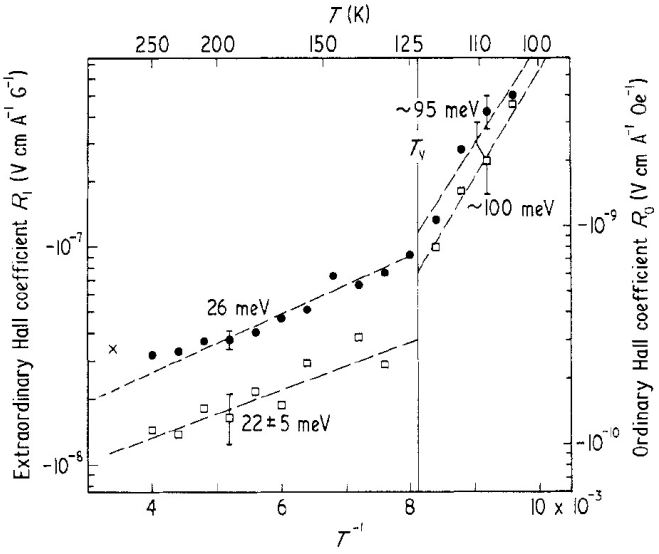

Fig. 2.2. The ordinary and extraordinary (anomalous) Hall coefficients as a function of temperature [34].

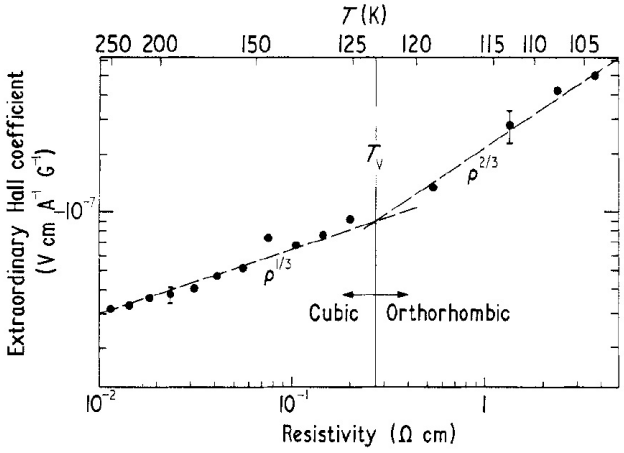

Fig. 2.3. The anomalous Hall coefficient as a function of the longitudinal resistivity. This figure gives the scaling exponent $\gamma \approx 1.33$ for $T < T_v$ and $\gamma \approx 1.66$ for $T > T_v$ [34].

2.1.1 Magnetite

An earlier experiment on the AHE in the insulating regime was done by Feng et al in the magnetite (Fe_3O_4) thin films [34], with the temperature varied from

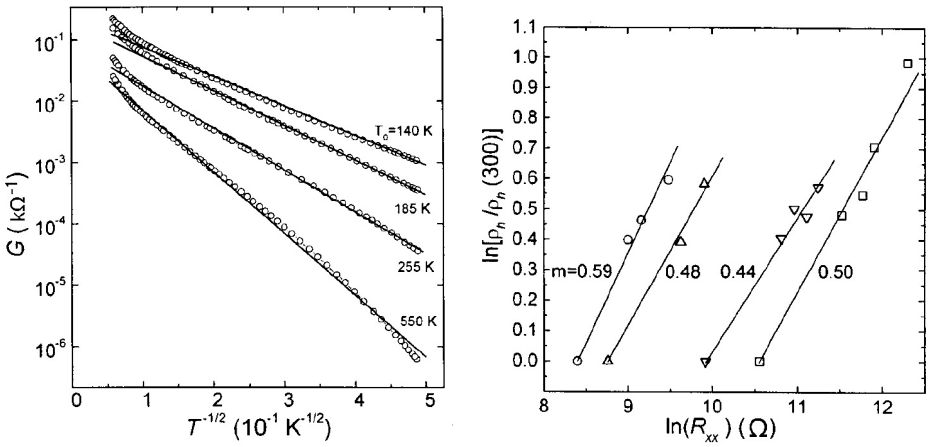

(a) (b)

Fig. 2.4. Experimental data from Ref. [35]. (a) Temperature dependencies of the conductance G_{xx} of insulating samples with various compositions. (b) The scaling relation between anomalous Hall resistivity and longitudinal one, with the resistivity varied by changing the T from $77 - 300$ K.

104K to room temperature to change the longitudinal conductivity (Figs. 2.1-2.2). The scaling relation $\sigma_{xy}^{AH} \propto \sigma_{xx}^{\gamma}$ was observed with $\gamma = 1.33 \sim 1.66$. It is important that the scaling exponent is related to the Verwey transition which occurred at $T_v = 123$K [63]. At the temperature below T_v, the scaling exponent was observed to be $\gamma \approx 1.33$, while above T_v it was about $\gamma \approx 1.66$ (Fig. 2.3). Moreover, the scaling of longitudinal conductivity versus T in these samples holds the form $\log \sigma_{xx} \propto 1/T$, which indicates the system was mostly in the nearest-neighbor hopping (activation E_3 hopping) conduction regime [64, 65].

For the samples of granular $(\mathrm{NiFe})_x/(\mathrm{SiO_2})_{1-x}$ films with $x < x_c \approx 0.6$, Aronzon et al reported the scaling between AHC and the longitudinal conductivity as $\sigma_{xy}^{AH} \propto \sigma_{xx}^{1.4\sim1.6}$, as shown in Fig. 2.4 [35, 36]. In their experiment the conductivities are also varied by changing the temperature between 77K to 300K. An characteristic phenomenon was observed in these samples that when M decreases as x decreases which leads to more highly insulating phase, the anomalous Hall coefficient R_s in-

creases much greater relative to bulk iron. This indicates anomalous charge Hall transport is dominated by the hopping conduction between different granules rather than by individual granules. Actually, a clear 1/2-type variable range hopping (VRH) conduction was observed in these samples described by the scaling of longitudinal conductivity versus temperature $\sigma_{xx} = \sigma_0 e^{-(T_0/T)^{1/2}}$ (see Fig. 2.4 (a)), where T_0 is a constant depending on the sample parameters such as the characteristic granular size, the localization length of the electron wave function in the insulator.

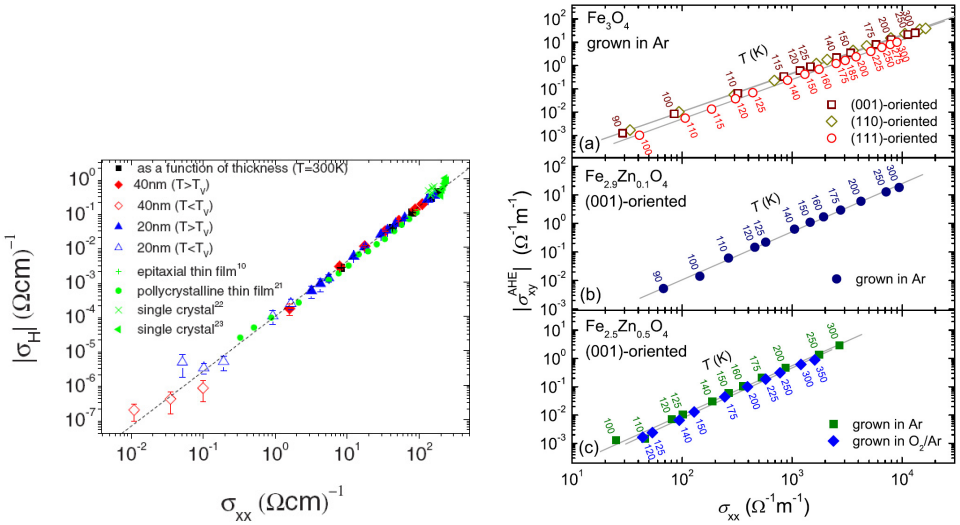

Fig. 2.5. (a) Relationship between the magnitude of the Hall conductivity at 11 kOe and the longitudinal conductivity for different Fe_3O_4 epitaxial thin films [43]. (b) Modulus of the anomalous Hall conductivity plotted versus longitudinal conductivity σ_{xx} for different epitaxial $Fe_{3-x}Zn_xO_4$ films in the temperature regime between 90 and 350K [44].

The recent experimental observations of this scaling are reported in epitaxial thin films by Fernández-Pacheco et al [43] and by Venkateshvaran et al [44], respectively. The former reported the scaling exponent $\gamma \approx 1.6$ (Fig. 2.5 (a)) and the later reported that $\gamma = 1.69 \pm 0.08$ (Fig. 2.5 (b)). It is interesting that these scalings

keep unchanged when T changes from below Verwey temperature T_v to above T_v, and they are valid over three decades of the longitudinal conductivity.

2.1.2 Anatase and rutile $Ti_{1-x}Co_xO_{2-\delta}$

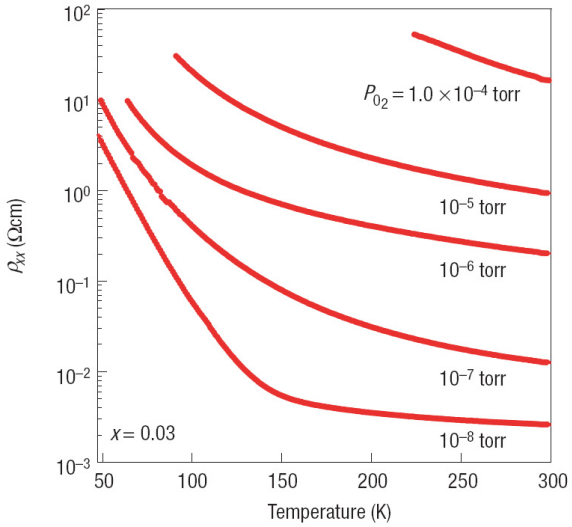

Fig. 2.6. Temperature dependence of the resistivity ρ_{xx} for $Ti_{0.97}Co_{0.03}O_{2-\delta}$ films grown under different oxygen pressures P_{O_2} [38].

Toyosaki et al has studied the anomalous Hall effect in the anatase and rutile $Ti_{1-x}Co_xO_{2-\delta}$ (δ is the oxygen deficiency) in the insulating regime [38]. The experimental data is shown in Figs. 2.6-2.7. The anatase and rutile phases of TiO_2 doped with Co are room temperature ferromagnetic semiconductors. The purpose of this experiment was to confirm the intrinsic regime of the ferromagnetic phase of $Ti_{1-x}Co_xO_{2-\delta}$. Namely, the ferromagnetic phase is not caused by the magnetic impurity segregation, but by spin-polarized charge carriers which mediate ferromagnetic exchange interaction between distant localized spins of magnetic impurities. The scaling $\sigma_{xy}^{AH} \propto \sigma_{xx}^{1.5\sim1.7}$ was observed with the temperature varying between 50K and 300K (Fig. 2.7). In the experiment the deficiency parameter δ is controlled by

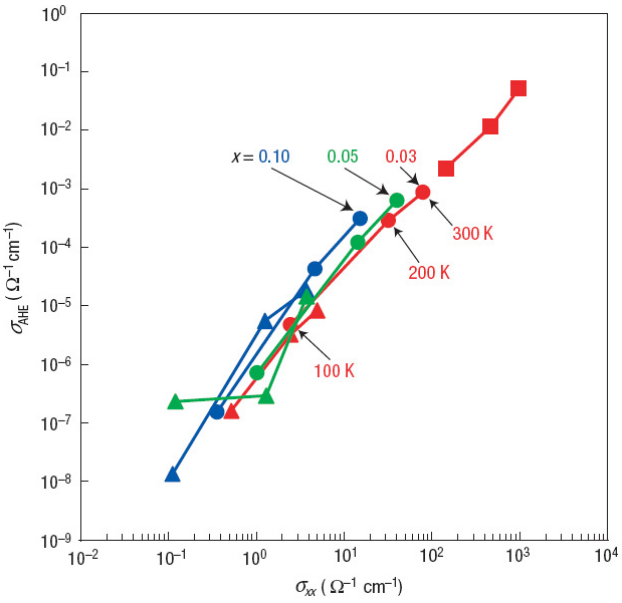

Fig. 2.7. Scaling relation between σ_{xy}^{AH} and σ_{xx}. The scaling exponent from the data in this figure is given by $\gamma = 1.5 \sim 1.7$ [38].

changing the oxygen pressure P_{O_2}. With decreasing the oxygen pressure, the deficiency δ increases and the electron density n of the samples increase accordingly. This leads to the increase of the longitudinal conductivity σ_{xx} (Fig. 2.6). The OHE and AHE have different dependence on n and x. The AHE increases with increasing Co concentration, i.e. increasing x, while OHE decreases with increasing n.

In experiment, one needs to subtract the OHE from the total Hall resistivity to obtain the anomalous Hall resistivity. This can be done by determining the ordinary Hall coefficient R_0 in the large external magnetic field case. In this case the AHE is saturated and the OHE keeps proportional to magnetic field. The AHE is more convenient to be measured with relatively larger x and larger n (or small P_{O_2}) values, in which situation the AHE dominates the Hall effect, while the OHE is small.

2.1.3 DMS $Ga_{1-x}Mn_xAs$

Experimental studies of the $Ga_{1-x}Mn_xAs$ digital ferromagnetic heterostructures done by Allen et al [39], which consist of submonolayers of MnAs separated by spacer layers of GaAs, have shown the scaling relation between the AHC and longitudinal conductivity $\sigma_{xy}^{AH} \propto \sigma_{xx}^{1.4\sim1.6}$ (Fig. 2.8). It was clearly demonstrated in this experiment that the VRH regime dominated the charge transport. Actually, the longitudinal resistance were observed to be of the hopping conduction type, $R_{xx} \propto T^{\alpha} \exp[(T_0/T)^{\beta}]$, with the parameter $\beta = 1/2, 1/3, 1/4$ having been observed for different samples (see Fig. 2.8 (a)). Another interesting phenomenon reported in the experiment by Allen et al is that the AHC can change sign when the sample grown temperature T_G was changed [39].

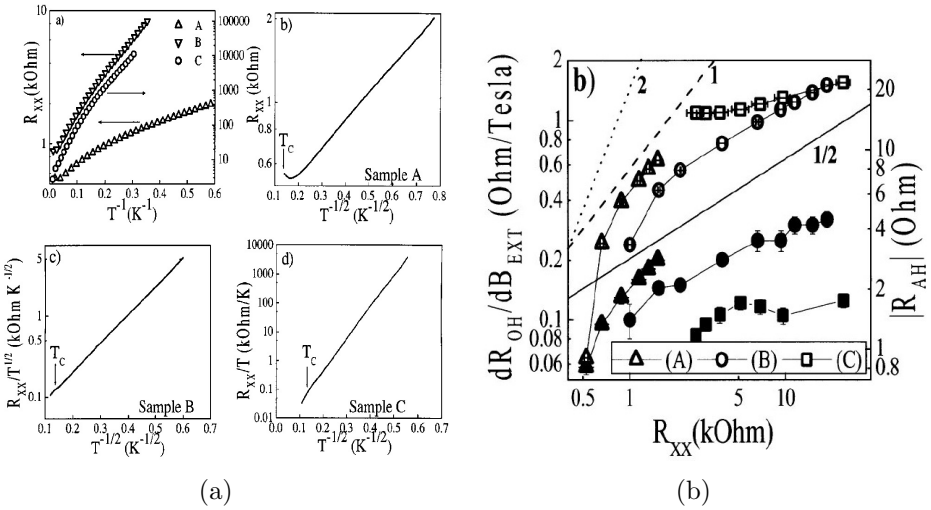

(a) (b)

Fig. 2.8. Experimental data from Ref. [39]. (a) Temperature dependence of the longitudinal resistance versus $1/T$ (a) and $1/T^{1/2}$ (b-d). The samples A, B, and C are grow in different temperatures. (b) Ordinary Hall component (filled symbols) and $|R_{AH}|$ (open symbols) as a function of R_{xx} on a log-log scale. Power-law slopes are shown as a comparison for the observed scalings by the lines labeled 1/2 (solid), 1 (dashed), and 2 (dotted).

A similar scaling relation in DMS $Ga_{1-x}Mn_xAs$ was reported by Shen et al [42]. In their experiment the scaling exponent γ for the transverse and longitudinal conductivities is mostly around $\gamma \approx 1.5$ in different samples. However, the variation of σ_{xx} was within one decade, and therefore the results observed in this experiment demonstrates only a possible scaling relation between AHC and σ_{xx}.

2.2 Discussions

Summarizing the experimental observations presented above, we can see the AHE in the disordered insulating regime has several important fundamental features. The first is that the scaling relation in the insulating AHE is generically observed in a wide range of different materials, which indicates this result is material-independent. Second, the observed scaling does not depend on the relevant parameters such as the impurity type (n or p type), electron or hole spins, magnetization, etc. Finally, this scaling relation is independent of specific types of hopping conduction mechanism (Mott VRH [66] or E-S hopping regime [67]), and even when σ_{xx} crosses over between different regimes (from VRH regime to nearest neighbor hopping regime, i.e. activation E_3 hopping regime [64, 65]). These important properties strongly indicates the underlying theory for the insulating AHE must be based on the physical mechanism which is generic in the disordered insulating regimes. Furthermore, the theoretical formalism used to evaluate the AHC in this regime should also be material independent.

3. THEORY OF THE AHE: METALLIC REGIME

In this section we review the AHE theory in the metallic regime with linear response formulas. Relative to the Kubo and Keldysh formalisms, the Boltzmann equation method has much clearer physical picture. However, since the Boltzmann equation studies the dynamics of the trace of the density matrix, the off-diagonal part of the density matrix which determines the coherent interband coupling effects are not naturally included. To study the coherent multiband effects, the Boltzmann equation usually needs to be properly modified. On the other hand, the full quantum mechanical studies of the quantum transport phenomena can be done based on the Kubo or Keldysh formalism. Nevertheless, for the sake of physical transparency, in this section we consider the SBE to discuss the intrinsic, side jump and skew scattering contributions to the AHE.

3.1 Semiclassical Boltzmann equation

The SBE describes the dynamics of the distribution function $f(\mathbf{r}, \mathbf{k}, t)$ for a many-body system in the semiclassical picture [68]

$$\frac{\partial f_l}{\partial t} + \dot{\mathbf{r}} \cdot \frac{\partial f_l}{\partial \mathbf{r}} + \dot{\mathbf{k}} \cdot \frac{\partial f_l}{\partial \mathbf{k}} = \left(\frac{\partial f_l}{\partial t} \right)_{coll}, \tag{3.1}$$

where l is the band index. The right hand side of above formula represents the collision term which may includes the disorder scattering, electron-electron and electron-phonon interactions, etc. In this work we consider only the disorder scattering, and then it can be given as

$$\left(\frac{\partial f_l}{\partial t} \right)_{coll} = -\sum_{l'} \int \frac{d^2\mathbf{k}'}{(2\pi)^2} \left[\omega_{k',l';k,l} f_l(k) - \omega_{k,l;k',l'} f_{l'}(k') \right], \tag{3.2}$$

where $\omega_{k',l';k,l}$ is the scattering rate from state (k,l) to state (k',l'). When the system is spatially homogeneous, we have $f(\mathbf{r},\mathbf{k},t) = f(\mathbf{k},t)$. We can then rewrite Eq. (3.1) in the form

$$\frac{\partial f_l}{\partial t} + e\mathbf{E}\cdot\mathbf{v}_{0l}\frac{\partial f_l}{\partial \epsilon_{\mathbf{k}}} = -\sum_{l'}\int \frac{d^2\mathbf{k}'}{(2\pi)^2}\left[\omega_{k',l';k,l}f_l(k) - \omega_{k,l;k',l'}f_{l'}(k')\right], \tag{3.3}$$

where $\mathbf{v}_{0l} = \frac{1}{\hbar}\frac{\partial \epsilon_l}{\partial \mathbf{k}}$ is the group velocity of the particle with momentum k. In the above equation we have used the equation of motion $\hbar\dot{\mathbf{k}} = e\mathbf{E}$. It is noteworthy in the semiclassical picture, we usually treat the particle as wave packet which has a narrow momentum distribution centered at k_c. In this way, one needs to replace the momentum k with k_c in above equation, which is then available to describe the dynamics of wave packets. The electric current reads

$$\mathbf{J} = e\sum_{l}\int \frac{d^2\mathbf{k}}{(2\pi)^2}f_l(\mathbf{k})\mathbf{v}_l, \tag{3.4}$$

with which one can derive the conductivities.

It can be seen in the SBE the disorder information comes from the scattering term in the right hand side. To obtain the correct physics based on SBE, all cautious should be paid to this term so that it describes the correct scattering process (in the semiclassical picture and up to linear order of external electric field). Note the AHE which is an effect due to coherent interband mixing. To capture the extrinsic contribution, one must explicitly include into the right hand side of the SBE the coherent interband mixing effect induced by the disorder scattering.

3.2 Theory of metallic AHE

3.2.1 A general picture of the metallic regime

Before we turn to the calculation of the AHC with different mechanisms, we present here a general picture for the AHE in the metallic regime. From Eq. (3.4) we know the current can be obtained through the following procedures: (a) to write down the correct form of the velocity by considering external electric field and disorder scattering; (b) to solve the nonequilibrium corrections to the distribution function. For both of them we keep only the terms up to the linear order of the electric field in the linear response theory. However, as for the disorder scattering, in principle one can consider up to any order correction. For the AHE, we shall see the distribution function and the semiclassical velocity in the SBE can be written down respectively in the following forms [29, 31]

$$\mathbf{v}_l = \frac{1}{\hbar}\frac{\partial \epsilon_l}{\partial \mathbf{k}} + e\mathcal{B}_l(\mathbf{k}) \times \mathbf{E} + \delta \mathbf{v}_l, \tag{3.5}$$

$$f_l(\mathbf{k}) = f_l^{(0)}(\mathbf{k}) + g_l(\mathbf{k}) + g_l^{adist}(\mathbf{k}), \tag{3.6}$$

where the second term in the right hand side of $\mathbf{v}_l$ is the anomalous velocity due to Berry curvature $\mathcal{B}_l$ and electric field, and the third term is the correction due to disorder scattering and will be specified later. Similarly, for the nonequilibrium distribution function the term g_l is the correction due to electric field in the presence of the normal disorder scattering. The contribution g_l^{adist} results from the fact that the particle acquires a position displacement upon disorder scattering [29], and represents an anomalous correction to the distribution function. We shall see the above decomposition is generally true for the linear response regime.

Substituting the formulas (3.5) and (3.6) to (3.4) and keeping up to linear order of electric field we can rewrite the Hall current in the following form

$$\begin{aligned}\mathbf{J}^H &= e\sum_l \int \frac{d^2\mathbf{k}}{(2\pi)^2}\big[f_l^{(0)}(\mathbf{k})e\mathcal{B}_l(\mathbf{k})\times\mathbf{E} + f_l^{(0)}(\mathbf{k})\delta\mathbf{v}_l + g_l(\mathbf{k})\frac{1}{\hbar}\frac{\partial\epsilon_l}{\partial\mathbf{k}} + g_l(\mathbf{k})\delta\mathbf{v}_l + \\ &\quad + g_l^{adist}(\mathbf{k})\frac{1}{\hbar}\frac{\partial\epsilon_l}{\partial\mathbf{k}} + g_l^{adist}(\mathbf{k})e\mathcal{B}_l(\mathbf{k})\times\mathbf{E} + g_l^{adist}(\mathbf{k})\delta\mathbf{v}_l\big], \qquad (3.7)\end{aligned}$$

where the fact that $g_l(\mathbf{k})$ is at least proportional to electric field E has been considered. The above formula can be further simplified due to the following arguments. First, for the correction to velocity we must have

$$\int \frac{d^2\mathbf{k}}{(2\pi)^2} f_l^{(0)}(\mathbf{k})\delta\mathbf{v}_l(\mathbf{k}) = 0, \qquad (3.8)$$

since the disorder scattering cannot lead to charge current without electric field. Thus the second term in the right hand side of the Eq. (3.7) is zero. It is noteworthy this result gives the property $\mathbf{v}_l(-\mathbf{k}) = -\mathbf{v}_l(\mathbf{k})$ in the case $f_l^{(0)}(-\mathbf{k}) = f_l^{(0)}(\mathbf{k})$. Second, although g_l^{adist} is a consequence of the disorder scattering induced displacement, a nonzero g_l^{adist} requires the presence of the external electric field. This indicates the function g_l^{adist} is also at least linear in the electric field $\mathbf{E}$. Moreover, the Hall current $\mathbf{J}^H$ must be an odd function of the electric field, which determines that the nonzero contribution from the next to the last term in Eq. (3.7) should be at least in cubic form of the electric field $\mathbf{E}$. Therefore in the linear response regime this term is also neglected. According to these analysis, we can finally simplify the Hall current to be

$$\begin{aligned}\mathbf{J}^H &= e\sum_l \int \frac{d^2\mathbf{k}}{(2\pi)^2}\big[f_l^{(0)}(\mathbf{k})e\mathcal{B}_l(\mathbf{k})\times\mathbf{E} + g_l(\mathbf{k})\frac{1}{\hbar}\frac{\partial\epsilon_l}{\partial\mathbf{k}} + g_l(\mathbf{k})\delta\mathbf{v}_l + \\ &\quad + g_l^{adist}(\mathbf{k})\frac{1}{\hbar}\frac{\partial\epsilon_l}{\partial\mathbf{k}} + g_l^{adist}(\mathbf{k})\delta\mathbf{v}_l\big]. \qquad (3.9)\end{aligned}$$

It is clear the first term gives the intrinsic contribution. This formula is generally true for the AHE in the linear response regime.

It is interesting that the above formula implies important symmetric properties of the nonequilibrium distribution functions $g_l(\mathbf{k})$ and $g_l^{adist}(\mathbf{k})$. In the Eq. (3.9), if we do the TR or spatial transformation (in $x-y$ plane), the Hall current $\mathbf{J}^H$ in the left hand side and the group velocity $\frac{1}{\hbar}\frac{\partial \epsilon_l}{\partial \mathbf{k}}$ in the right hand side change in the same way. Therefore a nonzero contribution of the corresponding terms to Hall current requires $g_l(\mathbf{k})$ and $g_l^{adist}(\mathbf{k})$ must be TR *invariant* and spatial inversion *even*. The Berry curvature is *odd* under the spatial inversion along x axis or y axis, but *even* under the inversion in both directions. Note $g_l(\mathbf{k})$ and $g_l^{adist}(\mathbf{k})$ are functions of the electric field $\mathbf{E}$, Berry curvature $\mathcal{B}$ and the momentum $\mathbf{k}$ (or group velocity $\frac{1}{\hbar}\frac{\partial \epsilon_l}{\partial \mathbf{k}}$). Up to the order linear in electric field and Berry curvature, the terms satisfying both TR symmetry and spatial inversion symmetry can only be in the following three possible forms: $\mathcal{B}\cdot(\mathbf{E}\times\mathbf{k})$, $\mathbf{E}\cdot\mathbf{k}$ and $\hat{e}_z\cdot(\mathbf{E}\times\mathbf{k})$. Since $g_l(\mathbf{k})$ results from the usual disorder scattering, it is independent of the Berry curvature. On the other hand, the term $g_l^{adist}(\mathbf{k})$ is the correction due to the disorder scattering induced displacement, which is the consequence of a non-zero Berry curvature. Bearing these properties in mind we can predict that

$$g_l^{adist}(\mathbf{k}) \sim \mathcal{B}\cdot(\mathbf{E}\times\mathbf{k}), \tag{3.10}$$

and $g_l(\mathbf{k}) = g_l^{\parallel}(\mathbf{k}) + g_l^{\perp}(\mathbf{k})$ with

$$g_l^{\parallel}(\mathbf{k}) \sim \mathbf{E}\cdot\mathbf{k}, \quad g_l^{\perp}(\mathbf{k}) \sim \hat{e}_z\cdot(\mathbf{E}\times\mathbf{k}). \tag{3.11}$$

In above formulas $g_l(\mathbf{k})$ and $g_l^{adist}(\mathbf{k})$ are linear in momentum. In principle they can be general odd functions of the momentum with the TR and spatial inversion symmetries preserved. It is straightforward to check that the product of $g_l^{\parallel}(\mathbf{k})$ and the group velocity $\frac{1}{\hbar}\frac{\partial \epsilon_l}{\partial \mathbf{k}}$ yields zero contribution to the Hall current and thus for the second term in Eq. (3.9) only $g_l^{\perp}(\mathbf{k})$ contributes to the Hall effect.

It is remarkable that so far we have not performed any specific calculations, but have already determined the basic properties of the nonequilibrium distribution functions. To obtain the Hall current, we only need to determine the proportional coefficients in formulas. (3.10) and (3.11) by solving the SBE. it is noteworthy the formula (3.9) may be further simplified for some special situation. For example, assume the electric field in the y direction $\mathbf{E} = E_y\hat{e}_y$ and in this case we only need to examine the current J_x^H. Then to the linear order of E_y we must have $g_l^{adist} \propto \alpha(\mathbf{k})E_y$ with $\alpha(-k_y, k_x) = \alpha(k_y, k_x)$. If the velocity correction in the x direction is proportional to k_y, the integral of the last term in Eq. (3.9) over the momentum space also yields zero. The next step is to determine g_l, g_l^{adist}, and $\delta\mathbf{v}_l$ in the presence of disorder scattering.

3.2.2 Bloch state wave packet

For a lattice system with zero Berry's connection, it is easy to know the wave packet in band n centered at position $\mathbf{r}_c$ and with the average momentum $\mathbf{k}_c$ can be constructed in the following

$$\Psi_{n,\mathbf{k}_c,\mathbf{r}_c}(\mathbf{r},t) = \frac{1}{\sqrt{V}}\sum_{\mathbf{k}} |w_{\mathbf{k}_c,\mathbf{r}_c}(\mathbf{k})e^{i\mathbf{k}\cdot(\mathbf{r}-\mathbf{r}_c)}u_{n\mathbf{k}}(\mathbf{r}), \tag{3.12}$$

where $|w_{\mathbf{k}_c,\mathbf{r}_c}(\mathbf{k})|$ is a real function describing the $\mathbf{k}$-distribution of wave packet. When a momentum-space Berry connection $\mathcal{A}_n(\mathbf{k})$ (gauge field in $\mathbf{k}$ space) is included into the Hamiltonian, the position operator transforms to be $\mathbf{r} \to i\partial_{\mathbf{k}} + \mathcal{A}_n(\mathbf{k})$, with $\mathcal{A}_n(\mathbf{k}) = i\hbar\langle u_{n\mathbf{k}}|\partial_{\mathbf{k}}|u_{n\mathbf{k}}\rangle$. Then the new wave function whose dynamics governed by the new Hamiltonian is simply related to the old one by a U(1) phase transformation in the momentum space:

$$\Psi_{n,\mathbf{k}_c,\mathbf{r}_c}(\mathbf{r},t) \to \Psi_{n,\mathbf{k}_c,\mathbf{r}_c}(\mathbf{r},t)e^{\frac{i}{\hbar}\int_{\mathbf{k}_c}^{\mathbf{k}}\mathcal{A}_n(\mathbf{k})\cdot d\mathbf{k}}. \tag{3.13}$$

Thus the wave packet with a momentum gauge potential can finally be defined by

$$\Psi_{n,\mathbf{k}_c,\mathbf{r}_c}(\mathbf{r},t)=\frac{1}{\sqrt{V}}\sum_{\mathbf{k}}|w_{\mathbf{k}_c,\mathbf{r}_c}(\mathbf{k})e^{\frac{i}{\hbar}\int_{\mathbf{k}_c}^{\mathbf{k}}\mathcal{A}_n(\mathbf{k})\cdot d\mathbf{k}+i\mathbf{k}\cdot(\mathbf{r}-\mathbf{r}_c)}u_{n\mathbf{k}}(\mathbf{r}). \tag{3.14}$$

In the literature the integral form of the phase factor is always written in the form $i\int_{\mathbf{k}_c}^{\mathbf{k}}\mathcal{A}_n(\mathbf{k})\cdot d\mathbf{k}\simeq i\mathcal{A}_n(\mathbf{k})\cdot(\mathbf{k}-\mathbf{k}_c)$, which is not exact but can give the same result for SBE [11,69]. Based on the above definition of wave packet, we can introduce the the Lagrangian to describe the dynamics of the wave packet [69]

$$\begin{aligned}\mathcal{L} &= \langle\Psi_{n,\mathbf{k}_c,\mathbf{r}_c}|i\hbar\partial_t-H_0-eV(\mathbf{r})|(\Psi_{n,\mathbf{k}_c,\mathbf{r}_c}\rangle\\ &= \hbar\mathbf{k}_c\cdot\dot{\mathbf{r}}_c+\hbar\dot{\mathbf{k}}_c\cdot\mathcal{A}_n(\mathbf{k}_c)-\epsilon_n(\mathbf{k}_c)+eV(\mathbf{r}_c),\end{aligned} \tag{3.15}$$

where $V(\mathbf{r}_c)$ represents the electric potential. The dynamics of the wave packet then reads

$$\hbar\dot{\mathbf{k}}_c = e\mathbf{E}(\mathbf{r}_c), \tag{3.16}$$

$$\dot{\mathbf{r}}_c = \mathbf{v}_{0n}-e\mathbf{E}\times\mathcal{B}_n(\mathbf{k}_c), \tag{3.17}$$

where $\mathcal{B}_n(\mathbf{k}_c)=\nabla_{\mathbf{k}_c}\times\mathcal{A}_n(\mathbf{k}_c)$ is the Berry curvature for band n. The second term in the equation of $\dot{\mathbf{r}}_c$ gives the anomalous velocity. When considering the disorder scattering, this term needs to be further modified.

3.2.3 Disorder scattering and modified Boltzmann equation

Now we consider the scattering transition rate $\omega_{k',l';k,l}$ in the Boltzmann equation. The exact form of the transition rate can be obtained by T-matrix element of the disorder potential V (the total Hamiltonian reads $H=H_0+V$)

$$\omega_{q'q}=2\pi|T_{q'q}|^2\delta(\epsilon_{q'}-\epsilon_q), \tag{3.18}$$

where the T matrix is defined by $T_{q'q} = \langle q'|V|\psi_q\rangle$, with $|\psi_q\rangle$ the exact eigenstate of the total Hamiltonian. Here we have simplified the notation of the band and momentum indices by q. The exact eigenstate $|\psi_q\rangle$ can be derived by a perturbation expansion in powers of disorder potential $V_{q'q} = \langle q'|V|q\rangle$ and thus

$$\begin{aligned} |\psi_q\rangle &= |q\rangle + \sum_{q''} \frac{V_{q'q}}{\epsilon_q - \epsilon_{q''} + i0^+}|q''\rangle + \sum_{q_1 q_2} \frac{V_{q_1 q} V_{q_2 q_1}}{(\epsilon_q - \epsilon_{q_1} + i0^+)(\epsilon_q - \epsilon_{q_2} + i0^+)}|q_2\rangle + \\ &\quad + \cdots . \end{aligned} \tag{3.19}$$

The transition rate can be accordingly expanded in powers of disorder potential

$$\omega_{q'q} = \omega^{(2)}_{q',q} + \omega^{(3)}_{q',q} + \omega^{(4)}_{q',q} + \cdots , \tag{3.20}$$

with

$$\begin{aligned} \omega^{(2)}_{q',q} &= 2\pi \langle |V_{q'q}|^2 \rangle_{dis} \delta(\epsilon_{q'} - \epsilon_q), \\ \omega^{(3)}_{q',q} &= 2\pi \left(\sum_{q''} \frac{\langle V_{q'q} V_{qq''} V_{q''q'} \rangle_{dis}}{\epsilon_q - \epsilon_{q''} + i0^+} + c.c. \right) \delta(\epsilon_{q'} - \epsilon_q) \\ \omega^{(4)}_{q',q} &= 2\pi \left| \sum_{q''} \frac{\langle V_{q'q''} V_{q''q} \rangle_{dis}}{\epsilon_q - \epsilon_{q''} + i0^+} \right|^2 \delta(\epsilon_{q'} - \epsilon_q) + \\ &\quad + 2\pi \left(\sum_{q_1 q_2} \frac{\langle V_{q'q} V_{qq_1} V_{q_1 q_2} V_{q_2 q'} \rangle_{dis}}{(\epsilon_q - \epsilon_{q_1} + i0^+)(\epsilon_q - \epsilon_{q_2} + i0^+)} + c.c. \right) \delta(\epsilon_{q'} - \epsilon_q). \\ &\cdots \end{aligned} \tag{3.21}$$

It is easy to see $\omega^{(2)}_{q',q}$ is symmetric upon the exchange $q \leftrightarrow q'$. For the higher orders, generally there is no symmetric property. Then we can define the symmetric and antisymmetric terms through $\omega^{s/a}_{q'q} = (\omega_{q'q} \pm \omega_{qq'})/2$, with which we have $\omega_{q'q} = \omega^s_{q'q} + \omega^a_{q'q}$. It is straightforward to check

$$\omega^{(3a)}_{q',q} = (2\pi)^2 \sum_{q''} \delta(\epsilon_q - \epsilon_{q''}) \mathrm{Im} \langle V_{q'q} V_{qq''} V_{q''q'} \rangle_{dis} \delta(\epsilon_{q'} - \epsilon_q). \tag{3.22}$$

Similarly, $\omega^{(4a)}_{q',q}$ can be resulted from the imaginary part of the second term in the right hand side of the equation for $\omega^{(4)}_{q',q}$. The antisymmetric term has clear physics. For $\omega^{(3a)}_{q',q}$, for example, the term $\mathrm{Im}(V_{q'q}V_{qq''}V_{q''q'})$ is actually the Berry phase gained after the closed state evolution $q' \to q \to q'' \to q'$ induced by disorder scattering. This result actually indicates the skew scattering is also related to geometric phase. However, the magnitude of this phase depends on both the SOC and the disorder potential.

For SO coupled system, an important phenomenon is that the disorder scattering from state q to q' will be accompanied with a shift in the center of mass coordinate of the wave packet. This can be seen by the following formula

$$\begin{aligned}\frac{d\mathbf{r}_c}{dt} &= \frac{d}{dt}\langle\Psi_{n,\mathbf{k}_c,\mathbf{r}_c}|\mathbf{r}|\Psi_{n,\mathbf{k}_c,\mathbf{r}_c}\rangle \\ &= \frac{d\epsilon_{n,\mathbf{k}_c}}{d\mathbf{k}_c} + \frac{d}{dt}\Big\{\int_{cell}\sum_{\mathbf{k}} w^*_{\mathbf{k}_c,\mathbf{r}_c}(\mathbf{k})u_{n\mathbf{k}}(\mathbf{r})i\frac{\partial}{\partial\mathbf{k}}\big[w_{\mathbf{k}_c,\mathbf{r}_c}(\mathbf{k})u_{n\mathbf{k}}(\mathbf{r})\big]\Big\}, \quad (3.23)\end{aligned}$$

where $w_{\mathbf{k}_c,\mathbf{r}_c}(\mathbf{k}) = |w_{\mathbf{k}_c,\mathbf{r}_c}(\mathbf{k})|e^{\frac{i}{\hbar}\int^{\mathbf{k}}_{\mathbf{k}_c}\mathcal{A}_n(\mathbf{k})\cdot d\mathbf{k}}$. From above equation we get the side jump upon scattering $\delta\mathbf{r}_{q',q} = \mathbf{A}_{l'}(\mathbf{k}') - \mathbf{A}_l(\mathbf{k})$ (note the index $q = (l,\mathbf{k})$). This formula is not gauge invariant. The gauge invariant expression of the side jump upon disorder scattering is given by Sinitsyn et al [26]

$$\delta\mathbf{r}_{q',q} = \mathbf{A}_{l'}(\mathbf{k}') - \mathbf{A}_l(\mathbf{k}) - (\partial_{\mathbf{k}'} + \partial_{\mathbf{k}})\arg[\langle u_{l'\mathbf{k}'}|u_{l\mathbf{k}}\rangle]. \quad (3.24)$$

It is trivial to know that $\delta\mathbf{r}_{q',q} = -\delta\mathbf{r}_{q,q'}$. It is important that $\delta\mathbf{r}_{q',q}$ is totally determined by the initial and final states during the scattering, independent of the details of the disorder potential and the scattering process. This indicates the spatial shift of center of mass coordinate upon scattering is completely a consequence of SO coupling. The impurity scattering only results in the transition between quantum states.

We consider only the elastic scattering, which requires the initial and final states are the same in the energy. However, the position shift leads to the electric potential energy change $\Delta U_{q,q'} = e\mathbf{E}\cdot\delta\mathbf{r}_{q,q'}$. The energy conservation then requires the kinetic energies of the final and initial states satisfy $\epsilon_q - \epsilon_{q'} = \Delta U_{q,q'}$. We modify the right hand side of the Boltzmann equation (3.3) into

$$\begin{aligned}\omega_{q',q} f_l(k) - \omega_{q,q'} f_{l'}(k') &\rightarrow \omega_{q',q} f(\epsilon_q) - \omega_{q,q'} f(\epsilon_{q'} + e\mathbf{E}\cdot\delta\mathbf{r}_{q,q'}) \\ &= \omega_{q',q} f(\epsilon_q) - \omega_{q,q'} f(\epsilon_{q'}) - \omega_{q,q'}\frac{\partial f_0}{\partial \epsilon_{q'}} e\mathbf{E}\cdot\delta\mathbf{r}_{q,q'}. \quad (3.25)\end{aligned}$$

The Boltzmann equation can now be written as

$$\frac{\partial f_l}{\partial t} + e\mathbf{E}\cdot\mathbf{v}_{0l}\frac{\partial f_l}{\partial \epsilon_{\mathbf{k}}} = -\sum_{q'}\Big[\omega_{q',q} f(\epsilon_q) - \omega_{q,q'} f(\epsilon_{q'}) - \omega_{q,q'}\frac{\partial f_0}{\partial \epsilon_{q'}} e\mathbf{E}\cdot\delta\mathbf{r}_{q,q'}\Big]. \quad (3.26)$$

On the other hand, the position displacement $\delta\mathbf{r}_{q',q}$ results in a correction to the velocity which is given by the product of $\delta\mathbf{r}_{q',q}$ and the transition rate

$$\delta\mathbf{v}_q = -\sum_{q'}\omega_{q',q}\delta\mathbf{r}_{q',q}. \quad (3.27)$$

3.2.4 Intrinsic, side jump, and skew scattering

Now we study the three types of contribution to AHE in the metallic regime. To simplify the right hand side of the Boltzmann equation (3.26) we consider the following result

$$\begin{aligned}\sum_{q'}\omega_{q',q}f(\epsilon_q) &= \sum_{q'}\omega^{(s)}_{q',q}f(\epsilon_q)+\sum_{q'}\omega^{(a)}_{q',q}f(\epsilon_q)\\ &= \sum_{q'}\omega^{(s)}_{q',q}f(\epsilon_q)\\ &= \sum_{q'}\omega_{q,q'}f(\epsilon_q),\end{aligned} \tag{3.28}$$

where in the second line we have used the identity $\sum_{q'}\omega^{(a)}_{q',q}f(\epsilon_q)=0$. The physical meaning of this identity is that the summation of net transition rate from a state q to all other states (given by $\sum_{q'}\omega_{q',q}-\sum_{q'}\omega_{q,q'}=2\sum_{q'}\omega^{(a)}_{q',q}$) should always be zero. The Boltzmann equation then takes the form

$$\frac{\partial f_l}{\partial t}+e\mathbf{E}\cdot\mathbf{v}_{0l}\frac{\partial f_l}{\partial\epsilon_{\mathbf{k}}} = -\sum_{q'}\big[\omega_{q,q'}[f(\epsilon_q)-f(\epsilon_{q'})]-\omega_{q,q'}\frac{\partial f_0}{\partial\epsilon_{q'}}e\mathbf{E}\cdot\delta\mathbf{r}_{q,q'}\big]. \tag{3.29}$$

To solve the Boltzmann equation, we shall split the distribution function into three terms $f_l(\mathbf{k})=f_{0l}(\mathbf{k})+g_l(\mathbf{k})+g_l^{adist}(\mathbf{k})$ as having been mentioned in subsection 3.2.1. We consider the steady solution that $\partial_t f_l=0$. Then the nonequilibrium terms satisfy the following equations

$$e\mathbf{E}\cdot\mathbf{v}_{0l}\frac{\partial f_{0l}}{\partial\epsilon_{\mathbf{k}}} = -\sum_{q'}\big[\omega_{q',q}(g_q-g_{q'})\big], \tag{3.30}$$

and

$$\sum_{q'}\omega_{q',q}\big[(g_q^{adist}-g_{q'}^{adist})-\frac{\partial f_0}{\partial\epsilon_{q'}}e\mathbf{E}\cdot\delta\mathbf{r}_{q,q'}\big]=0. \tag{3.31}$$

It can be verified that in the linear response regime the Eqs. (3.29) to (3.31) are self-consistent. Eq. (3.30) can be solved by rewriting it into a matrix form [70]. For this we denote by $\vartheta(\mathbf{k})$ the angle between the velocity $\mathbf{v}_{0l}(\mathbf{k})$ and the electric field, and define the scattering operator

$$S[g_l] = \sum_{l'} \int \frac{d^2\mathbf{k}}{(2\pi)^2} \omega_{q',q} \big[g_{l'}(\mathbf{k}) - g_{l'}(\mathbf{k}') \big]. \tag{3.32}$$

For the functions $f_1 = |\mathbf{v}_{0l}(\mathbf{k})| \cos\vartheta_l(\mathbf{k})$ and $f_2 = |\mathbf{v}_{0l}(\mathbf{k})| \sin\vartheta_l(\mathbf{k})$, we obtain straightforwardly that

$$S\left[\begin{pmatrix} f_1 \\ f_2 \end{pmatrix} \right] = \begin{pmatrix} \frac{1}{\tau_l^{\parallel}(\mathbf{k})} & -\frac{1}{\tau_l^{\perp}(\mathbf{k})} \\ \frac{1}{\tau_l^{\perp}(\mathbf{k})} & \frac{1}{\tau_l^{\parallel}(\mathbf{k})} \end{pmatrix} \begin{pmatrix} f_1 \\ f_2 \end{pmatrix}, \tag{3.33}$$

where longitudinal and transverse life times are defined by

$$\frac{1}{\tau_l^{\parallel}(\mathbf{k})} = \sum_{l'} \int \frac{d^2\mathbf{k}}{(2\pi)^2} \omega_{q',q} \left(1 - \frac{|\mathbf{v}_{0l'}(\mathbf{k}')|}{|\mathbf{v}_{0l}(\mathbf{k})|} \cos\big[\vartheta_l(\mathbf{k}) - \vartheta_{l'}(\mathbf{k}') \big] \right), \tag{3.34}$$

$$\frac{1}{\tau_l^{\perp}(\mathbf{k})} = \sum_{l'} \int \frac{d^2\mathbf{k}}{(2\pi)^2} \omega_{q',q} \frac{|\mathbf{v}_{0l'}(\mathbf{k}')|}{|\mathbf{v}_{0l}(\mathbf{k})|} \sin\big[\vartheta_l(\mathbf{k}) - \vartheta_{l'}(\mathbf{k}') \big]. \tag{3.35}$$

According to the analysis of the Eq. (3.11), we may make the ansatz for the solution to $g_l(\mathbf{k})$ as

$$\begin{aligned} g_l(\mathbf{k}) &= -e \frac{\partial f_{0l}}{\partial \epsilon_{\mathbf{k}}} \mathbf{E} \cdot \big[A_l \mathbf{v}_{0l} + B_l \mathbf{v}_{0l} \times \hat{e}_z \big] \\ &= -eEv_{0l} \frac{\partial f_{0l}}{\partial \epsilon_{\mathbf{k}}} \big[A_l \cos\vartheta_l(\mathbf{k}) + B_l \sin\vartheta_l(\mathbf{k}) \big]. \end{aligned} \tag{3.36}$$

The two parameters $A_l(\mathbf{k})$ and $B_l(\mathbf{k})$ obtained through the inversion of the scattering operator in Eq. (3.32)

$$A_l(\mathbf{k}) = \frac{\tau_l^{\parallel}(\mathbf{k})}{1+(\tau_l^{\parallel}/\tau_l^{\perp})^2}, \quad B_l(\mathbf{k}) = \frac{\tau_l^{\perp}(\mathbf{k})}{1+(\tau_l^{\perp}/\tau_l^{\parallel})^2}. \tag{3.37}$$

For the anomalous Hall system in the metallic regime, usually the transverse life is much larger than the longitudinal one, i.e. $\tau_l^{\perp} \gg \tau_l^{\parallel}$. We then have $A_l \approx \tau_l^{\parallel}$ and $B_l \approx (\tau_l^{\parallel})^2/\tau_l^{\perp}$. The formulas (3.36) and (3.37) consist of the general solution for the Eq. (3.30).

The term in the solution proportional to $B_l \approx (\tau_l^{\parallel})^2/\tau_l^{\perp}$ is nonzero only for asymmetric disorder scattering processes. This can be seen from the asymmetric property of the function $\sin[\vartheta(\mathbf{k})-\vartheta(\mathbf{k}')]$ in the formula (3.35). Therefore the lowest order contribution to skew scatterings comes from $\omega_{q',q}^{(3a)}$. The solution of $g_l^{adist}(\mathbf{k})$ to Eq. (3.31) can be solved in a similar ansatz, but the result depends on the form of $\delta\mathbf{r}_{q,q'}$ which is determined by specific models.

To see clearly the properties of the contributions from disorder scattering in different orders, we expand Eq. (3.30) in powers of disorder potential. Accordingly, we denote by $g_l(\mathbf{k}) = g_l^{(2s)} + g_l^{(3)} + g_l^{(4)} + \cdots$, where $g_l^{(3)}$ and $g_l^{(4)}$ correspond to the contribution from the 3rd and 4th order disorder scatterings, respectively. The lowest order solution $g_l^{(2s)}$ is given by

$$g_l^{(2s)}(\mathbf{k}) = -eEv_{0l}\frac{\partial f_{0l}}{\partial \epsilon_{\mathbf{k}}}\tau_l^{(2)\parallel}(\mathbf{k})\cos\vartheta_l(\mathbf{k}). \tag{3.38}$$

with the longitudinal life time given by

$$\frac{1}{\tau_l^{(2)\parallel}(\mathbf{k})} = \sum_{l'}\int\frac{d^2\mathbf{k}}{(2\pi)^2}\omega_{q',q}^{(2)}\left(1-\frac{|\mathbf{v}_{0l'}(\mathbf{k}')|}{|\mathbf{v}_{0l}(\mathbf{k})|}\cos\big[\vartheta_l(\mathbf{k})-\vartheta_{l'}(\mathbf{k}')\big]\right). \tag{3.39}$$

The solutions to $g_l^{(3)}$ and $g_l^{(4)}$ are governed by the following equations

$$\sum_{q'}\left[\omega_{q',q}^{(2s)}(g_q^{(3)}-g_{q'}^{(3)})\right]+\sum_{q'}\left[\omega_{q',q}^{(3s)}(g_q^{(2s)}-g_{q'}^{(2s)})+\omega_{q',q}^{(3a)}(g_q^{(2s)}+g_{q'}^{(2s)})\right]=0, \quad (3.40)$$

$$\sum_{q'}\left[\omega_{q',q}^{(2s)}(g_q^{(4)}-g_{q'}^{(4)})\right]+\sum_{q'}\left[\omega_{q',q}^{(4s)}(g_q^{(2s)}-g_{q'}^{(2s)})+\omega_{q',q}^{(4a)}(g_q^{(2s)}+g_{q'}^{(2s)})\right]=0, \quad (3.41)$$

The solution of $g_l^{(2s)}(\mathbf{k})$ has been obtained from Eqs. (3.38), and the higher contributions can be solved in terms of $g_l^{(2s)}(\mathbf{k})$. It is clear from the above two equations that we can split the solutions into $g_l^{(3)}=g_l^{(3a)}+g_l^{(3s)}$ and $g_l^{(4)}=g_l^{(4a)}+g_l^{(4s)}$, where $g_l^{(a/s,n)}$ $(n=3,4)$ corresponds to the contributions from asymmetric and symmetric terms in the disorder scattering.

Now we can present the explicit formula for different contributions to the AHE. According to the result in Eq. (3.9), the anomalous Hall current reads

$$\begin{aligned}\mathbf{J}^H &= e\sum_l\int\frac{d^2\mathbf{k}}{(2\pi)^2}\Big\{f_{0l}e\mathcal{B}_l(\mathbf{k})\times\mathbf{E}+(g_l^{(2s)}+g_l^{(3)}+g_l^{(4)})(\frac{1}{\hbar}\frac{\partial\epsilon_l}{\partial\mathbf{k}}+\delta\mathbf{v}_l)+\\ &\quad +g_l^{adist}(\mathbf{k})\frac{1}{\hbar}\frac{\partial\epsilon_l}{\partial\mathbf{k}}+g_l^{adist}(\mathbf{k})\delta\mathbf{v}_l\Big\}\\ &= e\sum_l\int\frac{d^2\mathbf{k}}{(2\pi)^2}\Big\{f_{0l}e\mathcal{B}_l(\mathbf{k})\times\mathbf{E}+g_l^{(2s)}\delta\mathbf{v}_l+(g_l^{(3a)}+g_l^{(4a)})\frac{1}{\hbar}\frac{\partial\epsilon_l}{\partial\mathbf{k}}+\\ &\quad +g_l^{(3s)}\delta\mathbf{v}_l+g_l^{adist}(\mathbf{k})\frac{1}{\hbar}\frac{\partial\epsilon_l}{\partial\mathbf{k}}+g_l^{adist}(\mathbf{k})\delta\mathbf{v}_l\Big\}. \quad (3.42)\end{aligned}$$

Let the electric field in the y direction. The AHC given from above formula can be written as

$$\sigma_{xy}^{AH}=\sigma_{xy}^{int}+\sigma_{xy}^{sj1}+\sigma_{xy}^{sj2}+\sigma_{xy}^{sk1}+\sigma_{xy}^{sk2}+\sigma_{xy}^{adist}. \quad (3.43)$$

The first term gives the intrinsic contribution which is due to the anomalous velocity and equilibrium distribution function

$$\sigma_{xy}^{int} = e^2 \sum_l \int \frac{d^2\mathbf{k}}{(2\pi)^2} f_{0l}(\mathbf{k}) \mathcal{B}_{l,z}(\mathbf{k}). \tag{3.44}$$

The second and third terms are the side jump contributions given by

$$\sigma_{xy}^{sj1} = e \sum_l \int \frac{d^2\mathbf{k}}{(2\pi)^2} [g_l^{(2s)}(\mathbf{k})/E_y] \sum_{q'} \omega_{q'q} \delta \mathbf{r}_{q'q}. \tag{3.45}$$

$$\sigma_{xy}^{sj2} = e \sum_l \int \frac{d^2\mathbf{k}}{(2\pi)^2} [g_l^{(3s)}(\mathbf{k})/E_y] \sum_{q'} \omega_{q'q} \delta \mathbf{r}_{q'q}. \tag{3.46}$$

We separate the side jump contributions into two, since they come from different orders of disorder scattering. The next two terms are called skew scattering contributions from the 3rd and 4th order impurity scatterings and are given by

$$\sigma_{xy}^{sk1} = \frac{e}{\hbar} \sum_l \int \frac{d^2\mathbf{k}}{(2\pi)^2} [g_l^{(3)}(\mathbf{k})/E_y] \frac{\partial \epsilon_l}{\partial k_x}, \tag{3.47}$$

$$\sigma_{xy}^{sk2} = \frac{e}{\hbar} \sum_l \int \frac{d^2\mathbf{k}}{(2\pi)^2} [g_l^{(4)}(\mathbf{k})/E_y] \frac{\partial \epsilon_l}{\partial k_x}, \tag{3.48}$$

and the last term reads

$$\sigma_{xy}^{adist} = \frac{e}{\hbar} \sum_l \int \frac{d^2\mathbf{k}}{(2\pi)^2} [g_l^{adist}(\mathbf{k})/E_y] \frac{\partial \epsilon_l}{\partial k_x}. \tag{3.49}$$

By a simple analysis, one can find the dependence of the correction to distribution function on disorder concentration n_i that $g_l^{(2s)}, g_l^{(3s)}, g_l^{(3a)} \propto 1/n_i$ and $g_l^{adist}, g_l^{(4)} \propto n_i^0$.

As a result we have the following general properties (note the longitudinal conductivity $\sigma_{xx} \propto \tau_l^{(2)\|}(\mathbf{k}) \propto n_i^{-1}$ in the lowest order)

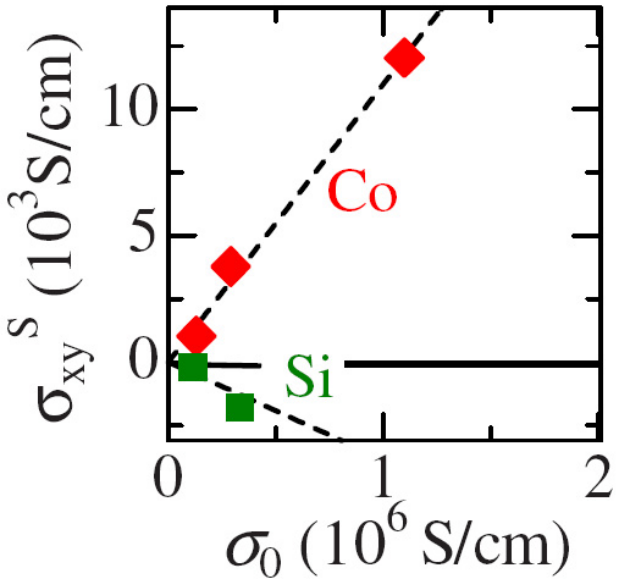

Fig. 3.1. Measurement of the skew-scattering-induced AHC σ_{xy} versus the lowest temperature conductivity σ_0 (the inverse of residual resistivity) for the Co-doped and Si-doped ion samples [24].

$$
\begin{aligned}
\sigma_{xy}^{int} &\propto n_i^0 \propto \sigma_{xx}^0, \\
\sigma_{xy}^{sj1} &\propto n_i^0 \propto \sigma_{xx}^0, \\
\sigma_{xy}^{sj2} &\propto n_i^0 \propto \sigma_{xx}^0, \\
\sigma_{xy}^{adist} &\propto n_i^0 \propto \sigma_{xx}^0, \\
\sigma_{xy}^{sk2} &\propto n_i^0 \propto \sigma_{xx}^0, \\
\sigma_{xy}^{sk1} &\propto n_i^{-1} \propto \sigma_{xx}.
\end{aligned}
$$

From these results we expect the skew scattering from 3rd order asymmetric disorder scattering dominates the AHE contribution in the clean limit. In the moderate metallic regime, the AHE is characterized by the scaling relation $\sigma_{xy} \propto \sigma_{xx}^0$, which

results from several different physical mechanisms. Further concrete results of the AHC requires the information of the model Hamiltonian of the specific materials. In experiment, the skew scattering regime is observed in the high conductivity condition with $\sigma_{xx} > 10^6$ $(\Omega\text{cm})^{-1}$ (see Fig. 3.1), and the scattering independent contribution is observed in the case with 10^4 $(\Omega\text{cm})^{-1} < \sigma_{xx} < 10^6$ $(\Omega\text{cm})^{-1}$ (see Fig. 3.2). It is noteworthy although the contributions characterized by σ_{xy}^{sj2} and σ_{xy}^{sk2} are independent of disorder concentration n_i, they do depend on the disorder potential strength. In experiment how to separate the intrinsic contribution from other contributions in the moderate disorder scattering is a challenging issue [2].

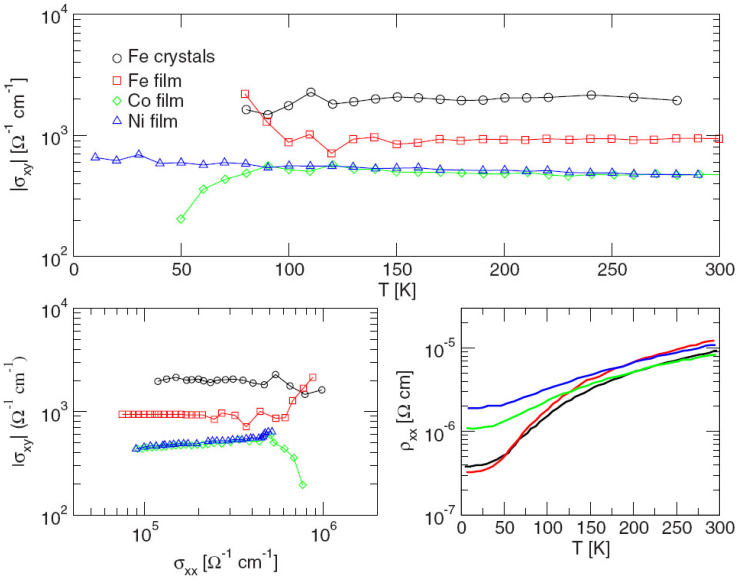

Fig. 3.2. Measurements of the σ_{xy} and ρ_{xx} versus temperature in single-crystal Fe and in thin foils of Fe, Co, and Ni. The lower left panel shows the scaling relation between σ_{xy} and σ_{xx} [2, 23].

3.3 Discussions

The results in (3.50) are obtained in the general case, independent of specific models, indicating the scaling relations $\sigma_{xy} \propto \sigma_{xx}$ and $\sigma_{xy} \propto \sigma_{xx}^0$ are universal for

AHE in the corresponding metallic regimes, independent of material details such as the charge carrier type, band structure, and types of the SO coupling. This result also tells the scaling exponent γ for the power-law relation between σ_{xy} and σ_{xx} cannot exceed unity in the metallic regime, and therefore the microscopic theories for metals cannot explain the observed scaling in the insulating regime.

4. LOCALIZED HOPPING CONDUCTION REGIME

For an ideal semiconductor material without disorder, the band structure of the system has a bulk gap and thus describes an insulator when the Fermi energy is in the band gap. Impurity donor (or acceptor) doping creates bound states below the conduction band (or above the valence band). The bound state spectra for the same type of impurities are the same when each impurity is treated as isolated, and thus each bound level for different impurities are degenerate. This degeneracy is lifted by taking into account the influence on a site from other impurity states. Due to the spatially random distribution of the impurities, the influences between different impurity sites are random and the resultant bound state energies are then randomized. This can also be understood by the result that the effective potential produced at an impurity site by the environment around it is random through the system. In this way the system becomes disordered amorphous when the Fermi energy crosses the bound states. At low temperature the electronic properties of the amorphous semiconductors are determined by the impurity states.

4.1 Localized states

A fundamental property of an impurity bound state is characterized by its ionization energy E_{ion} which is needed to move the an electron (hole) from the donor (acceptor) level to the bottom (top) of the conduction (valence) band. When the temperature $T > E_{ion}/k_B$ with k_B the Boltzmann constant, the impurities are thermally ionized and contribute electrons (holes) to the conduction (valence) band. The activated band electrons or hole will then dominate the charge transport in the system. On the other hand, at low temperature the electrons (holes) are captured by donors (acceptors), and the only possible transport mechanism is the phonon-assisted hopping of electrons (holes) between impurity sites [66, 71], which will be studied in the next section.

Here we present an introduction to the localized state on impurity sites, which can be studied with the effective mass method. The basic idea is given below. For a donor impurity site (case for acceptor site is similar), the bound levels are below the bottom of the conduction band. When the ground bound level is close to the bottom of the conduction band relative to the semiconductor band gap, the impurity is called shallow, which is the typical case for the present work. An important property of the bound state centered at a shallow impurity is that localization length ξ is much larger than the lattice constant. Therefore the in the Fourier expansion of the bound state wave function the only a narrow range of wave vectors compared to the FBZ will be dominant. According to the discussion in section 1 (see Eq. (1.11)), the typical dispersion relation is quadratic in momentum around the bottom of conduction band, which is analogy to the vacuum electron but with an effective mass usually smaller than the free electron mass m_0. The bound state can then be obtained similar to the case that a vacuum electron experiences an attractive potential. Under this picture, the bound state wave function of an impurity site can be approximately written in the form of a Bloch wave function at the bottom of the conduction band, modulated by a spatially large-scale hydrogen-like function. This hydrogen-like function is the solution to the effective Hamiltonian for the electrons at the bottom of conduction band plus the impurity potential [72, 73], described by

$$H = H_0 + U(\mathbf{r}), \tag{4.1}$$

where H_0 is the effective Hamiltonian for the band electrons in the bottom of the conduction band, and $U(\mathbf{r})$ is the impurity potential. As mentioned above, without considering the SO coupling the term H_0 can generally be simplified as a quadratic function of momentum $H_0 = \mathbf{p}^2/2m$ with m is the effective mass of the electron.

Furthermore, in the spatial scale much larger than the lattice constant, the impurity potential can be described by

$$U(\mathbf{r}) = -e^2/(\kappa r), \tag{4.2}$$

where κ is the dielectric permittivity of the lattice. The bound state wave function for the Hamiltonian (4.1) takes the form [72–74]

$$\Psi(\mathbf{r}) = u_{l,\mathbf{k}_{min}}(\mathbf{r})\Phi(\mathbf{r}), \tag{4.3}$$

where l is the conduction band index, $\mathbf{k}_{min}$ is the momentum corresponding to the bottom of the conduction band, $u_{n,\mathbf{k}_{min}}$ is the periodic part of the Bloch wave function with the momentum $\mathbf{k}_{min}$, and $\Phi(\mathbf{r})$ satisfies

$$\left(-\frac{\hbar^2}{2m}\nabla^2 - \frac{e^2}{\kappa r}\right)\Phi(\mathbf{r}) = E\Phi(\mathbf{r}). \tag{4.4}$$

The spectrum of the bound levels followed from above equation reads

$$E_n = -\frac{1}{n^2}\frac{e^2 m}{2\hbar^2\kappa^2}, \quad n = 1, 2, 3, \cdots . \tag{4.5}$$

It is clear the ground state energy is determined by two parameters: the effective mass m and the dielectric dielectric permittivity κ. The ground state wave function is given by

$$\Phi_g(\mathbf{r}) = (\pi a^3)^{-1/2} e^{-r/a}, \tag{4.6}$$

with the effective Bohr radius $a = \hbar^2\kappa/me^2$ characterizing the localization of the ground localized state on the impurity site. In the typical semiconductors, the effective mass of conduction band electron is usually much smaller than m_0 and the dielectric permittivity constant is very large. The binding energy of the ground

bound state is then typically small relative to the case in Hydrogen atom. The localization length $\xi = a$ then turns to be much larger than the lattice constant. For example, in GaAs considering the donor doping [75], the parameters $m \approx 0.066m_0$ and $\kappa \approx 12.6$. Then we have the binding energy $E_b \approx 5.67$meV and the localization length $\xi \approx 100$Å.

When the SO coupling is present, the original Hamiltonian changes to be $H_0 \to H_0 + H_{SO}$. The exact solution of the bound state on impurity site may be difficult to study when the SO coupling is complicated. Practically, we may consider the following two typical situations. First, when the SO coupling is weak, the solution can be obtained by neglecting the SO term first, and the SO term is then treated as a perturbation to calculate the bound state for the total Hamiltonian [75]. Another case is the strong SO coupling case, in which case besides the position dependent property, the effective Hamiltonian becomes a matrix in internal (local angular-momentum) space. The solution in this situation can usually be simplified with symmetry considerations. To study this issue, we consider below the acceptor doping which creates bound state above the top of the valence band.

For the valence band of semiconductor, the local atomic orbital is p state. Without the SO coupling, the valence band is sixfold degenerate at Γ point $\mathbf{k} = 0$ ($J = l \otimes s = 1 \otimes 1/2 = 3/2 \oplus 1/2$) [52]. By generalizing the effective mass method to the present case one may write down the bound state wave function in the following form

$$\Psi(\mathbf{r}) = \sum_{m=1}^{6} u_{m,0}(\mathbf{r})\Phi_m(\mathbf{r}), \tag{4.7}$$

with the function $\Phi_m(\mathbf{r})$ satisfying the following equation [75]

$$\sum_{m'=1}^{6}\left[\sum_{ij}^{3}\left(H_0 + H_{SO}\right)^{ij}_{mm'}\hat{p}_i\hat{p}_j + U(\mathbf{r})\delta_{mm'}\right]\Psi_{m'}(\mathbf{r}) = E\Phi_m(\mathbf{r}). \tag{4.8}$$

Here i, j are Cartesian indices and $\hat{\mathbf{p}} = -i\hbar\nabla$ is the momentum operator. When the SO coupling of the type (1.2) is present, the six fold degeneracy at $\mathbf{k} = 0$ is partially lifted, splitting into group of states characterized by $J = 1/2$ and $J = 3/2$, respectively. The gap Δ between $J = 1/2$ and $J = 3/2$ at $\mathbf{k} = 0$ depends on the SO coupling strength (see Eq. (1.10)). In the strong SO coupling limit, the band with $J = 1/2$ moves far away from the one with $J = 3/2$ and the coupling between them around $\mathbf{k} = 0$ can be neglected. In this way the Hamiltonian in the local on-site angular momentum space can be reduce to a 4×4 matrix. The Hamiltonian for the present valence band is described by the Luttinger model, as described in section 1. The general formula is given by [3]

$$H = \frac{1}{2m_0}\big[(\gamma_1 + \frac{5}{2}\gamma_2)\hat{p}^2 - 2\gamma_3(\hat{\mathbf{p}}\cdot\mathbf{J})^2 + 2(\gamma_3 - \gamma_2)\sum_i \hat{p}_i^2 J_i^2\big] + U(\mathbf{r}), \tag{4.9}$$

with the Luttinger parameters γ_1, γ_2 and γ_3 being material dependent. The last term in the Luttinger SO coupling Hamiltonian breaks the continuous rotational symmetry. Excluding the impurity potential, the dispersion relation of the Luttinger Hamiltonian is obtained by

$$E_{l,h}(\mathbf{k}) = \frac{\hbar^2}{2m_0}\Big\{\gamma_1 k^2 \pm \big[4\gamma_2^2 k^4 + 12(\gamma_3^2 - \gamma_2^2)(k_x^2 k_y^2 + k_y^2 k_z^2 + k_z^2 k_x^2\big]^{1/2}\Big\}, \tag{4.10}$$

where l (for $+$ sign) and h (for $-$ sign) represent the light and heavy hole bands, respectively. It is clear the isoenergetic surface of the spectrum is no longer spherically symmetric.

In many semiconductors such as Ge and GaAs [76], the anisotropy of the isoenergetic surface is weak, and one may consider the spherical approximation, which is described by approximately taking $\gamma_3 = \gamma_2$. Under this condition the Hamiltonian becomes

$$H = \frac{1}{2m_0}\big[(\gamma_1 + \frac{5}{2}\gamma_2)\hat{p}^2 - 2\gamma_2(\hat{\mathbf{p}}\cdot\mathbf{J})^2\big] + U(\mathbf{r}). \tag{4.11}$$

It is easy to see the above Hamiltonian preserves the continuous rotational symmetry, and thus the total angular momentum is a good quantum number. This is an important advantage of the spherical approximation.

The orbital motion of the valence band hole includes the local on-site angular momentum state and the dynamics corresponding to the hopping between lattice sites. The former bears an analogy to the spin of an electron, and the later accordingly leads to orbital angular momentum $\mathbf{L} = \mathbf{r} \times \mathbf{p}/\hbar$. Then the total angular momentum $\mathbf{j}$ can be written as

$$\mathbf{j} = \mathbf{J} + \mathbf{L}. \tag{4.12}$$

We would like to comment that this decomposition is actually an approximation since spin $\mathbf{J}$ and the orbital angular momentum $\mathbf{L}$ do not exactly commute. However, the spin $\mathbf{J}$ characterizes the motion in scale smaller than the lattice constant, while $\mathbf{L}$ characterizes the motion in the whole lattice system. The non-commutation property between them is negligible. The wave function satisfying Schrödinger equation with the Hamiltonian (4.11) can be written down in the following form [77]

$$\Phi_{j,j_z}(\mathbf{r}) = (2j+1)\sum_{l}(-1)^{l-3/2+M}R_{j,l}(r)\sum_{l_z,\mu}\begin{pmatrix} l & 3/2 & j \\ l_z & \mu & -j_z \end{pmatrix} Y_{l,l_z}(\theta,\phi)\chi_\mu. \tag{4.13}$$

Here Y_{l,l_z} is the spherical harmonic, $\begin{pmatrix} l & 3/2 & j \\ l_z & \mu & -j_z \end{pmatrix}$ is the Wigner $3-j$ symbol with $j_z = l_z + \mu$, and χ_μ is the eigenstate (3/2 spinor) of J_z with eigenvalue $\mu = -3/2, -1/2, 1/2, 3/2$. The rest thing is to work out the solution of $R_{j,l}(r)$ for the ground state. The ground state for the spherical model with the impurity potential (4.2) is described with total angular momentum $j = 3/2$ [75]. Thus the corresponding

orbital angular momentum can only be $l = 0, 2$. Substituting Eq. (4.13) into the formula (4.8) we obtain for $R_{3/2,0}(r)$ and $R_{3/2,2}(r)$ by

$$(1+\alpha)\big(\frac{d}{dx}-\frac{1}{x}\big)\big(\frac{d}{dx}+\frac{3}{x}\big)R_{3/2,2} + (1-\alpha)\big(\frac{d}{dx}-\frac{1}{x}\big)\frac{dR_{3/2,0}}{dx} + 2\alpha\big(-\lambda+\frac{2}{x}\big)R_{3/2,2}=0, \tag{4.14}$$

$$(1+\alpha)\big(\frac{d}{dx}+\frac{2}{x}\big)\frac{dR_{3/2,0}}{dx} + (1-\alpha)\big(\frac{d}{dx}+\frac{2}{x}\big)\big(\frac{d}{dx}+\frac{3}{x}\big)R_{3/2,2} + 2\alpha\big(-\lambda+\frac{2}{x}\big)R_{3/2,0}=0, \tag{4.15}$$

where $\alpha = (\gamma_1 - 2\gamma_2)/(\gamma_1 + 2\gamma_2) = m_l/m_h$ is the ratio between the masses of the light and heavy holes with $m_l = m_0/(\gamma_1 + 2\gamma_2)$ and $m_h = m_0/(\gamma_1 - 2\gamma_2)$, $x = r m_h e^2/\kappa\hbar^2$ and $\lambda = -2E_g\kappa^2\hbar^2/e^4 m_h$ are dimensionless atomic units [75]. Note the parameter $0 \le \alpha \le 1$. It is easy to see for $\alpha = 1$ which corresponds to $\gamma_2 = 0$, one has $\lambda = 1$. Gel'mont and D'yakonov [78] found that for $\alpha \to 0$, the result $\lambda = 4/9$, with which one can obtain the ground state energy $E_g = 4m_h e^4/(18\kappa^2\hbar^2)$. For the material Ge, one has $\alpha = 0.13$ and the ground state energy reads $E_g \approx 8.1$meV [79]. For InSb, one has $\alpha = 0.03$ and $E_g \approx 8$meV [75].

From the Eqs. (4.14) and (4.14) we can also derive the asymptotic behavior of the radial wave functions. By considering $x \to \infty$, we have

$$(1+\alpha)\frac{d^2}{dx^2})R_{3/2,2} + (1-\alpha)\frac{d^2}{dx^2}\frac{dR_{3/2,0}}{dx} - 2\alpha\lambda R_{3/2,2} = 0, \tag{4.16}$$

$$(1+\alpha)\frac{d^2}{dx^2}R_{3/2,0} + (1-\alpha)\frac{d^2}{dx^2}R_{3/2,2} - 2\alpha\lambda R_{3/2,0} = 0. \tag{4.17}$$

The above equations can be simplified by defining $R_+ = R_{3/2,2} + R_{3/2,0}$ and $R_- = R_{3/2,2} - R_{3/2,0}$ which are decoupled and satisfy

$$\frac{d^2}{dx^2}R_+ - \alpha\lambda R_+ = 0, \tag{4.18}$$

and

$$\frac{d^2}{dx^2}R_- - \lambda R_- = 0. \tag{4.19}$$

The bound state solutions to above two equations then take the form

$$R_+ \sim A_0 e^{-(\alpha\lambda)^{1/2}x},\ R_- \sim A_0 e^{-\lambda^{1/2}x},\ x \to \infty. \tag{4.20}$$

Therefore, for the large distance from the impurity center, the wave function of the bound state is in the exponentially decaying form. This property is general for the impurity bound states.

It is noteworthy so far we consider only the localized states for the case of single impurity (from now on we consider only the ground bound states for the impurity sites). The bound state spectrum is determined by the impurity type (donor or acceptor) and the host material band structure. A real system includes many impurities randomly distributed in the material, with the ground state energy the same for all the impurities if the influence between them is excluded. This degeneracy is lifted by taking into account the influence on a site from other impurity states. Due to the spatially random distribution of the impurities, the influences between different impurity sites are random and the resultant ground state energies are then randomized. This can also be understood by the result that the effective potential produced at an impurity by the environment around it is random through the system. In this way the electronic properties of the material depend on the parameters, i.e. the typical random on-site energy difference $\epsilon_{i\alpha} - \epsilon_{j\beta}$ (α, β are spin indices)

between two neighbor impurity sites (i and j) and the typical hopping coefficient $t_{i\alpha,j\beta}$ between them due to the overlapping of their bound states. The coefficient generally decays exponentially with distance according to the asymptotic behavior given in Eq. (4.20). When the impurity of concentration is high, the randomness of the on-site energy is reduced, while the impurity states overlap strongly. In this case one typically has the condition $|t_{i\alpha,j\beta}| \gg |\epsilon_{i\alpha} - \epsilon_{j\beta}|$ and the bound states lose their localization character. At low concentration the coupling energy between two neighbor impurity states due to overlapping is much smaller than their relevant on-site energy difference

$$\left| \frac{t_{i\alpha,j\beta}}{\epsilon_{i\alpha} - \epsilon_{j\beta}} \right| \ll 1, \tag{4.21}$$

and thus the states are localized. In this situation the electronic wave functions of the impurity states around Fermi energy do not extend throughout the system and the dc conductivity will vanish at zero temperature. Namely, the system becomes an Anderson insulator. A more general description of the disordered insulator can be obtained with the scaling theory of the localization. Denote by $g(L)$ the dimensionless conductance of a hypercube material with edge length L via [80]

$$g(L) = \frac{2\hbar}{e^2} G(L), \tag{4.22}$$

with $G(L)$ is the conductance of the material. The magnitude of $g(L)$ will determine the localization transition of the system. The logarithmic derivative of $g(L)$ versus material size L is defined below [81]

$$\frac{d \ln g(L)}{d \ln L} = \beta(g), \tag{4.23}$$

where $\beta(g)$ is a function solely dependent on g. It can be seen if $\beta(g) > 0$ when $L \to \infty$, the conductance $g(L)$ diverges and it describes a metal. Oppositely, if

$\beta(g) < 0$ when $L \to \infty$, the system is an insulator. The asymptotic form of $\beta(g)$ can be determined in the weak and strong disorder limits. In the weak limit, the conductance satisfies Ohm's law and thus $G(L) = \sigma L^{d-2}$, where σ is the conductivity and d is the dimensionality of the material. This gives

$$\lim_{G\to\infty} \beta(g) = d - 2. \tag{4.24}$$

On the other hand, in the strong disorder limit, all states a exponentially localized and the conductance satisfies $G(L) = G_0 e^{-L/a}$, which follows that

$$\lim_{G\to 0} \beta(g) = \ln G - \ln G_0. \tag{4.25}$$

Eqs. (4.24) and (4.25) lead to the following important results (we assume $\beta(g)$ is a monotonic function of $g(L)$). For the dimensionality $d \leq 2$, one has always $\beta(g) < 0$, and therefore the metallic phase is always absent. One should remember here only the disorder effect is taken into account. Including the electron-electron interaction will greatly complicate the phase diagram in the low dimensional case with $d \leq 2$. For $d = 3$, one has $\beta(g) \leq 1$. One can then expect around some critical value of the conductance $G = G_c$ the function $\beta(g)$ changes sign. Namely, $\beta(g) < 0$ for $G < G_c$, while $\beta(g) > 0$ for $G > G_c$. This indicates for a three dimensional system when the conductance is larger than G_c, it is in metallic phase. Otherwise, for $G < G_c$ it becomes an insulator. For the present disordered system, when the condition (4.21) is satisfied, one can expect the result $G < G_c$ and the material is in the insulating regime.

For the disordered insulating regime, the charge transport cannot occur at zero temperature. At low but finite temperature, the charge transport for such system will be dominated by the hopping of electrons/holes between impurity sites, assisted by the electron-phonon interaction [66, 71]. Due to the electron-phonon interaction,

the random on-site energy difference will be compensated by emitting or absorbing phonons during the hopping process.

4.2 Hopping conduction

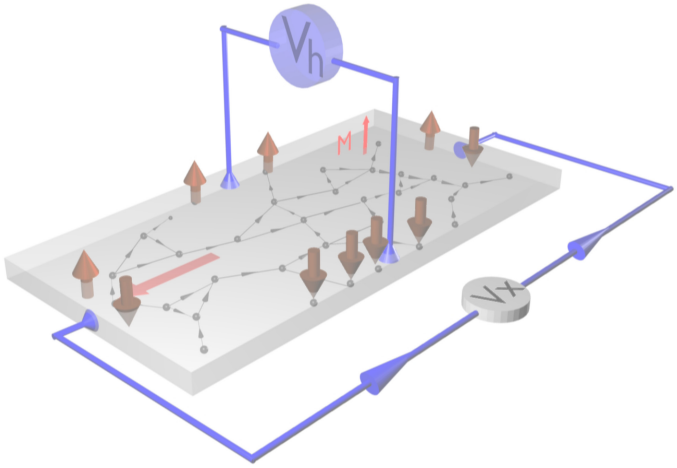

Fig. 4.1. AHE in the insulating regime. In this regime charge transport occurs via hopping between impurity sites.

The simplest case in the hopping transition is the one-phonon process through two impurity sites, which is time-reversal (TR) invariant and dominates the longitudinal charge transport [66, 71]. To capture the Hall effect (Fig. 4.1), one requires the hopping process to break the TR symmetry, which may occur in the process through more than two impurity sites. Holstein first found the hopping through three sites, is the minimum requirement to obtain the ordinary Hall effect (OHE) from theory [82]. In this case the quantum jump of a particle from site i to site j has two different choices for the hopping path. The total hopping amplitude is obtained by adding up the direct and indirect (through the intermediate k-site) hopping terms from i to j site. The two hopping paths give rise to an interference term for the transition rate, which breaks TR symmetry and is responsible for the Hall current in the hopping conduction regime. For the OHE, the interference is a reflection of the

Aharonov-Bohm effect, and for AHE it reflects the Berry phase due to SO coupling. Furthermore, the dominant contribution to the Hall transport will be given by the one- and two-real-phonon processes through triads [82].

4.2.1 A general picture for the hopping

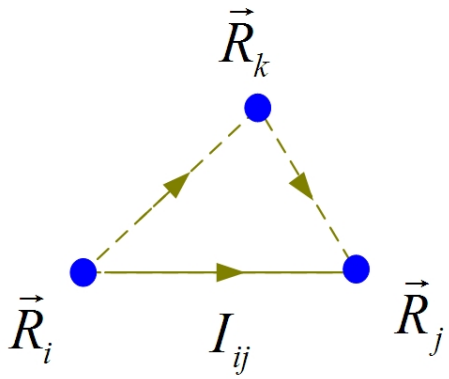

Fig. 4.2. Current with three-site hopping process.

Note the hopping between two impurity sites is a quantum process with the transition amplitude resulting from the superposition of many different hopping paths. Fig. 4.2 depicts the hopping processes from site i to site j through up to three sites, which consist of the dominant contribution to the longitudinal and Hall transports. The quantum jump through three sites (through triads) has two different choices for the hopping path. One is the direct hopping from i to j site without intermediate site, and another is called indirect hopping, in which the particle first goes to the third site, and then hops from k to j site. The total hopping amplitude is obtained by adding up the direct and indirect hopping terms from i to j site, which results in an interference term and contributes to the Hall effect. The hopping matrix between i and j sites can be generally written as

$$A_{ij} = A_{ij}^{dir} + A_{ij}^{ind}, \tag{4.26}$$

where A_{ij}^{dir} describes the direct term from i to j site, and A_{ij}^{ind} describes the indirect hopping term, say, from i to k and then to j site. Furthermore, both the direct and indirect hopping matrixes may include all possible multi-phonon processes. In later discussions we shall see these multi-phonon processes can be classified by the number of real phonons included in the corresponding process. In this way we get

$$A_{ij}^{dir} = \sum_{n} A_{ij}^{(m)dir}, \tag{4.27}$$

$$A_{ij}^{ind} = \sum_{n} A_{ij}^{(m)ind}, \tag{4.28}$$

where m indicates the number of real phonons. It is noteworthy, a process with m real phonons can include any number of virtual phonons which are emitted (or absorbed) and later reabsorbed (or remitted) in the intermediate process. For the Hall effect the hopping matrix includes a geometric phase, for which they can be rewritten as

$$A_{ij}^{(m)dir} = A_{(m)ij}^{(0)dir} e^{i\phi_1}, \quad A_{ij}^{(m)ind} = A_{(m)ij}^{(0)ind} e^{i\phi_2}. \tag{4.29}$$

Let $\phi = \phi_1 - \phi_2$. We then have

$$|A_{ij}^{(m)}|^2 = |A_{(m)ij}^{(0)dir}|^2 + |A_{(m)ij}^{(0)ind}|^2 + Re[A_{(m)ij}^{(0)dir} A_{(m)ij}^{*(0)ind}] \cos\phi + Im[A_{(m)ij}^{*(0)dir} A_{(m)ij}^{(0)ind}] \sin\phi, \tag{4.30}$$

and the transition rate for the m-phonon process is given by Fermi golden rule

$$P_{ij}^{(m)} = \frac{2\pi}{\hbar} \sum_{phonon\ modes} |A_{(m)ij}|^2 \delta(\epsilon_i - \epsilon_j \pm \Delta\mathcal{E}_{phonon}^{(m)}), \tag{4.31}$$

where the summation is over all modes for the m-phonon process considered, and $\Delta\mathcal{E}^{(m)}_{phonon}$ represents the energy variation with respect to absorbing and emission of the m real phonons. Note between direct and indirect hopping paths of different number of real phonons there will be no interference. The Hall effect is a consequence of geometric phase. When the phase $\phi \to -\phi$, e.g. when the external magnetic field (for normal Hall effect) or the magnetization (for anomalous Hall effect) inverts, the Hall conductivity must change sign. On the other hand, the only term changes sign in Eq. (4.30) with this transformation is the one with $\sin\phi$. Therefore we know the transition contributing to the Hall effect is

$$P^{(m)(H)}_{ij} = \frac{2\pi}{\hbar} \sum_{phonon\ \ modes} Im[A^{*(0)dir}_{(m)ij}\, A^{(0)ind}_{(m)ij}] \sin\phi\delta(\epsilon_i - \epsilon_j \pm \Delta\mathcal{E}^{(m)}_{phonon}), \qquad (4.32)$$

while the transition corresponding to the longitudinal charge transport is

$$\begin{aligned} P^{(0)}_{(m)ij} \;\; = \;\; & \frac{2\pi}{\hbar} \sum_{phonon\ \ modes} \left(|A^{(0)dir}_{(m)ij}|^2 + |A^{(0)ind}_{(m)ij}|^2 + Re[A^{(0)dir}_{(m)ij} A^{*(0)ind}_{(m)ij}] \cos\phi\right) \times \\ & \times\delta(\epsilon_i - \epsilon_j \pm \Delta\mathcal{E}^{(m)}_{phonon}). \end{aligned} \qquad (4.33)$$

The total transition rate is a summation of $P^{(m)}_{ij}$, mamely

$$P_{ij} = \sum_m P^{(m)}_{ij}. \qquad (4.34)$$

It is noteworthy in above analysis we consider only one intermediate site for the indirect hopping process. Certainly, the general indirect hopping process may include one or more intermediate sites, and each such kind of process can also be classified by number of real phonons included in the whole transition. For the Hall effect in the hopping conduction regime, the dominant contribution comes from the processes with only one intermediate site and up to two real phonons in the whole transition. Any process including more than one intermediate site or more than two

real phonons gives merely a negligible high order contribution. On the other hand, for longitudinal conductivity only the direct hopping with one real phonon absorbed or emitted needs to be considered.

4.2.2 Two-site hopping process

In this subsection we consider the two-site direct hopping process with the impurity states being well localized if no electron-phonon coupling is considered, and show how the conduction takes place when the electron-phonon interaction opens up. Consider two adjacent impurity sites i and j connected by a vector $\mathbf{R}$. The Hamiltonian is given by

$$H = H_0 + \frac{1}{\kappa}\frac{e^2}{|\mathbf{r}-\mathbf{R}_i|} - \frac{1}{\kappa}\frac{e^2}{|\mathbf{r}-\mathbf{R}_j|} + V_a(\mathbf{r}), \tag{4.35}$$

where H_0 gives the effective mass term, $V_a(\mathbf{r})$ is the potential due to other nearby ions and $\mathbf{R} = \mathbf{R}_j - \mathbf{R}_i$. We denote ϕ_i (ϕ_j) as the eigenstate of the isolated impurity site i (j), which has been studied in the section 1 with effective mass method. Then the full eigenstate of the impurity site can be obtained by perturbation theory, i.e. treating all other interaction except for the terms describing the isolated impurity site as the perturbation. Generally we can write down the perturbed eigenstates for i and j sites in the form

$$\psi_i = a_i\phi_i + a_j\phi_j, \quad \psi_j = b_i\phi_i + b_j\phi_j. \tag{4.36}$$

In the first order of the perturbation, we have $a_i = b_j = 1$, $a_j \approx w/\Delta$ and $b_i \approx -w/\Delta$, with w the coupling between ϕ_i and ϕ_j, and $\Delta = \epsilon_i - \epsilon_j$, i.e. the on-site energy difference. The localization means $|\Delta| \gg |w|$, in which case the transition between the two states is greatly reduced. Charge transport can take place through hopping when the phonon assistance is considered.

In the second quantization picture, the electron-phonon coupling Hamiltonian is given as

$$H_{el-ph} = i\sum_{\lambda} E_1 \vec{q}_\lambda \cdot \vec{e}_\lambda \left(\frac{\hbar}{2MN\omega}\right)^{1/2} (b_\lambda e^{i\vec{q}_\lambda\cdot\vec{r}} - b_\lambda^\dagger e^{-i\vec{q}_\lambda\cdot\vec{r}}). \tag{4.37}$$

Here E_1 is the coupling constant, M is atomic mass, N is the number of lattice sites, b_λ and $b_\lambda^\dagger$ are annihilation and creation operators with respect to the mode $\vec{q}_\lambda$. The dispersion relation of phonon field is assumed to be isotropic in different directions and reads $\omega = sq_\lambda$, with s the phonon velocity and taken as a constant. Now we derive the matrix element of transition between the two sites: $A_{ij} = \langle\psi_i|H_{el-ph}|\psi_j\rangle$. Specifically, we shall calculate $\langle n_q, \psi_i|H_{el-ph}|\psi_j, n_q+1\rangle$ and $\langle n_q+1\psi_i|H_{el-ph}|\psi_j, n_q\rangle$, respectively. It is straightforward to know

$$\begin{aligned} A_{ij} &= -\frac{w}{\Delta}\langle n_q, \phi_i|H_{el-ph}|\phi_i, n_q+1\rangle + \frac{w}{\Delta}\langle n_q, \phi_j|H_{el-ph}|\phi_j, n_q+1\rangle \\ &\quad + \langle n_q, \phi_i|H_{el-ph}|\phi_j, n_q+1\rangle - \frac{w^2}{\Delta^2}\langle n_q, \phi_j|H_{el-ph}|\phi_i, n_q+1\rangle. \end{aligned} \tag{4.38}$$

The fourth term in the right hand side of above equation can be neglected immediately since it is the second order perturbation with respect to w/Δ. On the other hand, the third term contains the phase factor $e^{i\vec{q}_\lambda\cdot\vec{r}}$, which oscillates quickly and is also negligible. In this way we obtain

$$A_{ij} = i\vec{q}_\lambda \cdot \vec{e}_\lambda \left[\frac{\hbar(n_q+1)}{2MN\omega_\lambda}\right]^{1/2} E_1 \frac{w}{\Delta}\left[\langle\phi_j|e^{i\vec{q}_\lambda\cdot\vec{r}}|\phi_j\rangle - \langle\phi_i|e^{i\vec{q}_\lambda\cdot\vec{r}}|\phi_i\rangle\right]. \tag{4.39}$$

Note $\phi_i(\vec{r}) = \phi(\vec{r}-\mathbf{R}_i) = \phi(\vec{r}-(\mathbf{R}_i-\mathbf{R}_j)-\mathbf{R}_j) = \phi(\vec{r}-\mathbf{R}-\mathbf{R}_j) = \phi_j(\vec{r}-\mathbf{R})$. We have $\langle\phi_j|e^{i\vec{q}_\lambda\cdot\vec{r}}|\phi_j\rangle - \langle\phi_i|e^{i\vec{q}_\lambda\cdot\vec{r}}|\phi_i\rangle = (e^{i\vec{q}_\lambda\cdot\vec{R}}-1)\langle\phi_i|e^{i\vec{q}_\lambda\cdot\vec{r}}|\phi_i\rangle$. For practical case, one

can consider the condition $q_\lambda a \ll 1$, with a the radius of the wave function $\phi_{i,j}$ [71]. Under this condition we have

$$\langle \phi_i | e^{i\vec{q}_\lambda \cdot \vec{r}} | \phi_i \rangle \approx \left[\frac{1}{1 + (qa/2)^2} \right]^2. \tag{4.40}$$

Thus we have

$$A_{ij} = iE_1 \vec{q}_\lambda \cdot \vec{e}_\lambda \left[\frac{\hbar(n_q + 1)}{2MN\omega_\lambda} \right]^{1/2} \frac{w}{\Delta} (e^{i\vec{q}_\lambda \cdot \vec{R}} - 1) \left[\frac{1}{1 + (qa/2)^2} \right]^2. \tag{4.41}$$

With the hopping matrix above, we evaluate the transition rate through Fermi-golden rule that

$$\begin{aligned} P_{ij} &= \frac{2\pi}{\hbar} \frac{V}{8\pi^3} \int |A_{ij}|^2 \delta(\hbar\omega_\lambda - \Delta) d^2\vec{q}_\lambda, \\ &= \frac{2\pi}{\hbar} \frac{V}{8\pi^3} E_1^2 \frac{\hbar w^2}{MN\Delta^2 s} \int (n_q + 1) q (1 - \cos \vec{q}_\lambda \cdot \vec{R}) \frac{\delta(\hbar qs - \Delta)}{\left[1 + (qa/2)^2\right]^4} d^2\vec{q}_\lambda, \\ &= \gamma_0 \int (n_q + 1) q (1 - \cos(qR\cos\theta)) \frac{\delta(\hbar qs - \Delta)}{\left[1 + (qa/2)^2\right]^4} q^2 \sin\theta d\theta d\phi dq. \end{aligned} \tag{4.42}$$

The constant γ_0 is defined via $\gamma_0 = \frac{VE_1^2}{4\pi^2} \frac{w^2}{MN\Delta^2 s}$. Note the integral

$$\int (1 - \cos(qR\cos\theta)) \sin\theta d\theta d\phi = 4\pi(1 - \sin(qR)/qR),$$

and then we reach

$$\begin{aligned} P_{ij} &= 4\pi\gamma_0 \int (n_q + 1) q^3 \big[1 - \frac{1}{qR} \sin(qR)\big] \frac{\delta(\hbar qs - \Delta)}{\left[1 + (qa/2)^2\right]^4} dq, \\ &\approx E_1^2 \frac{V}{\pi\hbar^4 s^5} \frac{w^2\Delta}{NM} (n_q + 1). \end{aligned} \tag{4.43}$$

Similarly, for the term $\langle n_q + 1 \psi_i | H_{el-ph} | \psi_j, n_q \rangle$, we get $P_{ij} = E_1^2 \frac{V}{\pi\hbar^4 s^5} \frac{w^2\Delta}{NM} n_q$. Note without electron-phonon coupling, the transition rate between the two localized

states is proportional to $|w/\Delta|^2$, which is very small. Thus from above result we can see the transition in the presence of election-phonon coupling is enhanced.

4.2.3 Longitudinal electric conductance

Let's go back to the transition rate $P_{ij}(q_\lambda)$ for specific mode q_λ, i.e. without integrating over q_λ. We have ($w \to W_{ij}$)

$$P_{ij}(\vec{q}_\lambda) = E_1^2(\vec{q}_\lambda \cdot \vec{e}_\lambda)^2 \frac{\hbar(n_q+1)}{2MN\omega_\lambda} \frac{W_{ij}^2}{\Delta^2} \quad \text{or} \quad E_1^2(\vec{q}_\lambda \cdot \vec{e}_\lambda)^2 \frac{\hbar n_q}{2MN\omega_\lambda} \frac{W_{ij}^2}{\Delta^2}. \tag{4.44}$$

From the Bose statistics we have $n_{q_\lambda} + 1/2 \pm 1/2 = \mp 1/(1 - e^{\pm\hbar\omega_\lambda/k_BT})$. The total transition rate can be rewritten as

$$\begin{aligned} P_{ij} &= \sum_{\vec{q}} \frac{2\pi}{\hbar} P_{ij}(\vec{q}_\lambda)\delta(\hbar\omega_{q_\lambda} - \Delta) \\ &= \sum_{\vec{q}} \frac{4\pi}{\hbar} E_1^2(\vec{q}_\lambda \cdot \vec{e}_\lambda)^2 \frac{\hbar}{2MN\omega_\lambda} \frac{W_{ij}^2}{(\epsilon_i - \epsilon_j)^2} \frac{1}{|1 - e^{-(\epsilon_i - \epsilon_j)/k_BT}|} \delta(\epsilon_i - \epsilon_j \pm \hbar\omega_\lambda) \\ &= \mathcal{Z} e^{\epsilon_i/k_BT} L_{ij}, \end{aligned} \tag{4.45}$$

with $\mathcal{Z} = \sum_i e^{-\epsilon_i/k_BT}$ and $L_{ij} = L_{ji}$ given by

$$L_{ij} = \mathcal{Z}^{-1} \sum_{\vec{q}} \frac{4\pi}{\hbar} E_1^2(\vec{q}_\lambda \cdot \vec{e}_\lambda)^2 \frac{\hbar}{2MN\omega_\lambda} \frac{W_{ij}^2}{(\epsilon_i - \epsilon_j)^2} \frac{1}{|e^{\epsilon_i/k_BT} - e^{\epsilon_j/k_BT}|} \delta(\epsilon_i - \epsilon_j \pm \hbar\omega_\lambda). \tag{4.46}$$

The current between i and j sites is calculated by

$$I_{ij} = e\big[P_{ij} f_i(1 - f_j) - P_{ji} f_j(1 - f_i)\big], \tag{4.47}$$

where f_i is the Fermi distribution function. Now we consider in the following two different simple cases.

First, if there is no external electric field, we shall obtain no longitudinal electric current between the two sites. This is easy to see from the following formula

$$\begin{aligned} I_{ij} &= e\mathcal{Z}(e^{\epsilon_i/k_BT}L_{ij}f_i - e^{\epsilon_j/k_BT}L_{ji}f_j) + e\mathcal{Z}(e^{\epsilon_i/k_BT}L_{ij} - e^{\epsilon_j/k_BT}L_{ji})f_if_j \\ &= e\mathcal{Z}L_{ij}\frac{e^{(\epsilon_i+\epsilon_j-\mu)/k_BT} - e^{(\epsilon_i+\epsilon_j-\mu)/k_BT}}{(e^{(\epsilon_i-\mu)/k_BT}+1)(e^{(\epsilon_j-\mu)/k_BT}+1)} \\ &= 0. \end{aligned} \tag{4.48}$$

Second, when an external electric field $\mathbf{E} = E\vec{e}_x$ is applied, the on-site energies and the chemical potential will change to be $\epsilon_i \to \tilde{\epsilon}_i = \epsilon_i + \delta\epsilon_i$ and $\mu_i \to \tilde{\mu}_i = \mu_i + \delta\mu_i$. The calculation of $\delta\epsilon_i$ and $\delta\mu_i$ should be done separately [75]. By a similar derivative we can obtain

$$I_{ij} = e\tilde{\mathcal{Z}}\tilde{L}_{ij}\frac{e^{(\tilde{\epsilon}_i+\tilde{\epsilon}_j-\tilde{\mu}_j)/k_BT} - e^{(\tilde{\epsilon}_i+\tilde{\epsilon}_j-\tilde{\mu}_i)/k_BT}}{(e^{(\tilde{\epsilon}_i-\tilde{\mu}_i)/k_BT}+1)(e^{(\tilde{\epsilon}_j-\tilde{\mu}_j)/k_BT}+1)}. \tag{4.49}$$

Here $\tilde{\mathcal{Z}}$ and $\tilde{L}_{ij}$ hold the same forms as $\mathcal{Z}$ and L_{ij}, with only the parameters ϵ_i, μ_i replaced by $\tilde{\epsilon}_i, \tilde{\mu}_i$. For the hopping conduction we are interested in the states with $|\tilde{\epsilon}_i - \tilde{\mu}_i| \gg k_BT$, which dominate the contribution to the conductivity. Then in the weak electric field case (thus $|\delta\mu_i|, |\delta\epsilon_i| \ll k_BT$), we have

$$I_{ij} = e\tilde{\mathcal{Z}}\tilde{L}_{ij}\frac{\delta\mu_i - \delta\mu_j}{k_BT} = e^2\tilde{\mathcal{Z}}\tilde{L}_{ij}\frac{U_{ij}}{k_BT}, \tag{4.50}$$

where $U_{ij} = (\delta\tilde{\mu}_i - \delta\tilde{\mu}_j)/e$ is the effective electric voltage between i and j. The above formula gives the conductance between the two neighbor sites as

$$G_{ij} = e^2\tilde{\mathcal{Z}}\frac{\tilde{L}_{ij}}{k_BT}. \tag{4.51}$$

Note the above result is just the microscopic conductance between two neighbor impurity sites. The macroscopic conductance/resistance of the material should be evaluated by considering all impurity sites connected to each other. Such a process

is nontrivial and can be done with percolation theory which will be introduced in the section 5.

4.2.4 Hopping through triads

The two-site direct hopping calculated in above section determines the longitudinal conductivity/resistivity, but cannot lead to Hall effect. This is because this term preserve TR symmetry, while the AHE breaks TR symmetry. To study the Hall effect, we shall calculate in this section the interference term in the hopping process through three sites (through triads).

Our theory is based on a minimal tight-binding Hamiltonian which is valid for both electron and hole carriers hopping between localized sites in the ferromagnetic system. With the particle-phonon coupling considered, the total Hamiltonian can be written as

$$\begin{aligned} H &= H_p + H_{p-ph} + H_{ph}, \\ H_p &= \sum_{\alpha} \epsilon_i \hat{c}^{\dagger}_{i\alpha}\hat{c}_{i\alpha} - \sum_{i\alpha,j\beta} t_{i\alpha,j\beta}\hat{c}^{\dagger}_{i\alpha}\hat{c}_{j\beta} + \sum_{i\alpha\beta} \mathbf{M}\cdot\tau_{\alpha\beta}\hat{c}^{\dagger}_{i\alpha}\hat{c}_{i\beta}, \\ H_{p-ph} &= i\sum_{i\alpha\lambda} g^i_{\lambda}(b_{\lambda}e^{i\vec{q}_{\lambda}\cdot\vec{r}} - b^{\dagger}_{\lambda}e^{-i\vec{q}_{\lambda}\cdot\vec{r}})\hat{c}^{\dagger}_{i\alpha}\hat{c}_{i\alpha} \\ H_{ph} &= \sum_{\lambda} \omega_{\lambda} b^{\dagger}_{\lambda} b_{\lambda}. \end{aligned} \tag{4.52}$$

Here H_p is the Hamiltonian for localized states (holes or electrons), H_{p-ph} gives the coupling between localized states and phonons, H_{ph} is the phonon energy, and the index α represents the local on-site total angular momentum state ("spin" of the electron or hole). The particle-phonon coupling g^i_{λ} can be found by comparing with Eq. (4.37), and the hopping matrix t_{ij} is generally off-diagonal due to SO coupling. The specific form of the relevant parameters (hopping matrix, spin operator, magnetization) depends on what material one considers, and will not affect the scaling between σ^{AH}_{xy} and σ_{xx} . In this work we consider that the magnetization is (nearly)

saturated and thus we assume $\mathbf{M} = M\hat{e}_z$, and can then rewrite the Hamiltonian H_p in the diagonal basis of the exchange term and obtain

$$H_p = \sum_{\alpha} \epsilon_{i\alpha} \hat{c}^{\dagger}_{i\alpha} \hat{c}_{i\alpha} - \sum_{i\alpha,j\beta} t_{i\alpha,j\beta} \hat{c}^{\dagger}_{i\alpha} \hat{c}_{j\beta}, \tag{4.53}$$

where $\epsilon_{i\alpha} = \epsilon_i + M\tau_{\alpha\alpha}$. The specific form of hopping coefficient $t_{i\alpha,j\beta}$ depends on the material we consider. For $Ga_{1-x}Mn_xAs$, for example, $t_{i\alpha,j\beta}$ describes the hopping between holes localized on the Mn impurities, and can be obtained by a unitary rotation $U(\mathbf{R})$ from the $\hat{e}_z$ direction to the hopping direction $i \to j$. We thus have $t_{i\alpha,j\beta} = [U^{\dagger}(\mathbf{R}_{ij}) t_{diag} U(\mathbf{R}_{ij})]_{\alpha\beta}$, where $t_{diag} = \mathrm{diag}[t_{3/2}, t_{1/2}, t_{-1/2}, t_{-3/2}]$ represents the situation that the hopping direction is along the z direction [83]. Another example is for the localized s-orbital electrons. In this case, the hopping is given by $t_{ij} = U^{\dagger}(\mathbf{R}_{ij})[\tilde{t}_{ij}(1 + i\vec{v}_{ij} \cdot \vec{\sigma})]U(\mathbf{R}_{ij})$. Here $\tilde{t}_{ij} = \mathrm{diag}[t_{1/2}, t_{-1/2}]$ and $\vec{v}_{ij} = \frac{\alpha}{\hbar} \int_{\vec{r}_i}^{\vec{r}_j} (\nabla V(\mathbf{r}) \times d\vec{r}')$ with $V(\mathbf{r})$ including the ion and external potentials, the spin-orbit coupling coefficient $\alpha = \hbar/(4m^2c^2)$ and m the effective mass of the electron.

Again, the localization regime requires that typically $|t_{i\alpha,j\beta}| \ll |\epsilon_{i\alpha} - \epsilon_{j\beta}|$. In this way, the coupling between states localized in different impurity sites can be treated with perturbation theory. In the first order perturbation to eigenstates, we have

$$|\alpha, \psi_i\rangle = |\alpha, \phi_i\rangle + \sum_{j \neq i, \beta} \frac{t_{i\alpha,j\beta}}{\epsilon_{i\alpha} - \epsilon_{j\beta}} |\beta, \phi_j\rangle. \tag{4.54}$$

The hopping matrix between i and j (with $i \neq j$) due to the particle-phonon coupling reads

$$\begin{aligned}
A_{ij}^{\alpha\beta} &= \langle \alpha, \psi_i | H_{p-ph} | \beta, \psi_j \rangle \\
&= \langle \alpha, \phi_i | H_{p-ph} | \beta, \phi_j \rangle + \sum_{k(\neq i),\alpha'} \frac{t^*_{i\alpha,k\alpha'}}{\epsilon_{i\alpha} - \epsilon_{k\alpha'}} \langle \alpha', \phi_k | H_{p-ph} | \beta, \phi_j \rangle + \\
&\quad + \sum_{k(\neq j),\beta'} \frac{t_{j\beta,k\beta'}}{\epsilon_{j\beta} - \epsilon_{k\beta'}} \langle \alpha, \phi_i | H_{p-ph} | \beta', \phi_k \rangle + \\
&\quad + \sum_{k(\neq i),k'(\neq j),\alpha',\beta'} \frac{t^*_{i\alpha,k\alpha'}}{\epsilon_{i\alpha} - \epsilon_{k\alpha'}} \frac{t_{j\beta,k\beta'}}{\epsilon_{j\beta} - \epsilon_{k\beta'}} \langle \alpha', \phi_k | H_{p-ph} | \beta', \phi_{k'} \rangle \\
&\approx \sum_{k(\neq i),\alpha'} \frac{t^*_{i\alpha,k\alpha'}}{\epsilon_{i\alpha} - \epsilon_{k\alpha'}} \langle \alpha', \phi_k | H_{p-ph} | \beta, \phi_j \rangle + \sum_{k(\neq j),\beta'} \frac{t_{j\beta,k\beta'}}{\epsilon_{j\beta} - \epsilon_{k\beta'}} \langle \alpha, \phi_i | H_{p-ph} | \beta', \phi_k \rangle \\
&\approx \sum_{\alpha'} \frac{t^*_{i\alpha,j\alpha'}}{\epsilon_{i\alpha} - \epsilon_{j\alpha'}} \langle \alpha', \phi_j | H_{p-ph} | \beta, \phi_j \rangle + \sum_{\beta'} \frac{t_{j\beta,i\beta'}}{\epsilon_{j\beta} - \epsilon_{i\beta'}} \langle \alpha, \phi_i | H_{p-ph} | \beta', \phi_i \rangle. \quad (4.55)
\end{aligned}$$

Since the particle-phonon coupling conserves spin, we can further obtain

$$A_{ij}^{\alpha\beta} = \frac{t^*_{i\alpha,j\beta}}{\epsilon_{i\alpha} - \epsilon_{j\beta}} \langle \beta, \phi_j | H_{p-ph} | \beta, \phi_j \rangle + \frac{t_{j\beta,i\alpha}}{\epsilon_{j\beta} - \epsilon_{i\alpha}} \langle \alpha, \phi_i | H_{p-ph} | \alpha, \phi_i \rangle, \quad i \neq j. \quad (4.56)$$

On the other hand, if $i = j$, we find $A_{ii}^{\alpha\beta} = \langle \alpha, \phi_i | H_{p-ph} | \beta, \phi_i \rangle \delta_{\alpha\beta}$. Together with these results we finally reach

$$\begin{aligned}
\sum_{ij} \hat{A}_{ij}^{\alpha\beta} &= i \sum_{ij\lambda} g_\lambda^i \big[\delta_{ij}\delta_{\alpha\beta} + (1 - \delta_{ij}) \frac{t_{j\beta,i\alpha}}{\epsilon_{j\beta} - \epsilon_{i\alpha}} \big] (b_\lambda e^{i\vec{q}_\lambda \cdot \vec{R}_i} - b_\lambda^\dagger e^{-i\vec{q}_\lambda \cdot \vec{R}_i}) \\
&\quad + i \sum_{ij\lambda} g_\lambda^i (1 - \delta_{ij}) \frac{t^*_{i\alpha,j\beta}}{\epsilon_{i\alpha} - \epsilon_{j\beta}} (b_\lambda e^{i\vec{q}_\lambda \cdot \vec{R}_j} - b_\lambda^\dagger e^{-i\vec{q}_\lambda \cdot \vec{R}_j}). \quad (4.57)
\end{aligned}$$

In the basis of phonon number states, we can write down the transition matrix in the form:

$$\begin{aligned} A_{ij}^{\alpha\beta} &= \langle \psi_i^\alpha, n_{q_\lambda} \mp 1 | H_{p-ph} | \psi_j^\beta, n_{q_\lambda} \rangle \\ &= i g_\lambda^{(\mp)} \big[\delta_{ij} \delta_{\alpha\beta} e^{\pm i\vec{q}_\lambda \cdot \vec{R}_i} + (1-\delta_{ij}) \frac{t_{j\beta,i\alpha}}{\epsilon_{j\beta} - \epsilon_{i\alpha}} (e^{\pm i\vec{q}_\lambda \cdot \vec{R}_i} - e^{\pm i\vec{q}_\lambda \cdot \vec{R}_j}) \big], \quad (4.58) \end{aligned}$$

with

$$g_\lambda^{(\mp)} = \pm E_1 (\vec{q}_\lambda \cdot \vec{e}_\lambda) \left[\frac{\hbar (n_{q_\lambda} + 1/2 \mp 1/2)}{2MN\omega_\lambda} \right]^{1/2}. \quad (4.59)$$

From the Eqs. (4.57) and (4.58) we can see the following important properties of the electron-phonon coupling process: a) A phonon can be absorbed or emitted, with the electron/hole jumped from one site to another site; b) A phonon can be absorbed or emitted, with the electron/hole staying at the same site! Certainly this process does not satisfy energy conservation, and can only be the intermediate process; c) When the electron/hole jump from site to site with assistance of phonons, the particle-phonon scattering does not flip spin, but the SO coupling can flip spin. Furthermore, here we only consider the particle-phonon scattering. If there is also the particle-magnon scattering, which does not conserve spin, the transition matrix will be more complicated (we have considered this in detail, but will not be introduced in this work).

Now we proceed to calculate the transition rate for the hopping process through three sites, in which the lowest-order process is the two-phonon process. From the hopping matrix obtained in Eqs. (4.57) and (4.58) we know the two-phonon processes include (a) direct hopping process (see Fig. 4.3): $|\psi_i^\alpha, n_q\rangle \to |\psi_i^\alpha, n_q \mp 1\rangle \to |\psi_j^\beta, n_q \mp 1, n_{q'} \mp 1\rangle$, and $|\psi_i^\alpha, n_q\rangle \to |\psi_j^\beta, n_q \mp 1\rangle \to |\psi_j^\beta, n_q \mp 1, n_{q'} \mp 1\rangle$ (and $n_q \longleftrightarrow n_{q'}$); (b)

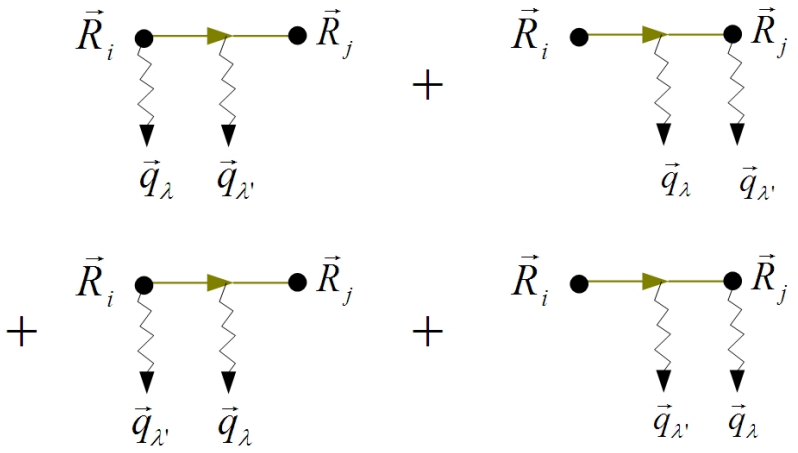

Fig. 4.3. Two-phonon direct hopping process. Here we only present the phonon-emission processes.

indirect hopping process (see Fig. 4.4): $|\psi_i^\alpha, n_q\rangle \to |\psi_k^\gamma, n_q \mp 1\rangle \to |\psi_j^\beta, n_q \mp 1, n_{q'} \mp 1\rangle$ (and $n_q \longleftrightarrow n_{q'}$). Specifically, we calculate the direct hopping matrix element by

$$\begin{aligned} A_{ij}^{\alpha\beta,dir} &= \frac{\langle \psi_j^\beta, n_q \mp 1, n_{q'} \mp 1|H_{p-ph}|\psi_i^\alpha, n_q \mp 1\rangle\langle \psi_i^\alpha, n_q \mp 1|H_{p-ph}|\psi_i^\alpha, n_q\rangle}{\pm\hbar\omega_\lambda} + \\ &+ \frac{\langle \psi_j^\beta, n_q \mp 1, n_{q'} \mp 1|H_{p-ph}|\psi_i^\alpha, n_{q'} \mp 1\rangle\langle \psi_i^\alpha, n_{q'} \mp 1|H_{p-ph}|\psi_i^\alpha, n_{q'}\rangle}{\pm\hbar\omega_{\lambda'}} \\ &+ \frac{\langle \psi_j^\beta, n_q \mp 1, n_{q'} \mp 1|H_{p-ph}|\psi_j^\beta, n_q \mp 1\rangle\langle \psi_j^\beta, n_q \mp 1|H_{p-ph}|\psi_i^\alpha, n_q\rangle}{\epsilon_{i\alpha} - \epsilon_{j\beta} \pm \hbar\omega_\lambda} \\ &+ \frac{\langle \psi_j^\beta, n_q \mp 1, n_{q'} \mp 1|H_{p-ph}|\psi_j^\beta, n_{q'} \mp 1\rangle\langle \psi_j^\beta, n_{q'} \mp 1|H_{p-ph}|\psi_i^\alpha, n_{q'}\rangle}{\epsilon_{i\alpha} - \epsilon_{j\beta} \pm \hbar\omega_{\lambda'}}, \end{aligned} \tag{4.60}$$

and the indirect hopping terms via

$$\begin{aligned} A_{ij}^{\alpha\beta,ind} &= \frac{\langle \psi_j^\beta, n_q \mp 1, n_{q'} \mp 1|H_{p-ph}|\psi_k^\gamma, n_q \mp 1\rangle\langle \psi_k^\gamma, n_q \mp 1|H_{p-ph}|\psi_i^\alpha, n_q\rangle}{\epsilon_{i\alpha} - \epsilon_{k\gamma} \pm \hbar\omega_\lambda + i\hbar s_+} + \\ &+ \frac{\langle \psi_j^\beta, n_q \mp 1, n_{q'} \mp 1|H_{p-ph}|\psi_k^\gamma, n_{q'} \mp 1\rangle\langle \psi_k^\gamma, n_{q'} \mp 1|H_{p-ph}|\psi_i^\alpha, n_{q'}\rangle}{\epsilon_{i\alpha} - \epsilon_{k\gamma} \pm \hbar\omega_{\lambda'} + i\hbar s_+}, \end{aligned} \tag{4.61}$$

where s_+ is a positive infinitesimal number. Note the Hall effect is contributed

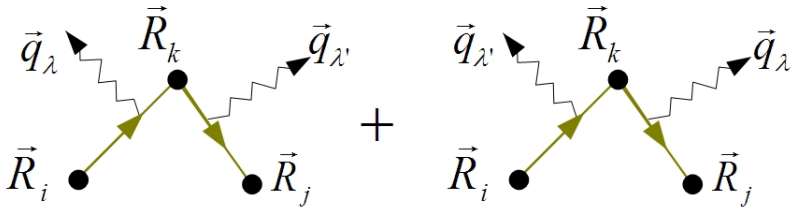

Fig. 4.4. Two-phonon indirect hopping process. Again we only present the phonon-emission processes.

from the interference between direct and indirect terms with $\pi/2$ out-of-phase in the zero geometric phase case. We will know this condition is satisfied when we have the following constrain: $\epsilon_{i\alpha} - \epsilon_{k\gamma} \pm \hbar\omega_\lambda = 0$ or $\epsilon_{i\alpha} - \epsilon_{k\gamma} \pm \hbar\omega_{\lambda'} = 0$. Note the two equalities cannot be fulfilled at the same time since this requires $\lambda = \lambda'$ which situation is negligible due to the small probability. Without loss of generality, we may consider the first condition, and thus we shall only keep the first term in the Eq. (4.61) for $A_{ij}^{\alpha\beta,ind}$. Another natural constrain is the energy conservation for the whole process: $\epsilon_{i\alpha} - \epsilon_{j\beta} \pm \hbar\omega_\lambda \pm \hbar\omega_{\lambda'} = 0$. Together with the two equalities, we have

$$\pm\hbar\omega_\lambda = \epsilon_{k\gamma} - \epsilon_{i\alpha}, \quad \pm\hbar\omega_{\lambda'} = \epsilon_{j\beta} - \epsilon_{k\gamma}. \tag{4.62}$$

With the above conditions we can rewrite the direct and indirect hopping matrix by

$$\begin{aligned} A_{ij}^{\alpha\beta,dir} \;=\; & \frac{1}{\epsilon_{k\gamma} - \epsilon_{i\alpha}} \big[\langle \psi_j^\beta, n_q \mp 1, n_{q'} \mp 1 | H_{p-ph} | \psi_i^\alpha, n_q \mp 1 \rangle \langle \psi_i^\alpha, n_q \mp 1 | H_{p-ph} | \psi_i^\alpha, n_q \rangle \\ & - \langle \psi_j^\beta, n_q \mp 1, n_{q'} \mp 1 | H_{p-ph} | \psi_j^\beta, n_{q'} \mp 1 \rangle \langle \psi_j^\beta, n_{q'} \mp 1 | H_{p-ph} | \psi_i^\alpha, n_{q'} \rangle \big] + \\ & + \frac{1}{\epsilon_{j\beta} - \epsilon_{k\gamma}} \big[\langle \psi_j^\beta, n_q \mp 1, n_{q'} \mp 1 | H_{p-ph} | \psi_i^\alpha, n_{q'} \mp 1 \rangle \langle \psi_i^\alpha, n_{q'} \mp 1 | H_{p-ph} | \psi_i^\alpha, n_{q'} \rangle \\ & - \langle \psi_j^\beta, n_q \mp 1, n_{q'} \mp 1 | H_{p-ph} | \psi_j^\beta, n_q \mp 1 \rangle \langle \psi_j^\beta, n_q \mp 1 | H_{p-ph} | \psi_i^\alpha, n_q \rangle \big], \end{aligned} \tag{4.63}$$

and

$$A_{ij}^{\alpha\beta,ind} = \frac{\langle\psi_j^\beta, n_q \mp 1, n_{q'} \mp 1|H_{p-ph}|\psi_k^\gamma, n_q \mp 1\rangle\langle\psi_k^\gamma, n_q \mp 1|H_{p-ph}|\psi_i^\alpha, n_q\rangle}{\epsilon_{i\alpha} - \epsilon_{k\gamma} \pm \hbar\omega_\lambda + i\hbar s_+}. \tag{4.64}$$

Substituting the result of (4.58) into above formulae yields

$$\begin{aligned} A_{ij}^{\alpha\beta,dir} &= -\frac{1}{\epsilon_{k\gamma} - \epsilon_{i\alpha}} \frac{t_{i\alpha,j\beta}}{\epsilon_{i\alpha} - \epsilon_{j\beta}} \left[g_\lambda^{(\mp)} g_{\lambda'}^{(\mp)} (e^{\pm i\vec{q}_{\lambda'}\cdot\vec{R}_j} - e^{\pm i\vec{q}_{\lambda'}\cdot\vec{R}_i})(e^{\pm i\vec{q}_\lambda\cdot\vec{R}_i} - e^{\pm i\vec{q}_\lambda\cdot\vec{R}_j}) \right] - \\ &\quad -\frac{1}{\epsilon_{j\beta} - \epsilon_{k\gamma}} \frac{t_{i\alpha,j\beta}}{\epsilon_{i\alpha} - \epsilon_{j\beta}} \left[g_\lambda^{(\mp)} g_{\lambda'}^{(\mp)} (e^{\pm i\vec{q}_\lambda\cdot\vec{R}_j} - e^{\pm i\vec{q}_\lambda\cdot\vec{R}_i})(e^{\pm i\vec{q}_{\lambda'}\cdot\vec{R}_i} - e^{\pm i\vec{q}_{\lambda'}\cdot\vec{R}_j}) \right] \\ &= \frac{t_{i\alpha,j\beta}}{(\epsilon_{i\alpha} - \epsilon_{k\gamma})(\epsilon_{j\beta} - \epsilon_{k\gamma})} \left[g_\lambda^{(\mp)} g_{\lambda'}^{(\mp)} (e^{\pm i\vec{q}_{\lambda'}\cdot\vec{R}_i} - e^{\pm i\vec{q}_{\lambda'}\cdot\vec{R}_j})(e^{\pm i\vec{q}_\lambda\cdot\vec{R}_i} - e^{\pm i\vec{q}_\lambda\cdot\vec{R}_j}) \right], \end{aligned} \tag{4.65}$$

and

$$\begin{aligned} A_{ij}^{\alpha\beta,ind} &= -\frac{1}{\epsilon_{i\alpha} - \epsilon_{k\gamma} \pm \hbar\omega_\lambda + i\hbar s_+} \frac{t_{i\alpha,k\gamma}}{\epsilon_{i\alpha} - \epsilon_{k\gamma}} \frac{t_{k\gamma,j\beta}}{\epsilon_{k\gamma} - \epsilon_{j\beta}} g_\lambda^{(\mp)} g_{\lambda'}^{(\mp)} \times \\ &\quad \times (e^{\pm i\vec{q}_\lambda\cdot\vec{R}_k} - e^{\pm i\vec{q}_\lambda\cdot\vec{R}_i})(e^{\pm i\vec{q}_{\lambda'}\cdot\vec{R}_j} - e^{\pm i\vec{q}_{\lambda'}\cdot\vec{R}_k}). \end{aligned} \tag{4.66}$$

The total transition rate due to two-phonon process is obtained by summing over all λ, λ' modes. We thus have

$$P_{ij}^{(2)} = \frac{2\pi}{\hbar} \sum_{\vec{q}_\lambda, \vec{q}_{\lambda'}} |A_{ij}^{\alpha\beta,dir}(\vec{q}_\lambda, \vec{q}_{\lambda'}) + A_{ij}^{\alpha\beta,ind}(\vec{q}_\lambda, \vec{q}_{\lambda'})|^2 \delta(\epsilon_{i\alpha} - \epsilon_{j\beta} \pm \hbar\omega_\lambda \pm \hbar\omega_{\lambda'}). \tag{4.67}$$

From the former discussion we already know the Hall effect is contributed from the interference between direct and indirect hopping amplitudes. A non-zero interference requires any randomness of the phase must be exactly canceled when calculating the phase difference between the two paths. From the Eq. (4.65) we can see $A_{ij}^{\alpha\beta,dir}$ contains no phase factor with respect to $\mathbf{R}_k$. Then after summation over phonon modes, only the term with respect to $e^{\pm i\vec{q}_\lambda\cdot\vec{R}_i \pm i\vec{q}_{\lambda'}\cdot\vec{R}_j}$ in $A_{ij}^{\alpha\beta,ind}$ (see Eq. (4.66)) needs

to be kept. With this result in mind, we obtain the contribution of two-phonon process to the Hall effect by

$$\begin{aligned} P_{ij}^{(2,H)} &= \frac{2\pi}{\hbar}\sum_{\vec{q}_\lambda,\vec{q}_{\lambda'}}(g_\lambda^{(\mp)}g_{\lambda'}^{(\mp)})^2\frac{1}{(\epsilon_{i\alpha}-\epsilon_{k\gamma})^2(\epsilon_{j\beta}-\epsilon_{k\gamma})^2}|t^*_{i\alpha,j\beta}+\frac{t_{i\alpha,k\gamma}t_{k\gamma,j\beta}}{\epsilon_{i\alpha}-\epsilon_{k\gamma}\pm\hbar\omega_\lambda+i\hbar s_+}|^2 \\ &\quad\times\delta(\epsilon_{i\alpha}-\epsilon_{j\beta}\pm\hbar\omega_\lambda\pm\hbar\omega_{\lambda'}). \end{aligned} \tag{4.68}$$

Using the result $1/(x+i\eta_+)=P(1/x)-i\pi\delta(x)$, we further get

$$\begin{aligned} P_{ij}^{(2,H)} &= \frac{(2\pi)^2}{\hbar}\sum_{\vec{q}_\lambda,\vec{q}_{\lambda'}}(g_\lambda^{(\mp)}g_{\lambda'}^{(\mp)})^2\frac{1}{(\epsilon_{i\alpha}-\epsilon_{k\gamma})^2(\epsilon_{j\beta}-\epsilon_{k\gamma})^2}\mathrm{Im}(t_{i\alpha,j\beta}t_{i\alpha,k\gamma}t_{k\gamma,j\beta}) \\ &\quad\times\delta(\epsilon_{i\alpha}-\epsilon_{j\beta}\pm\hbar\omega_\lambda\pm\hbar\omega_{\lambda'})\delta(\epsilon_{i\alpha}-\epsilon_{k\gamma}\pm\hbar\omega_\lambda) \\ &= \frac{(2\pi)^2}{\hbar}\sum_{\vec{q}_\lambda,\vec{q}_{\lambda'}}(g_\lambda^{(\mp)}g_{\lambda'}^{(\mp)})^2\frac{1}{(\epsilon_{i\alpha}-\epsilon_{k\gamma})^2(\epsilon_{j\beta}-\epsilon_{k\gamma})^2}\mathrm{Im}(t_{i\alpha,j\beta}t_{i\alpha,k\gamma}t_{k\gamma,j\beta}) \\ &\quad\times\delta(\epsilon_{k\gamma}-\epsilon_{j\beta}\pm\hbar\omega_{\lambda'})\delta(\epsilon_{i\alpha}-\epsilon_{k\gamma}\pm\hbar\omega_\lambda). \end{aligned} \tag{4.69}$$

Similarly, we can calculate the hopping with one- and three-phonon process, namely, in the direct hopping the particle emits or absorbs one phonon, while in the indirect hopping it emits or absorbs three phonons. However, to have a nonzero interference between the one- and three-phonon process, one must require in the later process effectively only one real phonon is absorbed or emitted. Such situation is realized when the three-phonon process actually includes two intermediate processes during which a phonon will be first emitted and then reabsorbed in a later time (or first absorbed and then remitted). This phonon is a virtual one. Therefore for the direct hopping we have $|\psi_i^\alpha,n_q\rangle\rightarrow|\psi_j^\beta,n_q\mp1\rangle$ (and $n_q\longleftrightarrow n_{q'}$), which gives the transition matrix as (for $\vec{q}_\lambda$ mode, see Fig. 4.5)

$$A_{ij}^{\alpha\beta,dir} = i\frac{t_{i\alpha,j\beta}}{\epsilon_{i\alpha}-\epsilon_{j\beta}}g_\lambda^{(\mp)}(e^{\pm i\vec{q}_\lambda\cdot\vec{R}_j}-e^{\pm i\vec{q}_\lambda\cdot\vec{R}_i}). \tag{4.70}$$

The indirect three-phonon hopping process is much more complicated, and has a lot of different processes such as (see Fig. 4.6 for the typical diagrams representing

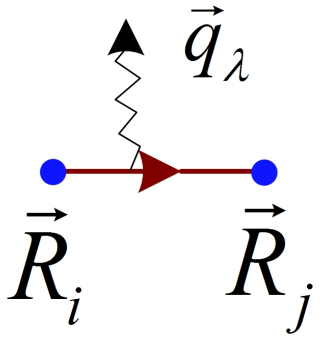

Fig. 4.5. The direct hopping process with one phonon emitted.

this process): (a) $|\psi_i^\alpha, n_{q'}\rangle \to |\psi_k^\gamma, n_{q'} \mp 1\rangle \to |\psi_j^\beta, n_q \mp 1, n_{q'} \mp 1\rangle \to |\psi_j^\beta, n_q \mp 1\rangle$, (b) $|\psi_i^\alpha, n_{q'}\rangle \to |\psi_k^\gamma, n_{q'} \mp 1\rangle \to |\psi_k^\beta, n_q \mp 1, n_{q'} \mp 1\rangle \to |\psi_j^\beta, n_q \mp 1\rangle$, (c) $|\psi_i^\alpha, n_{q'}\rangle \to |\psi_i^\alpha, n_{q'} \mp 1\rangle \to |\psi_k^\gamma, n_q \mp 1, n_{q'} \mp 1\rangle \to |\psi_j^\beta, n_q \mp 1\rangle$, (d) $|\psi_i^\alpha, n_q\rangle \to |\psi_i^\alpha, n_q \mp 1\rangle \to |\psi_k^\gamma, n_q \mp 1, n_{q'} \mp 1\rangle \to |\psi_j^\beta, n_q \mp 1\rangle$ (and $n_q \longleftrightarrow n_{q'}$), etc. However, we can simplify the discussion according to the results in the two-phonon process. First of all, according to the general discussion in the subsection 4.2.1, we know the Hall effect is contributed from the interference between direct and indirect terms with $\pi/2$ out-of-phase in the zero geometric phase case. This condition requires that one of the two intermediate processes should satisfy the energy conservation. Second, the direct hopping transition matrix with one-phonon includes only the phase factors $e^{\pm i\vec{q}_\lambda\cdot\vec{R}_j}, e^{\pm i\vec{q}_\lambda\cdot\vec{R}_i}$. Then in the three phonon-process we shall consider only the terms with such factors so that the random phase can be exactly canceled. Third, for the whole transition process the energy should be conserved. Bear in mind these conditions we obtain

$$\begin{aligned} A_{ij}^{\alpha\beta,ind} &= i\frac{1}{\epsilon_{i\beta}-\epsilon_{k\gamma}\pm\hbar\omega_{\lambda'}+i\hbar s_+}\frac{t_{i\alpha,k\gamma}}{(\epsilon_{i\alpha}-\epsilon_{k\gamma})^2}\frac{t_{k\gamma,j\beta}}{\epsilon_{k\gamma}-\epsilon_{j\beta}}g_\lambda^{(\mp)}|g_{\lambda'}^{(\mp)}|^2 e^{\pm i\vec{q}_\lambda\cdot\vec{R}_j} \\ &\quad -i\frac{1}{\epsilon_{j\beta}-\epsilon_{k\gamma}\pm\hbar\omega_{\lambda'}+i\hbar s_+}\frac{t_{i\alpha,k\gamma}}{\epsilon_{i\alpha}-\epsilon_{k\gamma}}\frac{t_{k\gamma,j\beta}}{(\epsilon_{k\gamma}-\epsilon_{j\beta})^2}g_\lambda^{(\mp)}|g_{\lambda'}^{(\mp)}|^2 e^{\pm i\vec{q}_\lambda\cdot\vec{R}_i}. \end{aligned} \tag{4.71}$$

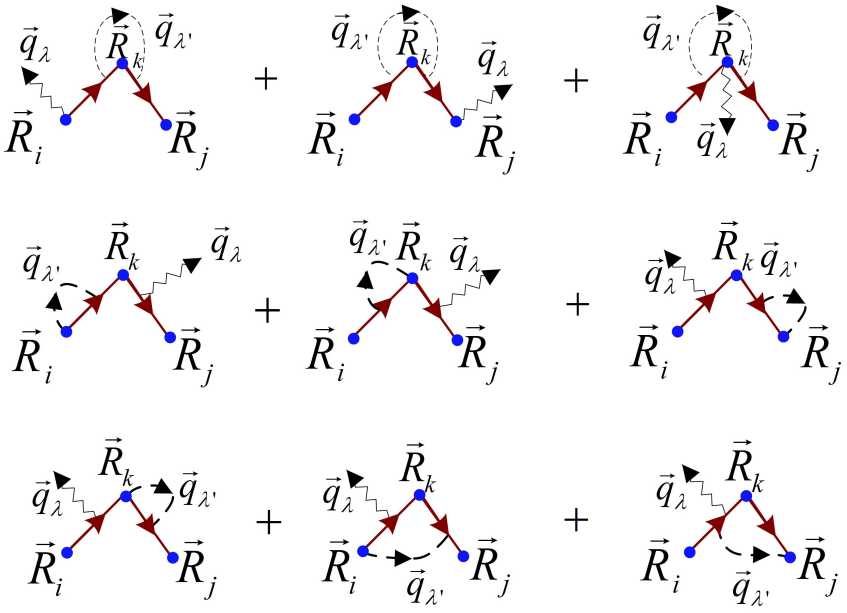

Fig. 4.6. Typical three-phonon (one real phonon) indirect hopping processes. In these diagrams the $\vec{q}_{\lambda'}$ is a virtual phonon. Also, we present only the phonon-emission processes.

The Hall transition rate arising from the interference between one- and three-phonon processes is obtained by the Fermi golden rule, similar as the procedure in the two-phonon process. The result is given by

$$\begin{aligned} P_{ij}^{(3,H)} &= \frac{(2\pi)^2}{\hbar}\sum_{\vec{q}_\lambda,\vec{q}_{\lambda'}}(g_\lambda^{(\mp)}g_{\lambda'}^{(\mp)})^2\mathrm{Im}(t_{i\alpha,j\beta}t_{i\alpha,k\gamma}t_{k\gamma,j\beta})\times \\ &\times \left[\frac{\delta(\epsilon_{i\alpha}-\epsilon_{j\beta}\pm\hbar\omega_\lambda)\delta(\epsilon_{i\alpha}-\epsilon_{k\gamma}\pm\hbar\omega_{\lambda'})}{(\epsilon_{i\alpha}-\epsilon_{j\beta})^2(\epsilon_{i\alpha}-\epsilon_{k\gamma})^2}+\right. \\ &\left.+\frac{\delta(\epsilon_{i\alpha}-\epsilon_{j\beta}\pm\hbar\omega_\lambda)\delta(\epsilon_{j\beta}-\epsilon_{k\gamma}\pm\hbar\omega_{\lambda'})}{(\epsilon_{i\alpha}-\epsilon_{j\beta})^2(\epsilon_{j\beta}-\epsilon_{k\gamma})^2}\right]. \end{aligned} \tag{4.72}$$

Together with Eqs. (4.69) and (4.72) we obtain the total Hall transition rate by

$$\begin{aligned}
P_{ij}^{(H)} &= P_{ij}^{(2,H)} + P_{ij}^{(3,H)} \\
&= \frac{(2\pi)^2}{\hbar} \sum_{\vec{q}_\lambda, \vec{q}_{\lambda'}} (g_\lambda^{(\mp)} g_{\lambda'}^{(\mp)})^2 \mathrm{Im}(t_{i\alpha,j\beta} t_{i\alpha,k\gamma} t_{k\gamma,j\beta}) \times \\
&\times \left[\frac{\delta(\epsilon_{i\alpha} - \epsilon_{j\beta} \pm \hbar\omega_\lambda)\delta(\epsilon_{i\alpha} - \epsilon_{k\gamma} \pm \hbar\omega_{\lambda'})}{(\epsilon_{i\alpha} - \epsilon_{j\beta})^2 (\epsilon_{i\alpha} - \epsilon_{k\gamma})^2} + \right. \\
&+ \frac{\delta(\epsilon_{i\alpha} - \epsilon_{j\beta} \pm \hbar\omega_\lambda)\delta(\epsilon_{j\beta} - \epsilon_{k\gamma} \pm \hbar\omega_{\lambda'})}{(\epsilon_{i\alpha} - \epsilon_{j\beta})^2 (\epsilon_{j\beta} - \epsilon_{k\gamma})^2} + \\
&\left. + \frac{\delta(\epsilon_{k\gamma} - \epsilon_{j\beta} \pm \hbar\omega_{\lambda'})\delta(\epsilon_{i\alpha} - \epsilon_{k\gamma} \pm \hbar\omega_\lambda)}{(\epsilon_{i\alpha} - \epsilon_{k\gamma})^2 (\epsilon_{j\beta} - \epsilon_{k\gamma})^2} \right]. \qquad (4.73)
\end{aligned}$$

We shall now sum above equation over all the phonon modes λ, λ'. Recall that $g_\lambda^{(\mp)}$ is given by the Eq. (4.59). By replacing the summation by the integration over over phonon modes we obtain

$$\begin{aligned}
P_{ij}^{(H)} &= \frac{(2\pi)^2}{\hbar} \frac{V^2}{(8\pi^3)^2} \int d^2\vec{q}_\lambda d^2\vec{q}_{\lambda'} (g_\lambda^{(\mp)} g_{\lambda'}^{(\mp)})^2 \mathrm{Im}(t_{i\alpha,j\beta} t_{i\alpha,k\gamma} t_{k\gamma,j\beta}) \times \\
&\times \left[\frac{\delta(\epsilon_{i\alpha} - \epsilon_{j\beta} \pm \hbar\omega_\lambda)\delta(\epsilon_{i\alpha} - \epsilon_{k\gamma} \pm \hbar\omega_{\lambda'})}{(\epsilon_{i\alpha} - \epsilon_{j\beta})^2 (\epsilon_{i\alpha} - \epsilon_{k\gamma})^2} + \right. \\
&+ \frac{\delta(\epsilon_{i\alpha} - \epsilon_{j\beta} \pm \hbar\omega_\lambda)\delta(\epsilon_{j\beta} - \epsilon_{k\gamma} \pm \hbar\omega_{\lambda'})}{(\epsilon_{i\alpha} - \epsilon_{j\beta})^2 (\epsilon_{j\beta} - \epsilon_{k\gamma})^2} + \\
&\left. + \frac{\delta(\epsilon_{k\gamma} - \epsilon_{j\beta} \pm \hbar\omega_{\lambda'})\delta(\epsilon_{i\alpha} - \epsilon_{k\gamma} \pm \hbar\omega_\lambda)}{(\epsilon_{i\alpha} - \epsilon_{k\gamma})^2 (\epsilon_{j\beta} - \epsilon_{k\gamma})^2} \right] \\
&= \sum_{\alpha\beta\gamma} E_1^4 \left(\frac{V}{\pi\hbar^4 c^5 NM} \right)^2 \mathrm{Im}(t_{i\alpha,j\beta} t_{i\alpha,k\gamma} t_{k\gamma,j\beta}) \times \\
&\times \left\{ |\Delta_{ij}\Delta_{ik}| \frac{1}{|e^{\epsilon_{i\alpha}/k_BT} - e^{\epsilon_{j\beta}/k_BT}|} \frac{1}{|1 - e^{-(\epsilon_{i\alpha} - \epsilon_{k\gamma})/k_BT}|} + \right. \\
&+ |\Delta_{ij}\Delta_{jk}| \frac{1}{|e^{\epsilon_{i\alpha}/k_BT} - e^{\epsilon_{j\beta}/k_BT}|} \frac{1}{|1 - e^{-(\epsilon_{j\alpha} - \epsilon_{k\gamma})/k_BT}|} + \\
&\left. + |\Delta_{ik}\Delta_{kj}| \frac{1}{|e^{\epsilon_{i\alpha}/k_BT} - e^{\epsilon_{k\beta}/k_BT}|} \frac{1}{|1 - e^{-(\epsilon_{k\alpha} - \epsilon_{j\gamma})/k_BT}|} \right\} e^{\epsilon_{i\alpha}/k_BT}, \qquad (4.74)
\end{aligned}$$

where $\Delta_{ij} = \epsilon_{i\alpha} - \epsilon_{j\beta}$. For simplicity, we rewrite the Hall transition rate in the form

$$P_{ij}^{(H)} = \mathcal{Z}\mathcal{L}_{ijk} e^{\epsilon_{i\alpha}/k_B T}, \tag{4.75}$$

with $\mathcal{L}_{ijk}$ given by Eq. (4.76)and

$$\begin{aligned}
\mathcal{L}_{ijk} &= \mathcal{Z}^{-1} \sum_{\alpha\beta\gamma} \left(\frac{V E_1^2}{\pi \hbar^4 c^5 N M} \right)^2 \mathrm{Im}(t_{i\alpha,j\beta} t_{i\alpha,k\gamma} t_{k\gamma,j\beta}) \times \\
&\times \left\{ |\Delta_{ij}\Delta_{ik}| \frac{1}{|e^{\epsilon_{i\alpha}/k_B T} - e^{\epsilon_{j\beta}/k_B T}|} \frac{1}{|1 - e^{-(\epsilon_{i\alpha} - \epsilon_{k\gamma})/k_B T}|} \right. \\
&\quad + |\Delta_{ij}\Delta_{jk}| \frac{1}{|e^{\epsilon_{i\alpha}/k_B T} - e^{\epsilon_{j\beta}/k_B T}|} \frac{1}{|1 - e^{-(\epsilon_{j\alpha} - \epsilon_{k\gamma})/k_B T}|} + \\
&\quad \left. + |\Delta_{ik}\Delta_{kj}| \frac{1}{|e^{\epsilon_{i\alpha}/k_B T} - e^{\epsilon_{k\beta}/k_B T}|} \frac{1}{|1 - e^{-(\epsilon_{k\alpha} - \epsilon_{j\gamma})/k_B T}|} \right\}.
\end{aligned} \tag{4.76}$$

It is straightforward to show an important property that

$$\mathcal{L}_{ijk} = \mathcal{L}_{jki} = \mathcal{L}_{kij} = -\mathcal{L}_{jik} = -\mathcal{L}_{ikj} = -\mathcal{L}_{kji}. \tag{4.77}$$

This result has several consequences. First, the current due to $P_{ij}^{(H)}$ between i and j sites may not be zero even when their voltages are equal $U_i = U_j$. This is actually a property of the Hall effect. The Hall current reads in this case

$$\begin{aligned}
I_{ij}^{(H)} &= e\big[P_{ij}^{(H)} f_i(1-f_j)(1-f_k) - P_{ji}^{(H)} f_j(1-f_i)(1-f_k)\big] + \\
&\quad + e\big[P_{ij}^{(H)} f_i f_k(1-f_j) - P_{ji}^{(H)} f_j f_k(1-f_i)\big] \\
&= e\big[P_{ij}^{(H)} f_i(1-f_j) - P_{ji}^{(H)} f_j(1-f_i)\big].
\end{aligned} \tag{4.78}$$

In the first equality of above formula, the first term corresponds to the electron-like transport, and the second one corresponds to the hole-like transport. Using the notation $\mathcal{L}_{ijk}$ we get

$$I_{ij}^{(H)} = e\mathcal{L}_{ijk}\big[f_i(1-f_j)e^{\epsilon_i/k_B T} + f_j(1-f_i)e^{\epsilon_j/k_B T}\big]. \tag{4.79}$$

Second, for an isolated triad composed of the three sites (i, j, k) with identical voltage, we can see the currents I_{ij}, I_{jk}, I_{ki} consist of the clockwise (or counter clockwise, depending on the magnetization and SO coupling of the system) circulating current. This result can be easily understood by comparing with the ordinary Hall effect in the semiclassical picture: The electrons/holes move along circular orbitals in the presence of an external magnetic field (similarly, in the quantum Hall effect with open boundary, a chiral edge current is obtained). Third, when a voltage difference between one and the other two sites (e.g. between k and i, j sites), the current through $i - j$ bond will be different in magnitude from the one through $j - k$ and $k - i$ bonds. In this way, a net current between i and j sites occurs. This is exactly consistent with the result of the Hall effect: an electric field leads to a transverse Hall current.

4.2.5 Linear response

Now we can derive the current between each pair of impurity sites in the linear response approximation. For convenience, we denote by $\tilde{I}_{ij}$ the current through the $i - j$ bond, and I_{ij} the net current between i and j sites. According to the results discussed in the former subsections, we have

$$\begin{aligned} \tilde{I}_{ij} &= \tilde{I}^{(0)}_{ij} + \tilde{I}^{(H)}_{ij} \\ &= e\big[P^{(0)}_{ij} f_i(1 - f_j) - P^{(0)}_{ji} f_j(1 - f_i)\big] + e\big[P^{(H)}_{ij} f_i(1 - f_j) - P^{(H)}_{ji} f_j(1 - f_i)\big]. \end{aligned} \tag{4.80}$$

From the subsection 4.2.3 we already know $\tilde{I}_{ij}^{(0)} = G_{ij}V_{ij}$. The term related to the Hall effect reads

$$\tilde{I}_{ij}^{(H)} = e\big[e^{\tilde{\epsilon}_i/k_BT}\sum_k \tilde{z}_{ijk}\tilde{\mathcal{L}}_{ijk}f_i(1-f_j) + e^{\tilde{\epsilon}_j/k_BT}\sum_k \tilde{z}_{ijk}\tilde{\mathcal{L}}_{ijk}f_j(1-f_i)\big], \tag{4.81}$$

where $\tilde{z}_{ijk} = e^{-(\tilde{\epsilon}_i+\tilde{\epsilon}_j+\tilde{\epsilon}_k)/k_BT}$, and k indicates the sites nearby i and j. In the typical situation we only need to consider one or two sites nearby the $i-j$ bond. Again, note in the hopping conduction regime, we are interested in the states with energy satisfying $|\tilde{\epsilon}_i - \mu_i| \gg k_BT$, which dominate the contribution to the charge transport. The above formula can be recast into

$$\tilde{I}_{ij}^{(H)} = e(1-f_i)(1-f_j)\big[\sum_k \tilde{z}_{ijk}\tilde{\mathcal{L}}_{ijk}(e^{\tilde{\mu}_i/k_BT} + e^{\tilde{\mu}_j/k_BT})\big]. \tag{4.82}$$

Note $\tilde{\mu}_i = \mu_0 + \delta\mu_i$, with $\delta\mu_i$ the correction to chemical potential at i site due to external electric field. The electric voltage difference can be defined by $V_{ij} = (\delta\mu_i - \delta\mu_j)/e$. The linear response requires that $|\delta\mu_i| \ll k_BT$. We then obtain in the linear order of the voltage difference that

$$\tilde{I}_{ij}^{(H)} = e^2(1-f_i)(1-f_j)\sum_k \tilde{z}_{ijk}\tilde{\mathcal{L}}_{ijk}e^{\mu_0/k_BT}\frac{2+V_i+V_j}{k_BT}. \tag{4.83}$$

The net current between i and j sites is obtained by the simple identity: $I_{ij} = \tilde{I}_{ij}^{(0)} + \frac{1}{2}(2\tilde{I}_{ij}^{(H)} - \tilde{I}_{kj}^{(H)} - \tilde{I}_{ji}^{(H)})$ and thus

$$\begin{aligned}\tilde{I}_{ij} &= I_{ij}^{(0)} + \frac{1}{2}e^2(1-f_i)(1-f_j)\sum_k \tilde{z}_{ijk}\tilde{\mathcal{L}}_{ijk}e^{\mu_0/k_BT}\frac{V_{ik}+V_{jk}}{k_BT} \\ &= G_{ij}V_{ij} + \sum_k F_{ijk}(V_{ik}+V_{jk}),\end{aligned} \tag{4.84}$$

where F_{ijk} is defined through

$$\begin{aligned}
F_{ijk} &= \frac{e^2}{2k_BT}(1-f_i)(1-f_j)\tilde{z}_{ijk}\tilde{\mathcal{L}}_{ijk}e^{\mu_0/k_BT} \\
&= \frac{e^2}{2k_BT}(1-f_i)(1-f_j)e^{\mu_0/k_BT}\sum_{\alpha\beta\gamma}\left(\frac{VE_1^2}{\pi\hbar^4c^5NM}\right)^2 \mathrm{Im}(t_{i\alpha,j\beta}t_{i\alpha,k\gamma}t_{k\gamma,j\beta})\times \\
&\quad\times\Bigg\{|\Delta_{ij}\Delta_{ik}|\frac{1}{|e^{\epsilon_{i\alpha}/k_BT}-e^{\epsilon_{j\beta}/k_BT}|}\frac{1}{|1-e^{-(\epsilon_{i\alpha}-\epsilon_{k\gamma})/k_BT}|}+ \\
&\quad+|\Delta_{ij}\Delta_{jk}|\frac{1}{|e^{\epsilon_{i\alpha}/k_BT}-e^{\epsilon_{j\beta}/k_BT}|}\frac{1}{|1-e^{-(\epsilon_{j\alpha}-\epsilon_{k\gamma})/k_BT}|}+ \\
&\quad+|\Delta_{ik}\Delta_{kj}|\frac{1}{|e^{\epsilon_{i\alpha}/k_BT}-e^{\epsilon_{k\beta}/k_BT}|}\frac{1}{|1-e^{-(\epsilon_{k\alpha}-\epsilon_{j\gamma})/k_BT}|}\Bigg\}. \qquad (4.85)
\end{aligned}$$

In the limit $|\epsilon_i-\mu_i|\gg k_BT$ and $|\epsilon_i-\epsilon_j|\gg k_BT$ this formula can be recast into

$$\begin{aligned}
F_{ijk} &= \frac{e^2}{2k_BT}\sum_{\alpha\beta\gamma}\left(\frac{VE_1^2}{\pi\hbar^4c^5NM}\right)^2 \mathrm{Im}(t_{i\alpha,j\beta}t_{i\alpha,k\gamma}t_{k\gamma,j\beta})\times \\
&\quad\times\Bigg\{|\Delta_{ij}\Delta_{ik}|e^{-\frac{1}{2k_BT}(|\epsilon_{j\beta}|+|\epsilon_{k\gamma}|+|\epsilon_{i\alpha}-\epsilon_{k\gamma}|+|\epsilon_{i\alpha}-\epsilon_{j\beta}|)}+ \\
&\quad+|\Delta_{ij}\Delta_{jk}|e^{-\frac{1}{2k_BT}(|\epsilon_{i\alpha}|+|\epsilon_{k\gamma}|+|\epsilon_{j\beta}-\epsilon_{k\gamma}|+|\epsilon_{i\alpha}-\epsilon_{j\beta}|)}+ \\
&\quad+|\Delta_{ik}\Delta_{kj}|e^{-\frac{1}{2k_BT}(|\epsilon_{i\alpha}|+|\epsilon_{j\beta}|+|\epsilon_{i\alpha}-\epsilon_{k\gamma}|+|\epsilon_{k\gamma}-\epsilon_{j\beta}|)}\Bigg\}. \qquad (4.86)
\end{aligned}$$

In the above formula we have rewritten $\epsilon_{i\alpha}-\mu_0$ as $\epsilon_{i\alpha}$ for simplicity. On the other hand, the direct conductance G_{ij} takes the form

$$G_{ij}=\frac{e^2}{k_BT}\sum_{\alpha\beta}\frac{VE_1^2}{\pi\hbar^4c^5NM}|t_{i\alpha,j\beta}|^2|\Delta_{ij}|e^{-\frac{1}{2k_BT}(|\epsilon_{i\alpha}|+|\epsilon_{j\beta}|+|\epsilon_{i\alpha}-\epsilon_{j\beta}|)}. \qquad (4.87)$$

To this step we have obtained the microscopic currents in a single triad by considering the electron-phonon scattering, from which the conductance and resistance for any single triad can be determined. The whole system is a macroscopic system which includes a large number of impurities randomly distributed in the material. The macroscopic physical quantity (e.g. the conductivities) for the whole system,

however, is not straightforward to evaluate based on the microscopic conductances obtained above. To perform this calculation, we shall resort to the percolation theory in the next section.

5. CONFIGURATION AVERAGING IN THE HOPPING REGIME

5.1 Percolation theory

Percolation theory is an approach to deal with the long-range connectivity in random systems. For example, take a regular lattice (e.g. cubic lattice), and randomly fill in it with sites (vertices) or bonds (edges) with a statistically independent probability p. Above a critical threshold p_c, the long-range connectivity first appears, namely, the long-range critical percolation path occurs when the density of randomly distributed sites reaches a critical value.

To employ the percolation theory for the AHE, we first map the present random impurity system to a random resistor network by connecting each pair of impurity sites with the direct resistor $Z_{ij} = 1/G_{ij}$. The Hall effect will be treated as a perturbation to the obtained resistor network. The charge transport will be dominated by some critical paths/clusters, i.e. the percolation paths/clusters, rather than by the whole resistor network. Therefore, the portions of the resistor network that have little contribution to the charge transport is negligible and can be treated as disconnected. To quantify this picture, we introduce a cut-off $G_c(T)$ for the direct conductance to redefine the connection and disconnection between any two impurity sites. When the conductance between two sites (e.g. i and j) satisfies $G_{ij} \geq G_c$, we say such two sites are connected with a finite resistor Z_{ij}. Otherwise, such two sites are treated as disconnected, i.e. $G_{ij} \to 0$. For this we reach a simplified resistor network determined by G_c. The average connectivity $\bar{n}$ per impurity site depends on the magnitude of the cut-off. It can expected that the choice of a smaller cut-off gives a larger average connectivity. Percolation path/cluster appears when the average connectivity per impurity site reaches some critical value n_c. This is equivalent to the case that the filling probability p of bonds reaches the threshold value p_c. To correctly describe the charge transport in the disordered insulating regime, the cut-off $G_c(T)$ should be properly chosen so that the long-range critical paths/clusters

appear and span the whole material. The charge transport is then dominated by such percolation path/cluster in the insulating regime. It is also noteworthy the cut-off cannot be too small. For example, if one chooses $G_c \to 0$, the resulted macroscopic resistivity/conductivity will be the exact since in this case one does not cut the connection between any pair of sites, but such a choice is meaningless according to former analysis. The macroscopic physical quantities will finally be obtained by averaging over the percolation path/cluter.

5.1.1 Random resistor network

Note the hopping coefficient $t_{i\alpha,j\beta}$ is generally an exponential decaying function of the distance between i and j sites. We can write down the direct conductance in the form

$$G_{ij} = G_0(T) e^{-2aR_{ij} - \frac{1}{2k_BT}(|\epsilon_{i\alpha}|+|\epsilon_{j\beta}|+|\epsilon_{i\alpha}-\epsilon_{j\beta}|)}, \tag{5.1}$$

where a^{-1} representing the localization length of the impurity states and $R_{ij} = |\mathbf{R}_i - \mathbf{R}_j|$. $G_0(T)$ gives at most a power law on temperature. To map the random impurity system to a random resistor network, we introduce the cut-off for the direct conductance in the following form

$$G_c(T) = G_0 e^{-\frac{\xi(T)}{k_BT}}, \tag{5.2}$$

where $\xi(T)/(k_BT)$ is a decreasing function of T, indicating the material is in the insulating regime. The form of $\xi(T)$ will be specified later. With the help of the cut-off $G_c(T)$, we can define the connectivity between two impurity sites. Namely, a

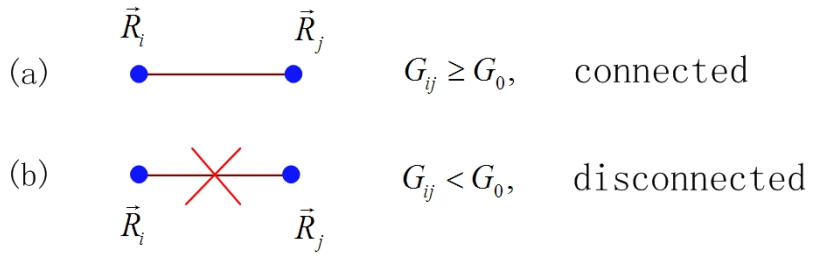

Fig. 5.1. Two sites i and j are connected when $G_{ij} \geq G_0$ and disconnected when $G_{ij} < G_0$.

pair of sites with conductances $G_{ij} \geq G_c(T)$ will be treated as connected. Otherwise, they are disconnected (see Fig. 5.1). The condition $G_{ij} \geq G_c$ is equivalent to

$$2aR_{ij} + \frac{1}{2k_BT}(|\epsilon_{i\alpha}| + |\epsilon_{j\beta}) \leq \xi(T)/k_BT. \tag{5.3}$$

To quantify the connectivity between impurity sites, as determined by above inequality, we calculate $n(\epsilon_i, \xi)$, the average number of sites connected to the site i with energy ϵ_i satisfying above condition. It is straightforward to know

$$n(\epsilon_i, \xi) = \int d\epsilon_j \int d^3\vec{r}_{ij}\rho(\epsilon_j, \vec{r}_{ij})\Theta\big(\xi(T)/k_BT - 2aR_{ij} - \frac{1}{2k_BT}(|\epsilon_{i\alpha}| + |\epsilon_{j\beta}|)\big), \tag{5.4}$$

where $\rho(\epsilon_j, \vec{r}_{ij})$ is the DOS. Consider the distribution of impurity sites is spatially homogeneous. We have for the DOS

$$\begin{aligned} \rho(\epsilon_j, \vec{r}_{ij}) &= \sum_i \delta(\epsilon - \epsilon_i)\delta(\vec{r} - \vec{r}_i) \\ &\approx \frac{1}{V}\sum_i \delta(\epsilon - \epsilon_i). \end{aligned} \tag{5.5}$$

Thus we have further from Eq. (5.4) that

$$\begin{aligned} n(\epsilon_i,\xi) &= \frac{1}{(2ak_BT)^3}\frac{4\pi}{3}\Big[\int_0^{\epsilon_i} d\epsilon_j\rho(\epsilon_j)(\xi-\epsilon_i)^3+\int_{\epsilon_i}^{\xi} d\epsilon_j\rho(\epsilon_j)(\xi-\epsilon_j)^3 \\ &\quad +\int_{-(\xi-|\epsilon_i|)}^{0}\rho(\epsilon_j)(\xi-|\epsilon_i|-|\epsilon_j|)^3\Big]. \end{aligned} \tag{5.6}$$

When $\rho(\epsilon)=\rho_0$ is a constant, we obtain [84]

$$n(\epsilon_i,\xi)=\frac{2\pi}{3}\frac{\rho_0}{(2ak_BT)^3}(\xi-|\epsilon_i|)^2(\xi^2-|\epsilon_i|^2). \tag{5.7}$$

5.1.2 Percolation cluster and configuration integral

Since the charge transport is through the critical percolation paths, the macroscopic physical quantities will be averaged over the percolation path/cluster. To derive the general formula for the configuration averaging of the physical quantities, we introduce another important parameter, $P_n(\epsilon_i,\xi)$, the probability that the n-th smallest resistor connected to the i site has the resistance less than $1/G_c$. The number $n(\epsilon_i,\xi)$ can then be given in terms of $P_n(\epsilon_i,\xi)$ and

$$n(\epsilon_i,\xi)=\sum_n P_n(\epsilon_i,\xi), \tag{5.8}$$

The function of $P_n(\epsilon_i,\xi)$ is calculated according to the following formula (Poisson distribution) [84]

$$\begin{aligned} P_n(\epsilon_i,\xi) &= \frac{1}{(n-1)!}\int_0^{n(\epsilon_i,\xi)} e^{-x}x^{n-1}dx \\ &= e^{-n(\epsilon_i,\xi)}\sum_{k=n}^{\infty}[n(\epsilon_i,\xi)]^k/k!. \end{aligned} \tag{5.9}$$

It is straightforward to confirm the equality (5.8) with the result (5.9). A characteristic quantity of the resistor network is the average number of connections per

impurity site $\bar{n} = \langle n(\epsilon_i)\rangle_c$, where the calculation of $\langle ...\rangle_c$ will be given later. The percolation path/cluster appears when $\bar{n}$ reaches the critical value n_c with proper choice of the cut-off $G_c(T)$.

The averaging of physical quantities along critical percolation path/cluster can be obtained based on the formula of P_n. Since the averaging is over critical percolation paths/clusters rather than over the whole system, the probability function in the averaging evaluation will not only be proportional to density of states, but also depend on the values of P_n. We consider first the general situation. Suppose a physical quantity $F(\epsilon_1, \epsilon_2, ..., \epsilon_N; \vec{r}_1, \vec{r}_2, ..., \vec{r}_N)$ is a function of N impurity sites, requiring that the i-th site have at least n_i sites connected to it satisfying the condition (5.3) (see Fig. 5.2). The averaging of such physical quantity is given by

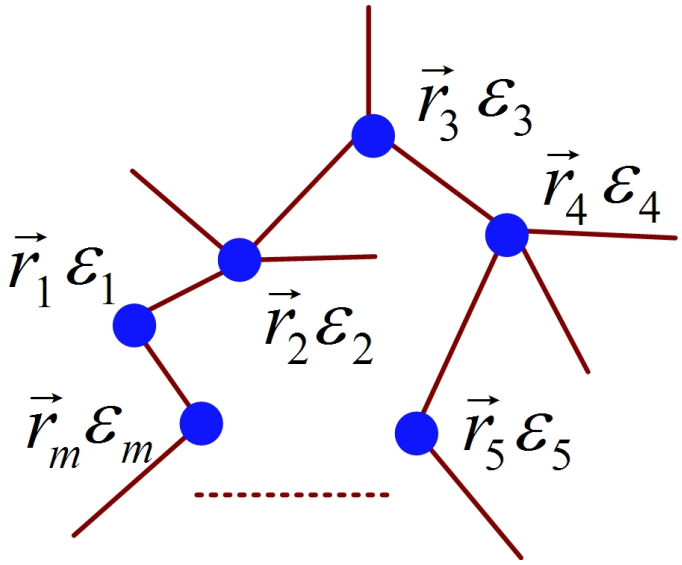

Fig. 5.2. Configuration integral of a general physical quantity composed of N impurity sites.

$$\begin{aligned}\langle F(\epsilon_1,...,\epsilon_N;\vec{r}_1,...,\vec{r}_N)\rangle_c &= \frac{1}{\mathcal{N}_F}\int d\epsilon_1...\int d\epsilon_N\int d^3\vec{r}_{12}...\int d^3\vec{r}_{N-1,N}\times \\ &\times \rho(\epsilon_1)\sum_{k=n_1}^{\infty}P_k(\epsilon_1)\rho(\epsilon_2)\sum_{k=n_2}^{\infty}P_k(\epsilon_2)...\rho(\epsilon_N)\times \\ &\times \sum_{k=n_N}^{\infty}P_k(\epsilon_N)F(\epsilon_1,\epsilon_2,...,\epsilon_N;\vec{r}_1,\vec{r}_2,...,\vec{r}_N), \qquad (5.10)\end{aligned}$$

with the normalization factor

$$\begin{aligned}\mathcal{N}_F &= \int d\epsilon_1\int d\epsilon_2...\int d\epsilon_N\int d^3\vec{r}_{12}\int d^3\vec{r}_{23}...\int d^3\vec{r}_{N-1,N}\times \\ &\times\rho(\epsilon_1)\sum_{k=n_1}^{\infty}P_k(\epsilon_1)\rho(\epsilon_2)\sum_{k=n_2}^{\infty}P_k(\epsilon_2)...\rho(\epsilon_N)\sum_{k=n_N}^{\infty}P_k(\epsilon_N). \qquad (5.11)\end{aligned}$$

It is clear that the probability function for the integral corresponding to the i-th site is given by $\rho(\epsilon_i)\sum_{k\geq\eta_i}P_k(\epsilon_i)$. The term $\sum_{k\geq\eta_i}P_k(\epsilon_i)$ entering the probability function is a consequence of the configuration averaging over the percolation cluster rather than over the whole impurity system. Moreover, this probability function also distinguishes the physical origins of the AHC and σ_{xx}. For σ_{xy}^{AH} one has $\eta_i = 3$, and for σ_{xx} one has $\eta_i = 2$. This indicates the averaging of σ_{xx} is performed along the one dimensional (1D) percolation path, while for AHE which is a two dimensional (2D) effect, one shall evaluate AHC over all triads connected in the 2D percolation cluster.

We can give several specific examples. The first example is the average value of $n(\epsilon_i,\xi)$ along the percolation path/cluster. Note $n(\epsilon_i,\xi)$ is a function of only one site. The averaging is straightforward and

$$\begin{aligned}\bar{n} &= \frac{\int d\epsilon_i n(\epsilon_i)\rho(\epsilon_i)\sum_{k=1}^{\infty}P_k(\epsilon_i)}{\int d\epsilon_\rho(\epsilon_i)\sum_{k=1}^{\infty}P_k(\epsilon_i)}, \\ &= \frac{\int d\epsilon_i n(\epsilon_i)\rho(\epsilon_i)n(\epsilon_i)}{\int d\epsilon_i n(\epsilon_i)\rho(\epsilon_i)}. \qquad (5.12)\end{aligned}$$

The hopping conduction occurs when the average value $\bar{n}$ reaches the critical value n_c. When the density of states $\rho(\epsilon)$ is a constant, we calculate straightforwardly

$$\begin{aligned}\bar{n} = \langle n(\epsilon,\xi)\rangle_c &= \frac{2\pi}{3}\frac{\rho_0}{(2ak_BT)^3}\frac{\int(\xi-|\epsilon_i|)^4(\xi^2-|\epsilon_i|^2)^2 d\epsilon_i}{\int(\xi-|\epsilon_i|)^2(\xi^2-|\epsilon_i|^2)d\epsilon_i} \\ &= 0.406\pi\rho_0\frac{1}{(2ak_BT)^3}\xi^4, \end{aligned} \tag{5.13}$$

from which we obtain the cut-off value ξ by

$$\xi(T) = \left[\frac{(2ak_BT)^3 n_c}{0.406\pi\rho_0}\right]^{1/4}. \tag{5.14}$$

Thus it gives

$$\xi\beta = \left(\frac{T_0}{T}\right)^{1/4}, \quad T_0 = 16\frac{a^3\bar{n}_c}{k_B\rho_0}, \tag{5.15}$$

which is the Mott law [66]. Accordingly, if we assume the density of states $\rho(\epsilon) \sim \epsilon^2$, we shall obtain the Efros-shklovskii (E-S) hopping regime [67].

Second, we give the formula for the longitudinal resistivity. Note the direct resistance is a function of two sites. We can therefore calculate the macroscopic longitudinal resistance by

$$\bar{R}_{xx} = \frac{N\int d\epsilon_i\int d\epsilon_j\int d^3\vec{r}_{ij}Z_{ij}(\epsilon_i,\epsilon_j;\vec{r}_{ij})\rho(\epsilon_i)\sum_{k=2}^{\infty}P_k(\epsilon_i)\rho(\epsilon_j)\sum_{k=2}^{\infty}P_k(\epsilon_j)}{\int d\epsilon_i\int d\epsilon_j\int d^3\vec{r}_{ij}\rho(\epsilon_i)\sum_{k=2}^{\infty}P_k(\epsilon_i)\rho(\epsilon_j)\sum_{k=2}^{\infty}P_k(\epsilon_j)}, \tag{5.16}$$

where N is the number of links along the percolation path. The above formula can be simplified by the fact that $\sum_{k=2}^{\infty}P_k(\epsilon_i) = n(\epsilon_i,\xi_c) - P_1(\epsilon_i,\xi_c) \propto [n(\epsilon_i,\xi_c)]^2$. We then reach

$$\bar{R}_{xx} = \frac{N\int d\epsilon_i\int d\epsilon_j\int d^3\vec{r}_{ij}Z_{ij}(\epsilon_i,\epsilon_j;\vec{r}_{ij})\rho(\epsilon_i)[n(\epsilon_i,\xi_c)]^2\rho(\epsilon_j)[n(\epsilon_j,\xi_c)]^2}{\int d\epsilon_i\int d\epsilon_j\int d^3\vec{r}_{ij}\rho(\epsilon_i)[n(\epsilon_i,\xi_c)]^2\rho(\epsilon_j)[n(\epsilon_j,\xi_c)]^2}. \tag{5.17}$$

The longitudinal resistivity is given by $\rho_{xx} = \bar{R}_{xx}/(n_d L_x)$, with n_d the density of the percolation paths and L_x the length of the material along x direction [84]. Accordingly, the longitudinal conductivity is obtained by $\sigma_{xx} = 1/\rho_{xx}$.

Finally, if the physical quantity is a function of three sites that consist of a triad, the averaging of such physical quantity is given by

$$\begin{aligned}
\bar{F}(\epsilon_1, \epsilon_2, \epsilon_3; \vec{r}_1, \vec{r}_2, \vec{r}_3) &= \frac{1}{\mathcal{N}_F^{(3)}} \int d\epsilon_1 d\epsilon_2 d\epsilon_3 \int d^3\vec{r}_{12} \int d^3\vec{r}_{23} F(\epsilon; \vec{r}) \rho(\epsilon_1) \times \\
&\quad \times \sum_{k=3}^{\infty} P_k(\epsilon_1)\rho(\epsilon_2) \sum_{k=3}^{\infty} P_k(\epsilon_2)\rho(\epsilon_3) \sum_{k=3}^{\infty} P_k(\epsilon_3) \\
&= \frac{1}{\mathcal{N}_F^{(3)}} \int d\epsilon_1 d\epsilon_2 d\epsilon_3 \int d^3\vec{r}_{12} \int d^3\vec{r}_{23} F(\epsilon; \vec{r}) \rho(\epsilon_1)[n(\epsilon_1)]^3 \times \\
&\quad \times \rho(\epsilon_2)[n(\epsilon_2)]^3 \rho(\epsilon_3)[n(\epsilon_3)]^3, \qquad (5.18)
\end{aligned}$$

with the normalization factor

$$\begin{aligned}
\mathcal{N}_F^{(3)} &= \int d\epsilon_1 d\epsilon_2 d\epsilon_3 \int d^3\vec{r}_{12} \int d^3\vec{r}_{23} \rho(\epsilon_1) \sum_{k=3}^{\infty} P_k(\epsilon_1)\rho(\epsilon_2) \sum_{k=3}^{\infty} P_k(\epsilon_2)\rho(\epsilon_3) \sum_{k=3}^{\infty} P_k(\epsilon_3) \\
&= \int d\epsilon_1 d\epsilon_2 d\epsilon_3 \int d^3\vec{r}_{12} \int d^3\vec{r}_{23} \rho(\epsilon_1)[n(\epsilon_1)]^3 \rho(\epsilon_2)[n(\epsilon_2)]^3 \rho(\epsilon_3)[n(\epsilon_3)]^3, \qquad (5.19)
\end{aligned}$$

In the next section we shall see the anomalous Hall conductivity/resistivity is calculated with this formula.

5.2 Configuration averaging of the AHC

In this section we provide the rigorous derivative of the configuration averaging of the AHC. From the above discussion we know the hopping conduction is dominated by the percolation path/cluster. Accordingly, in this regime the averaging number $\bar{n}$ of bonds connected to a site belonging to percolation path/cluster reaches the critical value n_c. Numerical solutions show the critical number is $n_c = 2.6 \sim 2.7$ for the appearance of the percolating path/cluster in the three dimension materials [86,87].

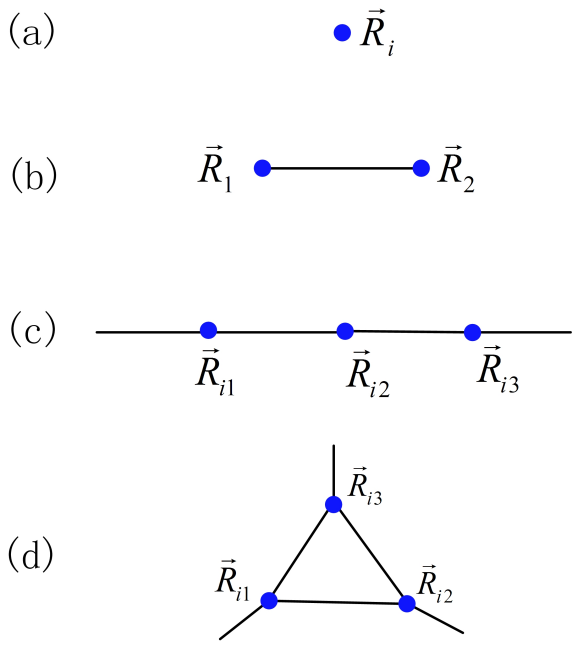

Fig. 5.3. Typical connectivity of the impurity sites in hopping conduction regime. (a) Isolated sites; (b) Single bonds; (c) 1D path. For each site, there are two bonds connecting to it; d) Triads, where each site has three bonds connecting to it.

This indicates the typical cases of the connectivity in the resister network include (Fig. 5.3): a) Isolated sites; b) Single bonds; c) For each site, there are two bonds connecting to it; d) Triads. Therefore the triads are sparsely distributed in the percolation cluster, as shown in Fig. 5.4. To derive a formula for the AHC, we can apply a total current I_0 in the longitudinal direction (along x axis), and then examine the transverse voltage (along y axis) induced by this current.

We consider the transverse voltage difference at the position x (for the region from $x - \Delta x$ to $x + \Delta x$). Assume in this region there are $N(x)$ triads distributed from the side $y = 0$ to the side $y = L_y$ (Note we consider the magnetization in z direction, and thus the system in this direction can be assumed to be uniform). The

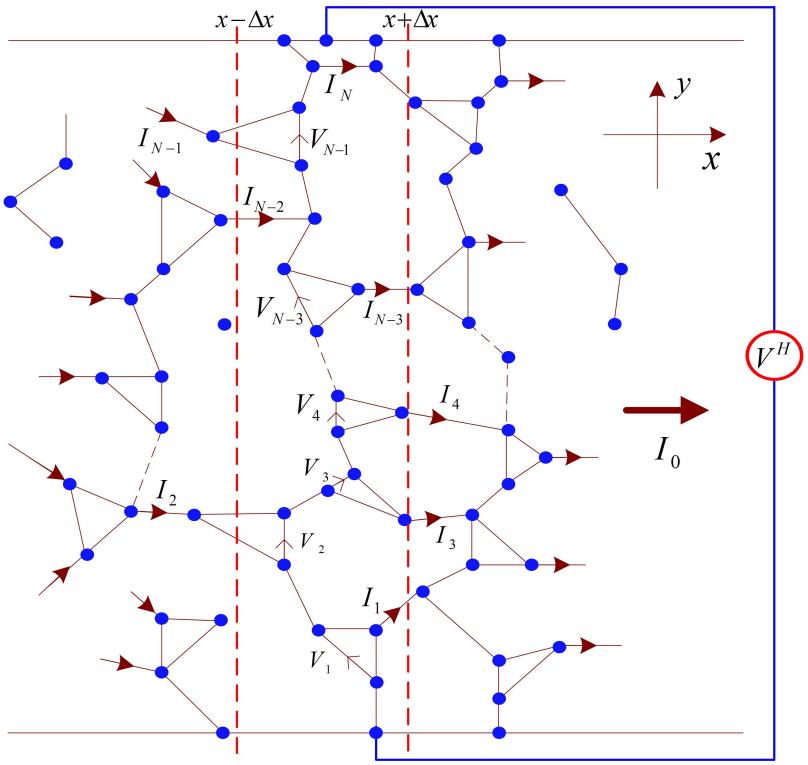

Fig. 5.4. Typical resistance network in the material. The present situation indicates V_{N-2}^H and V_N^H in the region from $x-\Delta x$ to $x+\Delta x$ are zero, where no triads form.

transverse voltage different is obtained by summing over the voltage drop of each triad in this region

$$V_y(x) = V_1^H + V_2^H + ... + V_N^H . \tag{5.20}$$

It is noteworthy for the general situation we allow some V_i^H's to be zero. In that case it means no triad forms for the incoming current I_i under the condition all direct conductances in a triad must be greater than G_c (see Fig. 5.4). To calculate V_i^H, the voltage contributed by the i-th triad, we employ perturbation theory to the Eq.

(4.84) [88]. First, in the zeroth order, we consider only the normal current, namely, the Hall current is zero and thus

$$\sum_j I_{ij} = \sum_j G_{ij} V_{ij}^{(0)} = 0. \tag{5.21}$$

Then, for the first-order perturbation, we have

$$\sum_j I_{ij} = \sum_j G_{ij} V_{ij}^{(0)} + \sum_j J_{ij}^{(H)} = 0, \tag{5.22}$$

which leads to $J_i^{(H)} = \sum_j J_{ij}^{(H)} = \sum_j \sum_i F_{ijk}(V_{jk}^{(0)} + V_{ik}^{(0)}) = -\sum_j G_{ij} V_{ij}^{(0)}$. The current $J_i^{(H)}$ can also be written as

$$\begin{aligned} J_i^{(H)} &= \sum_j \sum_i F_{ijk}(V_{jk}^{(0)} + V_{ik}^{(0)}) \\ &= \sum_{jk} F_{ikj}(V_{ij} + V_{kj}) \\ &= \frac{1}{2}\sum_{jk} F_{ijk}(V_{ik} + V_{jk} - V_{ij} - V_{kj}) \\ &= \frac{3}{2}\sum_{jk} F_{ijk} V_{jk}. \end{aligned} \tag{5.23}$$

Therefore, we obtain from the transformation indicated in Fig. 5.5 that

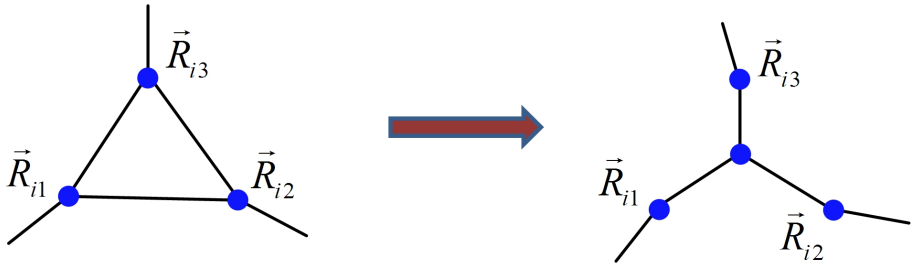

Fig. 5.5. Resistor network transformation.

$$V_i^{(H)} = V_{i_3 i_2}^{(H)} = \frac{G_{i_1 i_2} J_3^{(H)} - G_{i_1 i_3} J_2^{(H)}}{G_{i_1 i_2} G_{i_2 i_3} + G_{i_1 i_3} G_{i_2 i_3} + G_{i_3 i_1} G_{i_1 i_2}}$$
$$= \frac{3 I_i F_{i_1 i_2 i_3}^{(i)}}{G_{i_1 i_2} G_{i_2 i_3} + G_{i_1 i_3} G_{i_2 i_3} + G_{i_3 i_1} G_{i_1 i_2}}. \quad (5.24)$$

The total transverse voltage is then given by

$$V_y^H(x) = \sum_i V_i^H$$
$$= \sum_i \frac{3 I_i F_{i_1 i_2 i_3}^{(i)}}{G_{i_1 i_2} G_{i_2 i_3} + G_{i_1 i_3} G_{i_2 i_3} + G_{i_3 i_1} G_{i_1 i_2}}. \quad (5.25)$$

It is easy to confirm that $\sum_i^{N(x)} I_i = 2I_0$. For convenience, we denote $I_i = 2I_0 \lambda_i(x)$ with $\sum_i \lambda_i = 1$. Generally V_y^H is a function of position x. The average value of it can be obtained by

$$\bar{V}_y^H = 6 I_0 \frac{1}{L_x} \int dx \sum_i \lambda_i(x) \frac{F_{i_1 i_2 i_3}^{(i)}}{G_{i_1 i_2} G_{i_2 i_3} + G_{i_1 i_3} G_{i_2 i_3} + G_{i_3 i_1} G_{i_1 i_2}}, \quad (5.26)$$

where L_x is the length of the material in x direction. For a macroscopic system, one has the number $N(x) \to \infty$. Furthermore, we consider at the position x, for each $\lambda_i(x)$ there are $n_i(x)$ number triads that have such same current fraction λ_i. Thus we have

$$\bar{V}_y^H = 6 I_0 \frac{1}{L_x} \int dx \sum_{\{n_i\}} \sum_{j=1}^{n_i \gg 1} \lambda_i(x) \frac{F_{j_1 j_2 j_3}^{(j)}}{G_{j_1 j_2} G_{j_2 j_3} + G_{j_1 j_3} G_{j_2 j_3} + G_{j_3 j_1} G_{j_1 j_2}}. \quad (5.27)$$

To simplify this formula we extend the current distribution $\{\lambda_i\}$ for the region between $x - \Delta x$ and $x + \Delta x$ to the whole space along x direction, and then we can ex-

change the order of the integral and the first summation: $\frac{1}{L_x}\int dx \sum_{\{n_i\}} \lambda_i \sum_{j=1}^{n_i \gg 1} \rightarrow \sum_{\{\lambda_i\}} \lambda_i \frac{1}{L_x}\int dx \sum_{j=1}^{n_i(x)}$. The above equation then yields

$$\bar{V}_y^H = 6I_0 \sum_{\{n_i\}} \lambda_i \frac{1}{L_x} \int dx \sum_{j=1}^{n_i(x)\gg 1} \frac{F^{(j)}_{j_1 j_2 j_3}}{G_{j_1 j_2} G_{j_2 j_3} + G_{j_1 j_3} G_{j_2 j_3} + G_{j_3 j_1} G_{j_1 j_2}}. \tag{5.28}$$

The calculation $\frac{1}{L_x}\int dx \sum_{j=1}^{n_i(x)\gg 1}$ corresponds to the average of all possible configurations of the triads in the system, and it leads to

$$\bar{V}_y^H = 6I_0 \sum_{\{n_i\}} \bar{n}_i \lambda_i \langle \frac{F^{(i)}_{i_1 i_2 i_3}}{G_{i_1 i_2} G_{i_2 i_3} + G_{i_1 i_3} G_{i_2 i_3} + G_{i_3 i_1} G_{i_1 i_2}} \rangle_c, \tag{5.29}$$

where $\bar{n}_i$ is the average number of triads with input current I_i. Note the identity $\sum_i n_i \lambda_i = 1$ is independent of position x, and therefore we have also $\sum_i \bar{n}_i \lambda_i = 1$. We finally get

$$\bar{V}_y^H = 6I_0 \langle \frac{F_{i_1 i_2 i_3}}{G_{i_1 i_2} G_{i_2 i_3} + G_{i_1 i_3} G_{i_2 i_3} + G_{i_3 i_1} G_{i_1 i_2}} \rangle_c. \tag{5.30}$$

The transverse electric field is then given by

$$\begin{aligned} \bar{E}_y^H &= \frac{6I_0}{L_y} \langle \frac{F_{i_1 i_2 i_3}}{G_{i_1 i_2} G_{i_2 i_3} + G_{i_1 i_3} G_{i_2 i_3} + G_{i_3 i_1} G_{i_1 i_2}} \rangle_c \\ &= 6 j_0 L \langle \frac{F^{(i)}_{i_1 i_2 i_3}}{G_{i_1 i_2} G_{i_2 i_3} + G_{i_1 i_3} G_{i_2 i_3} + G_{i_3 i_1} G_{i_1 i_2}} \rangle_c, \end{aligned} \tag{5.31}$$

where $j_0 = I_0/(L_y L)$ is the longitudinal current density, with L the typical length of the triad. $L_y L$ means the area of the cross section. With above formula we obtain the Hall resistivity

$$\rho_{yx}^{AH} = 6L \langle \frac{F_{i_1 i_2 i_3}}{G_{i_1 i_2} G_{i_2 i_3} + G_{i_1 i_3} G_{i_2 i_3} + G_{i_3 i_1} G_{i_1 i_2}} \rangle_c, \tag{5.32}$$

and the Hall conductivity for the system

$$\sigma_{xy}^{AH} = 6L\sigma_{xx}^2\langle\frac{F_{i_1i_2i_3}}{G_{i_1i_2}G_{i_2i_3}+G_{i_1i_3}G_{i_2i_3}+G_{i_3i_1}G_{i_1i_2}}\rangle_c. \tag{5.33}$$

It is noteworthy that the above formula for the AHC differs from the former one derived by Burkov et al [50] in that the configuration integral in the former theory indeed applies to the whole impurity system rather than to the percolation cluster. The configuration averaging is not conducted over the whole impurity system, but over the percolation cluster which covers only portion of the impurity sites. Therefore the probability that an impurity site belonging to the percolation cluster must be taken into account for probability function, as derived in the previous subsection. The correct formula for the configuration integral, according to the Eq. (5.19), takes into account the key physics that the Hall currents are averaged over percolation cluster, and can therefore predict the correct scaling relation between the AHC and the longitudinal conductivity.

Before proceeding further we would like to present a few remarks on Eq. (5.33). First of all, this formula is generally valid for the disordered insulating regime, as long as the triads are sparsely distributed in the percolation cluster. Second, for different types of hopping regimes (Mott, E-S, and activation E3 hopping regimes), the functions of the DOS $\rho(\epsilon)$ and connectivity $n(\epsilon_i)$ in the configuration integral are different. Finally, the configuration integral is complicated, and is not easy to solve analytically.

6. SCALING RELATION BETWEEN ANOMALOUS HALL CONDUCTIVITY AND LONGITUDINAL CONDUCTIVITY

In this section we study in detail how to perform the configuration averaging derived in the previous section for the AHC, with which we shall determine the scaling relation between AHC and the longitudinal conductivity in the insulating hopping conduction regime. Configuration averaging is a highly nontrivial issue in the hopping regime. With different procedures it may result in very different outcomes. A special situation can be found in the AHE in the insulating manganites, where the anomalous Hall transport is a consequence of the scalar spin chirality composed of the manganese core spins and is dominated by the optimal triad rather than by all triads connected in the percolation cluster [48]. In that case no configuration averaging is needed and the conductivity of the single optimal triad determines the AHC of the system. Therefore the theory for the insulating manganites cannot predict any scaling relation between σ_{xy}^{AH} and σ_{xx} and therefore is not applicable to explain the scaling $\sigma_{xy}^{AH} \propto \sigma_{xx}^{1.4\sim1.75}$ as generically observed in many other insulating ferromagnetic materials, while it successfully explains the AHE in manganites. On the other hand, in another former theory of the AHE in the insulating regime Burkov et al obtain the AHC by replacing the configuration integral with the maximum value of the integrand [50]. This procedure did not predict the correct scaling relation between AHC and the longitudinal conductivity, either.

6.1 Formulas

The AHC needs to be obtained by averaging over all triads connected in the 2D percolation cluster. From the Eqs. (5.19) and (5.33) obtained in the previous section we get

$$\begin{aligned}\sigma_{xy}^{AH} &= \frac{6L\sigma_{xx}^2}{\mathcal{N}_F}\int d\epsilon_1 d\epsilon_2 d\epsilon_3 \int d^3\vec{r}_{12}\int d^3\vec{r}_{23}\rho(\epsilon_1)[n(\epsilon_1)]^3\rho(\epsilon_2)[n(\epsilon_2)]^3\rho(\epsilon_3)[n(\epsilon_3)]^3 \\ &\quad\times\frac{F_{123}}{G_{12}G_{23}+G_{13}G_{23}+G_{31}G_{12}} \\ &= 3L\sigma_{xx}^2\frac{k_BT}{e^2}\langle\frac{\sum_{\alpha\beta\gamma}\left[\mathrm{Im}(t_{i\alpha,j\beta}t_{j\beta,k\gamma}t_{k\gamma,i\alpha})T_{ijk}^{(3)}\right]}{|t_{ij}t_{jk}|^2T_{ij}^{(2)}T_{jk}^{(2)}+|t_{ik}t_{jk}|^2T_{ik}^{(2)}T_{jk}^{(2)}+|t_{ij}t_{ik}|^2T_{ij}^{(2)}T_{ik}^{(2)}}\rangle_c. \qquad (6.1)\end{aligned}$$

where $T_{jk}^{(2)}$ and $T_{ijk}^{(3)}$ are defined by

$$T_{ij}^{(2)} = |\Delta_{ij}|e^{-\frac{1}{2k_BT}(|\epsilon_{i\alpha}|+|\epsilon_{j\beta}|+|\epsilon_{i\alpha}-\epsilon_{j\beta}|)}, \qquad (6.2)$$

and

$$\begin{aligned}T_{ijk}^{(3)} &= |\Delta_{ij}\Delta_{ik}|e^{-\frac{1}{2k_BT}(|\epsilon_{j\beta}|+|\epsilon_{k\gamma}|+|\epsilon_{i\alpha}-\epsilon_{k\gamma}|+|\epsilon_{i\alpha}-\epsilon_{j\beta}|)}+ \\ &\quad+|\Delta_{ij}\Delta_{jk}|e^{-\frac{1}{2k_BT}(|\epsilon_{i\alpha}|+|\epsilon_{k\gamma}|+|\epsilon_{j\beta}-\epsilon_{k\gamma}|+|\epsilon_{i\alpha}-\epsilon_{j\beta}|)} \\ &\quad+|\Delta_{ik}\Delta_{kj}|e^{-\frac{1}{2k_BT}(|\epsilon_{i\alpha}|+|\epsilon_{j\beta}|+|\epsilon_{i\alpha}-\epsilon_{k\gamma}|+|\epsilon_{k\gamma}-\epsilon_{j\beta}|)}. \qquad (6.3)\end{aligned}$$

Note the hopping coefficient has the exponential decaying form $t_{i\alpha,j\beta} = t_{i\alpha,j\beta}^{(0)}e^{-aR_{ij}}$. Unfortunately, the configuration integral in the formula (6.1) is extremely complicated and the exact calculation of σ_{xy}^{AH} is impossible. However, instead of an exact calculation, it is possible to find the upper and lower limits of the AHC by imposing further restrictions in Eq. (6.1), with which the range of the scaling relation between σ_{xy}^{AH} and σ_{xx} can be determined.

By examining the formula of σ_{xy}^{AH} we see the denominator in the right hand side includes three terms in the summation, and in the numerator the function $T_{ijk}^{(3)}$

contains also three terms. We denote $\{|t_{ij}t_{jk}|^2 T_{ij}^{(2)} T_{jk}^{(2)}\}_{min,max}$ and $\{T_{ijk}^{(3)}\}_{min,max}$ as the minimum/maximum term out of the three ones in denominator and numerator, respectively. Then we have

$$\{\sigma_{xy}^{AH}\}_{min} \leq \sigma_{xy}^{AH} \leq \{\sigma_{xy}^{AH}\}_{max}, \tag{6.4}$$

with the lower and upper limits given by

$$\{\sigma_{xy}^{AH}\}_{min} = 3L\sigma_{xx}^2 \frac{k_B T}{e^2} \langle \frac{\{\sum_{\alpha\beta\gamma}[\mathrm{Im}(t_{i\alpha,j\beta}t_{j\beta,k\gamma}t_{k\gamma,i\alpha})T_{ijk}^{(3)}]\}_{min}}{\{|t_{ij}t_{jk}|^2 T_{ij}^{(2)} T_{jk}^{(2)}\}_{max}} \rangle_c, \tag{6.5}$$

$$\{\sigma_{xy}^{AH}\}_{max} = 3L\sigma_{xx}^2 \frac{k_B T}{e^2} \langle \frac{\{\sum_{\alpha\beta\gamma}[\mathrm{Im}(t_{i\alpha,j\beta}t_{j\beta,k\gamma}t_{k\gamma,i\alpha})T_{ijk}^{(3)}]\}_{max}}{\{|t_{ij}t_{jk}|^2 T_{ij}^{(2)} T_{jk}^{(2)}\}_{min}} \rangle_c. \tag{6.6}$$

The lower and upper limits correspond to different underlying physics. For the most general situation of charge transport through the resistor network, the choice of preferred paths for the current depends not only on the resistance magnitudes but also on the directional distribution of paths. The charge transport may prefer a short and straight path in the forward direction with larger resistance than a long and meandrous path with somewhat smaller resistance. Note this is an additional restriction complementary to the percolation theory for the charge transport [84], and it can quantitatively modify the averaging of the AHC. What bonds in a triad play the major role for the microscopic current flowing through it is determined by the optimization on the resistance magnitudes and spatial configuration of the three bonds. A quantitative description can be obtained by phenomenologically introducing an additional probability factor to restrict the charge transport, as initially done by Miller and Abraham [71], and later also by Pollak [84]. Here we only need to adopt this picture to present the two extreme situations corresponding to $\{\sigma_{xy}^{AH}\}_{min/max}$. The first one is that if we assume in each triad of the percolation cluster, it is the two

bonds with smaller direct conductances due to the spatial distribution that dominate the charge transport, we may keep the minimum term in the denominator (product of two smaller conductances) and maximum term in the numerator of Eq. (6.1) to get the upper limit of the AHC. For the opposite limit, the situation that the two bonds with larger conductances in each triad dominate the charge transport corresponds to the lower limit of the AHC. Conceivably, due to the complexity of real materials in the insulating regime, it is not surprising that the relation between σ_{xy}^{AH} and σ_{xx} may be quantitatively, though not qualitatively, affected by e.g. the distribution of impurity states, but should be within the range determined by the two limits. As a result, in the following we shall study $\{\sigma_{xy}^{AH}\}_{min}$ and $\{\sigma_{xy}^{AH}\}_{max}$ respectively, whose calculation can be simplified relative to the original integral.

6.2 The lower limit

We first consider the lower limit $\{\sigma_{xy}^{AH}\}_{min}$. The hopping conduction mechanism deals with the strong localization regime, in which case temperature dependence of the conductivities are dominated by exponential functions. It can then be expected the scaling relation between σ_{xy}^{AH} and σ_{xx} will be governed by the exponential functions in $\mathcal{G}_{ijk}$ and G_{ij}. To focus on the scaling relation, we first drop off the summation of the spin states. This procedure ignores an important physical consequence that the summation over spin-up and spin-down states contribute oppositely to the AHE (we shall return to this discussion later), but keeps the central result of the scaling relation unchanged between σ_{xy}^{AH} and σ_{xx}. Furthermore, in this calculation we first consider the approximation that the DOS is a constant around Fermi energy (it will be shown later the scaling relation is insensitive to the specific form of the DOS). By

substituting $T_{ij}^{(2)}$, $T_{ijk}^{(3)}$ and t_{ij} and examining the properties of these terms we can obtain

$$\begin{aligned}\{\sigma_{xy}^{AH}\}_{min} &= 3L\sigma_{xx}^2\frac{k_BT}{e^2}\frac{1}{t_{max}^{(0)}}\langle e^{a(r_{ij}+r_{jk}-r_{ik})}e^{\frac{1}{2k_BT}(|\epsilon_{i\alpha}|+|\epsilon_{j\beta}|+|\epsilon_{j\beta}-\epsilon_{k\gamma}|-|\epsilon_{i\alpha}-\epsilon_{k\gamma}|)}\rangle_c \\ &\simeq 3L\sigma_{xx}^2\frac{k_BT}{e^2}\frac{1}{t_{max}^{(0)}}\langle e^{a(r_{ij}+r_{jk}-r_{ik})}\rangle_c\langle e^{\frac{1}{2k_BT}(|\epsilon_{i\alpha}|+|\epsilon_{j\beta}|+|\epsilon_{j\beta}-\epsilon_{k\gamma}|-|\epsilon_{i\alpha}-\epsilon_{k\gamma}|)}\rangle_c,\end{aligned} \tag{6.7}$$

where the coefficient $t_{max}^{(0)}$ represents the maximum element in the matrix $t_{ij}^{(0)}$. In obtaining above equation we have considered the following restrictions

$$r_{ij}, r_{jk} < r_{ik}, \tag{6.8}$$

$$|\epsilon_{i\alpha}| < |\epsilon_{j\beta}| < |\epsilon_{k\gamma}|. \tag{6.9}$$

The percolation theory also gives another restriction in the formula (6.7) that $2ar_{ij} + \frac{1}{2k_BT}(|\epsilon_{i\alpha}| + |\epsilon_{j\beta}| + |\epsilon_{i\alpha} - \epsilon_{j\beta}|) \leq \xi/k_BT$. These restrictions will be fully considered in the next calculation. For convenience we simplify the notation $\epsilon_{i\alpha} \to \epsilon_i$ in following discussion. Using the inequalities

$$\begin{aligned}\langle e^{a(r_{ij}+r_{jk}-r_{ik})}\rangle_c &> e^{a\langle r_{ij}+r_{jk}-r_{ik}\rangle_c} \\ \langle e^{\frac{1}{2k_BT}(|\epsilon_i|+|\epsilon_j|+|\epsilon_i-\epsilon_j|)}\rangle_c &> e^{\frac{1}{2k_BT}\langle|\epsilon_i|+|\epsilon_j|+|\epsilon_j-\epsilon_k|-|\epsilon_i-\epsilon_k|\rangle_c},\end{aligned} \tag{6.10}$$

we further get the formula for the lower limit by

$$\{\sigma_{xy}^{AH}\}_{min} = 3L\sigma_{xx}^2\frac{k_BT}{e^2t_{max}^{(0)}}\langle R_{ijk}^{min}\rangle_c\langle\epsilon_{ijk}^{min}\rangle_c, \tag{6.11}$$

where $\langle R_{ijk}^{min}\rangle_c = e^{a\langle r_{ij}+r_{jk}-r_{ik}\rangle_c}\big|_{r_{ij},r_{jk}<r_{ik}}$, $\langle\epsilon_{ijk}^{min}\rangle_c = e^{0.5\beta\langle|\epsilon_i|+|\epsilon_j|+|\epsilon_j-\epsilon_k|-|\epsilon_i-\epsilon_k|\rangle_c}\big|_{|\epsilon_i|<|\epsilon_j|<|\epsilon_k|}$. We have neglected the spin indices for simplicity.

It is noteworthy in obtaining Eq. (6.11) we approximated the configuration averaging of the exponential functions to be the configuration averaging of the exponents. This approximation loses the information of the power-law dependence of the AHC on the temperature, and it requires the dominant temperature dependence of the AHC should be in the exponential form. In the hopping conduction regime this condition is generally satisfied according to the analysis in the beginning of this section. The configuration integral $\langle r_{ij}+r_{jk}-r_{ik}\rangle_c|_{r_{ij},r_{jk}<r_{ik}}$ is given by

$$\begin{aligned}\langle r_{ij}+r_{jk}-r_{ik}\rangle_c &= \frac{1}{\mathcal{N}_F^{(3)}}\int d\epsilon_i d\epsilon_j d\epsilon_k \int d^3\vec{r}_{ij}\int d^3\vec{r}_{jk}\rho(\epsilon_i)[n(\epsilon_i)]^3\times \\ &\quad \times\rho(\epsilon_j)[n(\epsilon_j)]^3\rho(\epsilon_k)[n(\epsilon_k)]^3(r_{ij}+r_{jk}-r_{ik}),\end{aligned} \tag{6.12}$$

with $r_{ij}, r_{jk} < r_{ik}$. We shall first perform this integral over position $\int d^3\vec{r}_{ij}\int d^3\vec{r}_{jk}$. We denote by $\vec{r}_{ij}=\vec{R}_1, \vec{r}_{jk}=\vec{R}_2$, and then $R_3 = r_{ik} = \sqrt{R_1^2+R_2^2-2R_1R_2\cos\theta}$ for convenience. The integral over position can be written as

$$I = \frac{1}{\mathcal{N}_r}\int d^3\vec{R}_1\int d^3\vec{R}_2(R_1+R_2-R_3), \tag{6.13}$$

where $\mathcal{N}_r = \int d^3\vec{R}_1\int d^3\vec{R}_2$. To write down the explicit formula of this integral, we apply the restrictions: $R_1, R_2 \le R_3$ and $R_i \le R_{i,max}$, with $R_{i,max}$ defined through the condition of the connectivity in percolation thoery

$$2ar_{ij}^{max}+\frac{1}{2k_BT}(|\epsilon_{i\alpha}|+|\epsilon_{j\beta}|+|\epsilon_{i\alpha}-\epsilon_{j\beta}|)=\xi/k_BT. \tag{6.14}$$

With the basic triangle geometry (Fig. 6.1) we can decompose the integral I into two terms given below

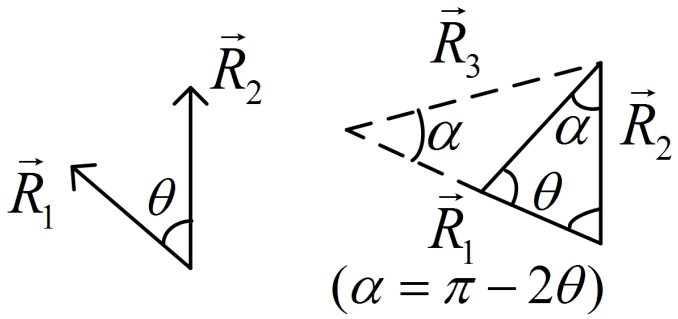

Fig. 6.1. Triangle geometry with $R_3 \geq R_1, R_2$ for the configuration integral over the position space.

$$
\begin{aligned}
I &= \frac{1}{\mathcal{N}_r} 8\pi^2 \int_0^{R_{2max}} dR_2 R_2^2 \Big[\int_{\pi/2}^{\pi} d\theta \int_0^{R_a} dR_1 R_1^2 \sin\theta \big(R_1 + R_2 - \\
&\quad - \sqrt{R_1^2 + R_2^2 - 2R_1 R_2 \cos\theta} \big) + \int_{\pi/3}^{\pi/2} d\theta \int_{2R_2\cos\theta}^{R_b} dR_1 R_1^2 \times \\
&\quad \times \sin\theta (R_1 + R_2 - \sqrt{R_1^2 + R_2^2 - 2R_1 R_2 \cos\theta}) \Big], \qquad (6.15)
\end{aligned}
$$

where in upper integral limit is given by

$$
\begin{aligned}
R_a &= \min\{R_{1max}, R_2 + \sqrt{\Lambda^2 - R_2^2 \sin^2\theta}\}, \\
R_b &= \min\{R_{1max}, \frac{R_2}{2\cos\theta}, R_2 \cos\theta + \sqrt{\Lambda^2 - R_2^2 \sin^2\theta}\}, \qquad (6.16)
\end{aligned}
$$

with

$$
\Lambda^2 = \frac{1}{4a^2} \Big[\frac{\xi}{k_B T} - \frac{1}{2k_B T} (|\varepsilon_i| + |\varepsilon_k| + |\varepsilon_i - \varepsilon_k|) \Big]^2. \qquad (6.17)
$$

From above formulas we can see the integral domain is not uniquely specified but has a complicated dependence on the the integral variables, which makes the Eq. (6.15) be still not analytically solvable. We can simplify this equation by amplifying

the integral domain. From the geometry of the triangle composed of (R_1, R_2, R_3), we can show the following two inequalities:

$$\frac{\int_{R_2\cos\theta+\sqrt{\Lambda^2-R_2^2\sin^2\theta}}^{R_{1max}} dR_1 R_1^2 \sin\theta(R_1+R_2-\sqrt{R_1^2+R_2^2-2R_1R_2\cos\theta})}{\int_{R_2\cos\theta+\sqrt{\Lambda^2-R_2^2\sin^2\theta}}^{R_{1max}} dR_1 R_1^2\sin\theta} \geq$$
$$\frac{\int_{0}^{R_2\cos\theta+\sqrt{\Lambda^2-R_2^2\sin^2\theta}} dR_1 R_1^2 \sin\theta(R_1+R_2-\sqrt{R_1^2+R_2^2-2R_1R_2\cos\theta})}{\int_{0}^{R_2\cos\theta+\sqrt{\Lambda^2-R_2^2\sin^2\theta}} dR_1 R_1^2\sin\theta}, \quad (6.18)$$

which is needed in the case $R_2\cos\theta+\sqrt{\Lambda^2-R_2^2\sin^2\theta} < R_{1max}$, and

$$\frac{\int_{R_b}^{R_{1max}} dR_1 R_1^2 \sin\theta(R_1+R_2-\sqrt{R_1^2+R_2^2-2R_1R_2\cos\theta})}{\int_{R_b}^{R_{1max}} dR_1 R_1^2\sin\theta} \geq$$
$$\frac{\int_{2R_2\cos\theta}^{R_b} dR_1 R_1^2 \sin\theta(R_1+R_2-\sqrt{R_1^2+R_2^2-2R_1R_2\cos\theta})}{\int_{2R_2\cos\theta}^{R_b} dR_1 R_1^2\sin\theta}, \quad (6.19)$$

when $R_b < R_{1max}$. The first inequality actually tells that when $\pi/2 < \theta < \pi$, the value of $R_1+R_2-R_3$ averaged in the range $R_a \leq R_1 \leq R_{1max}$ is no less than its value averaged in the range $0 \leq R_1 \leq R_a$. The second inequality indicates that for $\pi/3 < \theta < \pi/2$, the value of $R_1+R_2-R_3$ averaged in the range $R_b \leq R_1 \leq R_{1max}$ is no less than its value averaged in the range $2R_2\cos\theta \leq R_1 \leq R_a$. Based on these results, we find that

$$\begin{aligned} I \;\leq\; & \frac{1}{\mathcal{N}_r} 8\pi^2 \int_0^{R_{2max}} dR_2 R_2^2 \Big[\int_{\pi/2}^{\pi} d\theta \int_0^{R_{1max}} dR_1 R_1^2 \sin\theta \big(R_1+R_2- \\ & -\sqrt{R_1^2+R_2^2-2R_1R_2\cos\theta}\big) + \int_{\pi/3}^{\pi/2} d\theta \int_{2R_2\cos\theta}^{R_{1max}} dR_1 R_1^2 \sin\theta (R_1+R_2- \\ & -\sqrt{R_1^2+R_2^2-2R_1R_2\cos\theta})\Big], \end{aligned} \quad (6.20)$$

This formula can be rewritten as $I \simeq I_1 - I_2$, with

$$I_1 = \frac{1}{3\mathcal{N}_r} 8\pi^2 \int_0^{R_{2max}} dR_2 R_2^2 \Big[\int_{\pi/3}^{\pi} d\theta \sin\theta \int_0^{R_{1max}} dR_1 R_1^2 (R_1+R_2), \quad (6.21)$$

and

$$I_2 = \frac{1}{3\mathcal{N}_r} 8\pi^2 \int_0^{R_{2max}} dR_2 R_2 \int_0^{R_{1max}} dR_1 R_1 \big[(R_1+R_2)^2 - (R_1^2+R_2^2-R_1R_2)^{3/2}\big]. \tag{6.22}$$

By a straightforward calculation we obtain

$$I_1 \simeq \frac{2\pi^2}{\mathcal{N}_r} R_{max}^7, \tag{6.23}$$

and

$$I_1 \simeq \frac{2\pi^2}{\mathcal{N}_r} R_{max}^7, \tag{6.24}$$

where $R_{max} = \max\{R_{1max}, R_{2max}\}$. With above results we obtain now the integral over position by

$$I = I_1 - I_2 \simeq 0.424\pi^2 R_{max}^7/\mathcal{N}_r. \tag{6.25}$$

It is noteworthy in above calculation we amplified the integral domain, which may increase the value of the lower limit of the AHC. However, comparing with the original formula (6.87) for the lower limit, this is only a small amplification. A numerical study will be performed later to confirm this result. It is straightforward to find the normalization factor by

$$\begin{aligned} \mathcal{N}_r &= 8\pi^2\big[\int_0^{R_{2max}} dR_2 R_2^2 \int_{\pi/2}^{\pi} d\theta \int_0^{R_{1max}} dR_1 R_1^2 \sin\theta + \\ &\quad + \int_0^{R_{2max}} dR_2 R_2^2 \int_{\pi/3}^{\pi/2} d\theta \int_{2R_2\cos\theta}^{R_{1max}} dR_1 R_1^2 \sin\theta\big] \\ &= \frac{23}{18}\pi^2 R_{max}^6. \end{aligned} \tag{6.26}$$

We should emphasize that to this step we cannot cancel the function R_{max}^7 in the numerator of the Eq. (6.25) by the normalization factor $\mathcal{N}_r$. This is because both of them are only part of the original integral (6.12). To obtain the final result of the configuration averaging $\langle r_{ij}+r_{jk}-r_{ik}\rangle_c$ we need to further integrate over onsite energies. This gives

$$\langle r_{ij}+r_{jk}-r_{ik}\rangle_c = \frac{0.424}{23/18}\frac{\int d\epsilon_i d\epsilon_j d\epsilon_k \rho(\epsilon_i)[n(\epsilon_i)]^3\rho(\epsilon_j)[n(\epsilon_j)]^3\rho(\epsilon_k)[n(\epsilon_k)]^3 R_{max}^7}{\int d\epsilon_i d\epsilon_j d\epsilon_k \int \rho(\epsilon_i)[n(\epsilon_i)]^3\rho(\epsilon_j)[n(\epsilon_j)]^3\rho(\epsilon_k)[n(\epsilon_k)]^3 R_{max}^6}. \tag{6.27}$$

Substituting the formula of R_{max} (see the former definition) we obtain

$$\begin{aligned}\langle r_{ij}+r_{jk}-r_{ik}\rangle_c|_{r_{ij},r_{jk}<r_{ik}} &\simeq 0.332\frac{\beta}{2a}\frac{\int_{-\xi}^{\xi} d\epsilon_i d[n(\epsilon_i)]^3\rho(\epsilon_i)(\xi-|\epsilon_i|)^7}{\int_{-\xi}^{\xi} d\epsilon_i d[n(\epsilon_i)]^3\rho(\epsilon_i)(\xi-|\epsilon_i|)^6} \\ &= 0.156\beta\xi/a. \end{aligned} \tag{6.28}$$

With this we reach then $\langle R_{ijk}^{min}\rangle_c \simeq e^{0.156\beta\xi}$. So far in the calculation we have considered the approximation that the DOS $\rho(\epsilon)$ is a constant around Fermi energy. This approximation will be relaxed later.

Now we evaluate the configuration averaging of the energy function $\langle\epsilon_{ijk}^{min}\rangle_c$ under the condition $|\epsilon_i|<|\epsilon_j|<|\epsilon_k|$. For this we study $\langle|\epsilon_i|+|\epsilon_j|+|\epsilon_j-\epsilon_k|-|\epsilon_i-\epsilon_k|\rangle_c$, which is given by

$$\begin{aligned}\langle|\epsilon_i|+|\epsilon_j|+|\epsilon_j-\epsilon_k|-|\epsilon_i-\epsilon_k|\rangle_c &= \frac{1}{\mathcal{N}_\epsilon}\int d\epsilon_i d\epsilon_j d\epsilon_k \rho(\epsilon_i)[n(\epsilon_i)]^3\rho(\epsilon_j)[n(\epsilon_j)]^3\rho(\epsilon_k) \\ &\quad\times[n(\epsilon_k)]^3(|\epsilon_i|+|\epsilon_j|+|\epsilon_j-\epsilon_k|-|\epsilon_i-\epsilon_k|),\end{aligned} \tag{6.29}$$

where the normalization factor is calculated according to

$$\mathcal{N}_\epsilon = \int d\epsilon_i d\epsilon_j d\epsilon_k \rho(\epsilon_i)[n(\epsilon_i)]^3\rho(\epsilon_j)[n(\epsilon_j)]^3\rho(\epsilon_k)[n(\epsilon_k)]^3. \tag{6.30}$$

To simplify the above integral, we check $|\epsilon_j - \epsilon_k| - |\epsilon_i - \epsilon_k|$ with the restriction: $|\epsilon_i| < |\epsilon_j| < |\epsilon_k|$. For the case (i) $\mathrm{sgn}(\epsilon_i) = \mathrm{sgn}(\epsilon_j) = \mathrm{sgn}(\epsilon_k) = \pm 1$, we have

$$|\epsilon_j - \epsilon_k| - |\epsilon_i - \epsilon_k| = -|\epsilon_i - \epsilon_j|. \tag{6.31}$$

For (ii) $\mathrm{sgn}(\epsilon_i) = \mathrm{sgn}(\epsilon_j) = -\mathrm{sgn}(\epsilon_k) = \pm 1$, we have

$$|\epsilon_j - \epsilon_k| - |\epsilon_i - \epsilon_k| = -|\epsilon_i - \epsilon_j|. \tag{6.32}$$

For (iii) $\mathrm{sgn}(\epsilon_i) = \mathrm{sgn}(\epsilon_k) = -\mathrm{sgn}(\epsilon_j) = \pm 1$, we have

$$|\epsilon_j - \epsilon_k| - |\epsilon_i - \epsilon_k| = -|\epsilon_i - \epsilon_j|. \tag{6.33}$$

For (iv) $\mathrm{sgn}(\epsilon_j) = \mathrm{sgn}(\epsilon_k) = -\mathrm{sgn}(\epsilon_i) = \pm 1$, we have

$$|\epsilon_j - \epsilon_k| - |\epsilon_i - \epsilon_k| = |\epsilon_i - \epsilon_j|. \tag{6.34}$$

For this we have that

$$\langle |\epsilon_i| + |\epsilon_j| + |\epsilon_j - \epsilon_k| - |\epsilon_i - \epsilon_k| \rangle_c \simeq \langle |\epsilon_i| + |\epsilon_j| - \frac{1}{2}|\epsilon_i - \epsilon_j| \rangle_c. \tag{6.35}$$

This result is a consequence of the equal probabilities of the four situations (i-iv), and symmetric integral domain with respect to onsite energies below and above the Fermi energy. Furthermore we obtain

$$\begin{aligned}\frac{1}{2k_BT}\langle|\epsilon_i|+|\epsilon_j|-\frac{1}{2}|\epsilon_i-\epsilon_j|\rangle_c &= \frac{1}{2k_BT}\frac{\int d\epsilon_i\rho(\epsilon_i)[n(\epsilon_i)]^3|\epsilon_i|}{\int d\epsilon_i\rho(\epsilon_i)[n(\epsilon_i)]^3}+\\ &+\frac{1}{2k_BT}\frac{\int d\epsilon_j\rho(\epsilon_j)[n(\epsilon_j)]^3|\epsilon_j|}{\int d\epsilon_j\rho(\epsilon_j)[n(\epsilon_j)]^3}-\\ &-\frac{1}{4k_BT}\frac{\int d\epsilon_i\int d\epsilon_j\rho(\epsilon_i)[n(\epsilon_i)]^3\rho(\epsilon_j)[n(\epsilon_j)]^3|\epsilon_i-\epsilon_j|}{\int d\epsilon_i\int d\epsilon_j\rho(\epsilon_i)[n(\epsilon_i)]^3\rho(\epsilon_j)[n(\epsilon_j)]^3}\\ &= \frac{1}{2k_BT}(I_1+I_2-I_3),\end{aligned} \tag{6.36}$$

where $I_1 = I_2$ with

$$\begin{aligned}I_1 &= \frac{\int d\epsilon_i\rho(\epsilon_i)[n(\epsilon_i)]^3|\epsilon_i|}{\int d\epsilon_i\rho(\epsilon_i)[n(\epsilon_i)]^3}\\ &= \frac{\int_0^\xi d\epsilon_i(\xi-\epsilon_i)^9(\xi+\epsilon_i)^3\epsilon_i}{\int_0^\xi d\epsilon_i(\xi-\epsilon_i)^9(\xi+\epsilon_i)^3}\\ &= 0.112\xi,\end{aligned} \tag{6.37}$$

and

$$\begin{aligned}I_3 &= \frac{1}{2}\frac{\int d\epsilon_i\int d\epsilon_j\rho(\epsilon_i)[n(\epsilon_i)]^3\rho(\epsilon_j)[n(\epsilon_j)]^3|\epsilon_i-\epsilon_j|}{\int d\epsilon_i\int d\epsilon_j\rho(\epsilon_i)[n(\epsilon_i)]^3\rho(\epsilon_j)[n(\epsilon_j)]^3}\\ &= \frac{1}{2}\frac{\int_0^\xi d\epsilon_i\int_0^\xi d\epsilon_j(\xi-\epsilon_i)^9(\xi-\epsilon_j)^9(\xi+\epsilon_i)^3(\xi+\epsilon_j)^3|\epsilon_i-\epsilon_j|}{\int d\epsilon_i\int d\epsilon_j(\xi-\epsilon_i)^9(\xi-\epsilon_j)^9(\xi+\epsilon_i)^3(\xi+\epsilon_j)^3}\\ &= 0.0515\xi.\end{aligned} \tag{6.38}$$

Then from Eq. (6.36) we obtain

$$\frac{1}{2k_BT}\langle|\epsilon_i|+|\epsilon_j|+|\epsilon_j-\epsilon_k|-|\epsilon_i-\epsilon_k|\rangle_c|_{|\epsilon_i|<|\epsilon_j|<|\epsilon_k|} = 0.086\beta\xi, \tag{6.39}$$

which gives that $\langle \epsilon_{ijk}^{min} \rangle_c \simeq e^{0.086\beta\xi}$. Together with the results in Eq. (6.28) and Eq. (6.39) we get

$$\langle R_{ijk}^{min} \rangle_c \langle \epsilon_{ijk}^{min} \rangle_c \simeq e^{0.242\beta\xi}, \tag{6.40}$$

The lower limit of the AHC is then obtained by

$$\{\sigma_{xy}^{AH}\}_{min} = 3L\sigma_{xx}^2 \frac{k_B T}{e^2} \frac{1}{t_{max}^{(0)}} e^{0.242\beta\xi}. \tag{6.41}$$

Note the longitudinal conductivity σ_{xx} is calculated based on the 2-site function of G_{ij} which should be no less than G_c in a percolation path. The evaluation of σ_{xx} with percolation theory has been well studied in the published literatures [71, 84, 85]. It can be shown that the result of σ_{xx} equals G_c divided by the correlation length of the network and takes the form $\sigma_{xx} = \sigma_0(T)e^{-\beta\xi}$, where $\sigma_0(T)$ gives at most a power-law on T [84, 85]. Comparing this form with the lower limit of the AHC obtained above, we reach that

$$\begin{aligned} \{\sigma_{xy}^{AH}\}_{min} &= 3L\sigma_0^{0.242} \frac{k_B T}{e^2} \frac{1}{t_{max}^{(0)}} \sigma_{xx}^{1.758} \\ &\propto \sigma_{xx}^{\gamma}, \end{aligned} \tag{6.42}$$

with $\gamma \simeq 1.76$.

6.3 The upper limit

Now we calculate the upper limit of the AHC, which can be done in a fully similar procedure. From the Eq. (6.6) and by approximating the configuration averaging

of the exponential functions to be the configuration averaging of the exponents, we obtain

$$\{\sigma_{xy}^{AH}\}_{max} \simeq 3L\sigma_{xx}^2 \frac{k_B T}{e^2 t_{min}^{(0)}} \langle R_{ijk}^{max}\rangle_c \langle \epsilon_{ijk}^{max}\rangle_c, \tag{6.43}$$

where $t_{min}^{(0)}$ represents the minimum element in the matrix $t_{ij}^{(0)}$, the function $\langle R_{ijk}^{max}\rangle_c$ holds the same form as $\langle R_{ijk}^{min}\rangle_c$ but the restriction changes to be $R_1, R_2 > R_3$, and $\langle \epsilon_{ijk}^{max}\rangle_c = e^{0.5\beta\langle|\epsilon_i|+|\epsilon_j|+|\epsilon_j-\epsilon_k|-|\epsilon_i-\epsilon_k|\rangle_c}\big|_{|\epsilon_i|>|\epsilon_j|>|\epsilon_k|}$. Also, one should keep in mind the condition $R_i \leq R_i^{max}$ with R_i^{max} is always satisfied. The configuration integral $\langle R_1 + R_2 - R_3\rangle_c|_{R_1,R_2>R_3}$ is given by

$$\begin{aligned}\langle R_1 + R_2 - R_3\rangle_c &= \frac{1}{\mathcal{N}_F^{(3)}} \int d\epsilon_i d\epsilon_j d\epsilon_k \int d^3\vec{R}_1 \int d^3\vec{R}_2 \rho(\epsilon_i)[n(\epsilon_i)]^3 \times \\ &\times \rho(\epsilon_j)[n(\epsilon_j)]^3 \rho(\epsilon_k)[n(\epsilon_k)]^3 (R_1 + R_2 - R_3),\end{aligned} \tag{6.44}$$

which is the same as Eq. (6.12), but the restriction changes to be $R_1, R_2 > R_3$. To calculate the above configuration averaging we again consider first the integral under the new restriction

$$I = \frac{1}{\mathcal{N}_r} \int d^3\vec{R}_1 \int d^3\vec{R}_2 (R_1 + R_2 - \sqrt{R_1^2 + R_2^2 - 2R_1 R_2 \cos\theta}), \tag{6.45}$$

with $\mathcal{N}_r = \int d^3\vec{R}_1 \int d^3\vec{R}_2$. By applying the restrictions: $R_i \leq R_{i,max}$ and $R_1, R_2 \geq R_3$, and with the basic triangle geometry (Fig. 6.1) we obtain the above integral in the explicit form

$$\begin{aligned} I &= \frac{1}{\mathcal{N}_r} 8\pi^2 \int_0^{R_{2max}} dR_2 R_2^2 \int_0^{\pi/3} d\theta \int_{\frac{R_2}{2\cos\theta}}^{R_a} dR_1 R_1^2 \sin\theta (R_1 + R_2 - \\ &- \sqrt{R_1^2 + R_2^2 - 2R_1 R_2 \cos\theta}),\end{aligned} \tag{6.46}$$

where the upper limit for the integral reads

$$R_a \;=\; \min\{R_{1max}, 2R_2\cos\theta, R_2\cos\theta+\sqrt{\Lambda^2-R_2^2\sin^2\theta}\}. \tag{6.47}$$

Since the integral domain determined by R_a is again not uniquely specified, to calculate the above integral we still need to simplify it by amplifying the integral domain. For this we consider the following inequality:

$$\frac{\int_{R_2\cos\theta+\sqrt{\Lambda^2-R_2^2\sin^2\theta}}^{R_{1max}} dR_1R_1^2\sin\theta(R_1+R_2-\sqrt{R_1^2+R_2^2-2R_1R_2\cos\theta})}{\int_{R_2\cos\theta+\sqrt{\Lambda^2-R_2^2\sin^2\theta}}^{R_{1max}} dR_1R_1^2\sin\theta} \;\geq$$
$$\frac{\int_{\frac{R_2}{2\cos\theta}}^{R_2\cos\theta+\sqrt{\Lambda^2-R_2^2\sin^2\theta}} dR_1R_1^2\sin\theta(R_1+R_2-\sqrt{R_1^2+R_2^2-2R_1R_2\cos\theta})}{\int_{\frac{R_2}{2\cos\theta}}^{R_2\cos\theta+\sqrt{\Lambda^2-R_2^2\sin^2\theta}} dR_1R_1^2\sin\theta}, \tag{6.48}$$

which is needed in the case $R_2\cos\theta+\sqrt{\Lambda^2-R_2^2\sin^2\theta} < R_{1max}$. This inequality indicates that for $0<\theta<\pi/3$, the value of $R_1+R_2-R_3$ averaged in the range $R_a \leq R_1 \leq R_{1max}$ is no less than its value averaged in the range $R_2/(2\cos\theta) \leq R_1 \leq R_a$. Based on this result, we find that

$$I \;\leq\; \frac{1}{\mathcal{N}_r}8\pi^2\int_0^{R_{2max}} dR_2R_2^2\int_0^{\pi/3}d\theta\int_{\frac{R_2}{2\cos\theta}}^{R_{1max}} dR_1R_1^2\sin\theta(R_1+R_2-$$
$$-\sqrt{R_1^2+R_2^2-2R_1R_2\cos\theta}), \tag{6.49}$$

where the normalization factor reads $\mathcal{N}_r = 8\pi^2\int_0^{R_{2max}} dR_2R_2^2\int_0^{\pi/3}d\theta\int_{\frac{R_2}{2\cos\theta}}^{R_{1max}} dR_1R_1^2\sin\theta$. The integral can be separated into two parts $I=I_1-I_2$, where

$$I_1 = \frac{1}{\mathcal{N}_r}8\pi^2\int_0^{R_{2max}} dR_2R_2^2\int_0^{\pi/3}d\theta\sin\theta\int_{\frac{R_2}{2\cos\theta}}^{R_{1max}} dR_1R_1^2(R_1+R_2), \tag{6.50}$$

$$I_2 = \frac{1}{\mathcal{N}_r} 8\pi^2 \int_0^{R_{2max}} dR_2 R_2^2 \int_0^{\pi/3} d\theta \int_{\frac{R_2}{2\cos\theta}}^{R_{1max}} dR_1 R_1^2 \sin\theta \sqrt{R_1^2 + R_2^2 - 2R_1 R_2 \cos\theta}). \tag{6.51}$$

A straightforward calculation gives $I_1 \simeq 0.5694\pi^2 R_{max}^7/\mathcal{N}_r$, $I_2 \simeq 0.1965\pi^2 R_{max}^7/\mathcal{N}_r$, and therefore we have

$$I = I_1 - I_2 \simeq 0.3729\pi^2 R_{max}^7/\mathcal{N}_r. \tag{6.52}$$

The normalization factor yields $\mathcal{N}_r = 0.361\pi^2 R_{max}^6$. Similar as the procedure in lower limit we do now the configuration integral with respect to the on-site energies, which is derived by

$$\begin{aligned} \langle R_1 + R_2 - R_3 \rangle_c|_{R_1,R_2>R_3} &\simeq 1.03 \frac{\beta}{2a} \frac{\int_{-\xi}^{\xi} d\epsilon_i d[n(\epsilon_i)]^3 \rho(\epsilon_i)(\xi - |\epsilon_i|)^7}{\int_{-\xi}^{\xi} d\epsilon_i d[n(\epsilon_i)]^3 \rho(\epsilon_i)(\xi - |\epsilon_i|)^6} \\ &= 0.483\beta\xi/a. \end{aligned} \tag{6.53}$$

With this result we have $\langle R_{ijk}^{max} \rangle_c \simeq e^{0.483\beta\xi}$, which increases quite a bit in magnitude relative to the result in the lower limit. The physical understanding of this effect will be presented later.

Now we evaluate the configuration average $\langle \epsilon_{ijk}^{max} \rangle_c$ of the onsite energies. For this we calculate $\langle |\epsilon_i| + |\epsilon_j| + |\epsilon_i - \epsilon_k| - |\epsilon_j - \epsilon_k| \rangle_c$, with the restriction $|\epsilon_i| > |\epsilon_j| > |\epsilon_k|$. Similar to the procedure used in calculating the lower limit, the above integral can be simplified by examining $|\epsilon_i - \epsilon_k| - |\epsilon_j - \epsilon_k|$ with the present restriction. For the case i) $\mathrm{sgn}(\epsilon_i) = \mathrm{sgn}(\epsilon_j) = \mathrm{sgn}(\epsilon_k) = \pm 1$, we have $|\epsilon_i - \epsilon_k| - |\epsilon_j - \epsilon_k| = |\epsilon_i - \epsilon_j|$; for ii) $\mathrm{sgn}(\epsilon_i) = \mathrm{sgn}(\epsilon_j) = -\mathrm{sgn}(\epsilon_k) = \pm 1$, we have $|\epsilon_i - \epsilon_k| - |\epsilon_j - \epsilon_k| = |\epsilon_i - \epsilon_j|$; for iii) $\mathrm{sgn}(\epsilon_i) = \mathrm{sgn}(\epsilon_k) = -\mathrm{sgn}(\epsilon_j) = \pm 1$, we have $|\epsilon_i - \epsilon_k| - |\epsilon_j - \epsilon_k| = |\epsilon_i - \epsilon_j|$; and

for iv) $\mathrm{sgn}(\epsilon_j) = \mathrm{sgn}(\epsilon_k) = -\mathrm{sgn}(\epsilon_i) = \pm 1$, we have $|\epsilon_i - \epsilon_k| - |\epsilon_j - \epsilon_k| = -|\epsilon_i - \epsilon_j|$. Bearing these results in mind we obtain that

$$\langle |\epsilon_i| + |\epsilon_j| + |\epsilon_i - \epsilon_k| - |\epsilon_j - \epsilon_k| \rangle_c |_{|\epsilon_i|>|\epsilon_j|>|\epsilon_k|} \simeq \langle |\epsilon_i| + |\epsilon_j| + \frac{1}{2}|\epsilon_i - \epsilon_j| \rangle_c. \quad (6.54)$$

This formula is similar as the one for the upper limit, with the only difference being the last term with positive sign. The result is then simply given by

$$\frac{1}{2k_BT}\langle |\epsilon_i| + |\epsilon_j| + |\epsilon_j - \epsilon_k| - |\epsilon_i - \epsilon_k| \rangle_c |_{|\epsilon_i|>|\epsilon_j|>|\epsilon_k|} = \frac{1}{2k_BT}(I_1 + I_2 + I_3), \quad (6.55)$$

where $I_1 = I_2 = 0.112\xi$ and $I_3 = 0.0515\xi$. For this we get

$$\frac{1}{2k_BT}\langle |\epsilon_i| + |\epsilon_j| + |\epsilon_j - \epsilon_k| - |\epsilon_i - \epsilon_k| \rangle_c |_{|\epsilon_i|>|\epsilon_j|>|\epsilon_k|} = 0.1375\beta\xi. \quad (6.56)$$

Comparing the results (Eqs. (6.53) and (6.56)) obtained in the upper limit and those in the lower limit (Eqs. (6.28) and (6.39)), we can see configuration averaging over the position $\langle R_{ijk} \rangle_c$ undergoes a relatively large change in magnitude for the two limits. This result reflects an important property of the (variable range) hopping conduction regime presented below. In the VRH, the hopping process allows to go beyond between nearest neighbor impurity sites to minimize the resistivity. The optimization of the typical hopping length plays a major role in determining the scaling of the conductivities with respect to temperature [66]. The lower and upper limits correspond to the opposite extreme situations of the triad distribution which have distinct influences on the optimization of the hopping distances for the Hall transport and thus lead to very different results for the AHC after spatial averaging. We should emphasize that this remarkable difference between $\langle R_{ijk}^{max} \rangle_c$ and $\langle R_{ijk}^{min} \rangle_c$ is obtained under the approximation of a constant DOS around Fermi energy. One can expect this effect will be suppressed in the E-S hopping regime where the DOS is a parabolic function of the onsite energy and the difference between configuration

integrals with respect to energies become more important (refer to the discussion in section 6.5).

Together with the results in Eq. (6.53) and Eq. (6.56) we get

$$\langle R_{ijk}^{max}\rangle_c \langle \epsilon_{ijk}^{max}\rangle_c \simeq e^{0.6205\beta\xi}, \tag{6.57}$$

which gives rise to the upper limit of the AHC in the form

$$\{\sigma_{xy}^{AH}\}_{max} = 3L\sigma_{xx}^2 \frac{k_B T}{e^2} \frac{1}{t_{min}^{(0)}} e^{0.621\beta\xi}. \tag{6.58}$$

This result determines the upper limit of the AHC. Comparing this formula with the result of the longitudinal conductivity which takes the form $\sigma_{xx} = \sigma_0(T)e^{-\xi/k_BT}$, we reach finally

$$\begin{aligned} \{\sigma_{xy}^{AH}\}_{max} &= 3L\sigma_0^{0.621} \frac{k_B T}{e^2} \frac{1}{t_{min}^{(0)}} \sigma_{xx}^{1.379} \\ &\propto \sigma_{xx}^{\gamma}, \end{aligned} \tag{6.59}$$

with $\gamma \simeq 1.38$.

Based on the results obtained above we thus conclude

$$\{\sigma_{xy}^{AH}\}_{max} \propto \sigma_{xx}^{\gamma}, \tag{6.60}$$

where the exponent $1.38 \leq \gamma \leq 1.76$. It is noteworthy the maximum of the AH conductivity corresponds to the smaller power index $\gamma = 1.38$, while the minimum of it corresponds to the larger index $\gamma = 1.76$. This is reasonable since in the hopping conduction regime the longitudinal conductivity is a small value. The scaling predicted above is consistent with a rough estimate for σ_{xy}^{AH} and σ_{xx} presented below. Note the longitudinal charge transport is the 2nd order process with respect tothe transition matrix $t_{ij}^{(0)} e^{-aR_{ij}}$, while the Hall transport is the 3rd order process with

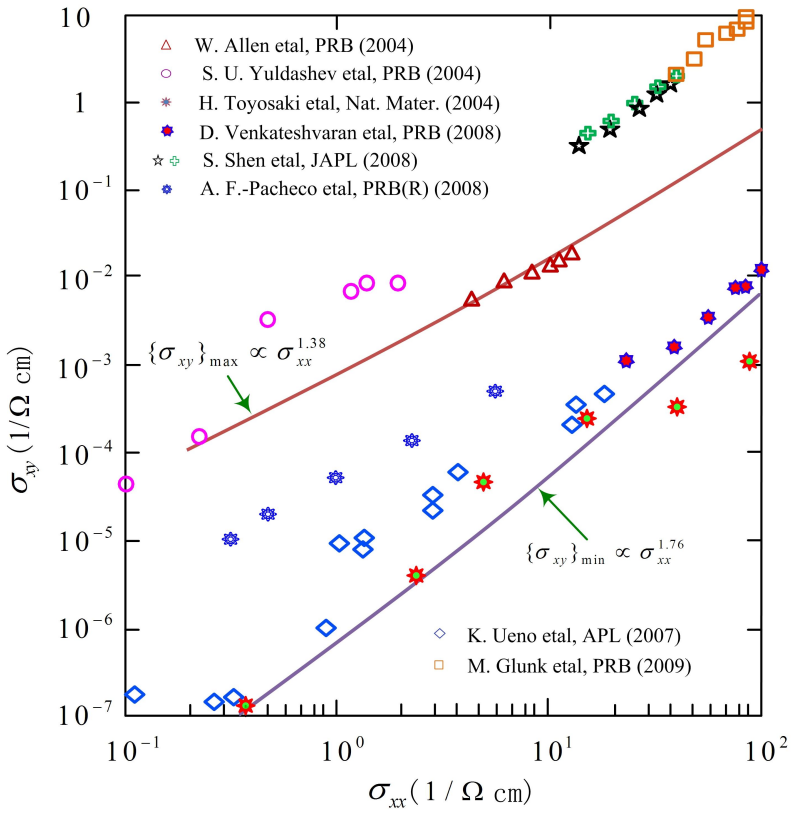

Fig. 6.2. Scaling relation between the Hall and longitudinal conductivity. The results derived from the present theory are compared with the experimental observations.

respect to the transition matrix. On the other hand, the configuration integral for σ_{xx} is along bonds in the percolation path, with the integrand proportional to $n^2(\epsilon_i)$, while for σ_{xx} it is over triads and the integrand is proportional to $n^3(\epsilon_i)$. Based on these properties a rough estimate gives the average scaling relation as $\sigma_{xy}^{AH} \sim \sigma_{xx}^{3/2}$. Furthermore, the range of the scaling relation $1.38 \leq \gamma \leq 1.76$ can be confirmed with a numerical calculation of the Eq. (6.1). Besides, a direct numerical study for the configuration integral (6.1) gives the scaling exponent $\gamma \approx 1.62$, which is consistent with our prediction of the lower and upper limits. Fig. 6.2 shows our theoretical prediction is consistent with the experimental observations of the scaling relation in this regime, hence completing the understanding of the phase diagram of the AHE.

6.4 Dependence of the AHC on DOS

So far in all calculations we have assumed the DOS to be a constant. For the ferromagnetic system with strong exchange interaction between local magnetic sites and charge carriers (e.g. in oxides, manganites, etc) and when the spin can be approximated to be fully polarized along the magnetization around Fermi level, one shall consider only the negative (relative to the magnetization direction) spin states for the calculation of AHC. In this case we do not need to sum over spin-up and spin-down states which contribute oppositely to the AHE. Then the approximation of a constant DOS ($\rho(\epsilon) \simeq \rho(\epsilon_F)$) is good enough and the previous results for the scaling relation are valid.

However, when the Fermi energy crosses both spin-up and -down impurity states, a symmetric DOS with $\rho(\epsilon) = \rho(-\epsilon)$ leads to zero AHC. This can be seen that under the transformation: $\epsilon_{i,\sigma} \to -\epsilon_{i,-\sigma}$, $\epsilon_{j,\sigma} \to -\epsilon_{j,-\sigma}$ and $\epsilon_{k,\sigma} \to -\epsilon_{k,-\sigma}$, we have $F_{ijk}(\epsilon_{i,\sigma}, \epsilon_{j,\sigma}, \epsilon_{k,\sigma}) \to -F_{ijk}(-\epsilon_{i,-\sigma}, -\epsilon_{j,-\sigma}, -\epsilon_{k,-\sigma})$, while the longitudinal conductance $G_{ij}(\epsilon_{i,\sigma}, \epsilon_{j,\sigma}) \to G_{ij}(-\epsilon_{i,-\sigma}, -\epsilon_{j,-\sigma})$. Therefore the AHC changes sign under this transformation, and the averaging over all spin states and the on-site energies below and above Fermi energy yields zero for the AHC. To have a nonzero anomalous Hall effect, we require the DOS around Fermi energy not to be exactly constant. Different situations can be studied separately in the following.

First, we consider the situation that the DOS varies slowly and monotonically versus on-site energy around Fermi level. Around the Fermi energy we can expand the DOS to the first order of ϵ:

$$\rho(\epsilon) \simeq \rho_0 + \frac{d\rho_0}{d\epsilon}\epsilon, \tag{6.61}$$

where ρ_0 is the DOS at Fermi level and $|\epsilon| \leq \xi$. The second term in the expansion is asymmetric in energy ϵ and will then contribute to the AHE. Substituting this expansion into the formula for σ_{xx}^{AH} we obtain

$$\begin{aligned}
\sigma_{xy}^{AH} &= \frac{6L\sigma_{xx}^2}{\mathcal{N}_F}\int d\epsilon_1 d\epsilon_2 d\epsilon_3 \int d^3\vec{r}_{12}\int d^3\vec{r}_{23}\rho(\epsilon_1)[n(\epsilon_1)]^3\rho(\epsilon_2)[n(\epsilon_2)]^3\rho(\epsilon_3)[n(\epsilon_3)]^3 \\
&\quad\times\frac{F_{123}}{G_{12}G_{23}+G_{13}G_{23}+G_{31}G_{12}} \\
&= \frac{6L\sigma_{xx}^2}{\mathcal{N}_F}\int d\epsilon_1 d\epsilon_2 d\epsilon_3 \int d^3\vec{r}_{12}\int d^3\vec{r}_{23}\rho_0^3[n(\epsilon_1)n(\epsilon_2)n(\epsilon_3)]^3 \\
&\quad\times\frac{F_{123}}{G_{12}G_{23}+G_{13}G_{23}+G_{31}G_{12}}+ \\
&\quad+\frac{6L\sigma_{xx}^2}{\mathcal{N}_F}\int d\epsilon_1 d\epsilon_2 d\epsilon_3 \int d^3\vec{r}_{12}\int d^3\vec{r}_{23}\rho_0^2\frac{d\rho_0}{d\epsilon}(\epsilon_1+\epsilon_2+\epsilon_3)[n(\epsilon_1)n(\epsilon_2)n(\epsilon_3)]^3 \\
&\quad\times\frac{F_{123}}{G_{12}G_{23}+G_{13}G_{23}+G_{31}G_{12}}. \qquad (6.62)
\end{aligned}$$

The first term in the last equality is zero according to above analysis. Furthermore, from the second we can see the DOS for the configuration integral is now simply a constant. Therefore all calculations in the former section are valid. We then get

$$\begin{aligned}
\sigma_{xy}^{AH} &= \frac{6L\sigma_{xx}^2}{\mathcal{N}_F}\int d\epsilon_1 d\epsilon_2 d\epsilon_3 \int d^3\vec{r}_{12}\int d^3\vec{r}_{23}\rho_0^2\frac{d\rho_0}{d\epsilon}(\epsilon_1+\epsilon_2+\epsilon_3)[n(\epsilon_1)n(\epsilon_2)n(\epsilon_3)]^3 \\
&\quad\times\frac{F_{123}}{G_{12}G_{23}+G_{13}G_{23}+G_{31}G_{12}} \\
&= 3L\sigma_{xx}^2\frac{d\rho_0}{d\epsilon_F}\frac{k_BT}{e^2}\langle\frac{\mathrm{Im}[\mathrm{tr}(t_{ik}t_{kj}t_{ji})]T_{ijk}^{(3)}(\epsilon_1+\epsilon_2+\epsilon_3)}{|t_{ij}t_{jk}|^2T_{ij}^{(2)}T_{jk}^{(2)}+|t_{ik}t_{jk}|^2T_{ik}^{(2)}T_{jk}^{(2)}+|t_{ij}t_{ik}|^2T_{ij}^{(2)}T_{ik}^{(2)}}\rangle_c. \qquad (6.63)
\end{aligned}$$

It is noteworthy that a similar equation was derived by Burkov et al [50]. However, our formula is new, since the configuration integral derived in this work is essentially different from the former theory. Our formalism is based on the configuration averaging over the percolation cluster, while in the work by by Burkov et al

the configuration averaging is indeed valid for the whole system rather than for 2D percolation cluster. By a similar procedure we obtain the minimum of the AHC by

$$\begin{aligned}\{\sigma_{xy}^{AH}\}_{min} &= 9L\sigma_{xx}^2\frac{k_BT}{e^2}\frac{1}{t_{max}^{(0)}}\frac{d\rho_0}{d\epsilon_F}\frac{M_0}{k_BT}\langle|\epsilon|\rangle_c e^{0.242\beta\xi} \\ &= 9L\sigma_0^{0.242}\frac{k_BT}{e^2}\frac{1}{t_{max}^{(0)}}\frac{d\rho_0}{d\epsilon_F}\frac{M_0}{k_BT}\langle|\epsilon|\rangle_c\sigma_{xx}^{1.758}. \end{aligned} \tag{6.64}$$

Also, the maximum of the AHC is given by

$$\begin{aligned}\{\sigma_{xy}^{AH}\}_{max} &= 9L\sigma_{xx}^2\frac{k_BT}{e^2}\frac{1}{t_{max}^{(0)}}\frac{d\rho_0}{d\epsilon_F}\frac{M_0}{k_BT}\langle|\epsilon|\rangle_c e^{0.621\beta\xi} \\ &= 9L\sigma_0^{0.621}\frac{k_BT}{e^2}\frac{1}{t_{max}^{(0)}}\frac{d\rho_0}{d\epsilon_F}\frac{M_0}{k_BT}\langle|\epsilon|\rangle_c\sigma_{xx}^{1.379}. \end{aligned} \tag{6.65}$$

The appearance of M_0/k_BT due to the summation over the spin-up and spin-down states. Note $\langle|\epsilon|\rangle_c = 0.112\xi$, we finally get

$$\{\sigma_{xy}^{AH}\}_{min} = 1.01L\sigma_0^{0.242}(T)\frac{M_0}{e^2}\frac{1}{t_{max}^{(0)}}\frac{d\rho_0}{d\epsilon_F}\xi(T)\sigma_{xx}^{1.758}, \tag{6.66}$$

and

$$\{\sigma_{xy}^{AH}\}_{max} = 1.01L\sigma_0^{0.621}(T)\frac{M_0}{e^2}\frac{1}{t_{max}^{(0)}}\frac{d\rho_0}{d\epsilon_F}\xi(T)\sigma_{xx}^{1.379}. \tag{6.67}$$

The functions $\sigma_0(T)$ and $\xi(T)$ affects the power-law of the AHC versus temperature. For the Mott hopping conduction regime, we have $\xi = k_BT\big(T_0/T\big)^{1/4}$. The dependence of $\sigma_0(T)$ on temperature can be determined through experiment observation. Generally we may assume

$$\sigma_0 \sim T^{-\delta}. \tag{6.68}$$

Then the Eqs. (6.66) and (6.67) give

$$\{\sigma_{xy}^{AH}\}_{min} \sim 1.01L\frac{M_0}{e^2}\frac{1}{t_{max}^{(0)}}\frac{d\rho_0}{d\epsilon_F}T^{0.75-0.242\delta}\sigma_{xx}^{1.758}, \tag{6.69}$$

$$\{\sigma_{xy}^{AH}\}_{max} \sim 1.01L\frac{M_0}{e^2}\frac{1}{t_{max}^{(0)}}\frac{d\rho_0}{d\epsilon_F}T^{0.75-0.621\delta}\sigma_{xx}^{1.379}. \tag{6.70}$$

Second, when the DOS has a local minimum but still larger than zero at the Fermi energy due to particle-particle interaction (coulomb interaction) [75], the first derivative of the DOS with respect to energy $d\rho/d\epsilon_F = 0$, Moreover, we assume the DOS has only a relatively small variation in the range $|\epsilon| < \xi$. In this way we can expand the DOS to the order of ϵ^3, which is the first asymmetric term in DOS expansion:

$$\rho(\epsilon) \simeq \rho_0 + \frac{1}{2}\frac{d^2\rho_0}{d\epsilon^2}\epsilon^2 + \frac{1}{6}\frac{d^3\rho_0}{d\epsilon^3}\epsilon^3. \tag{6.71}$$

It is easy to show the scaling law between σ_{xy}^{AH} and σ_{xx} is the same as before, but the power-law will be changed. By a similar procedure we obtain

$$\{\sigma_{xy}^{AH}\}_{min} \simeq 0.002L\sigma_0^{0.242}(T)\frac{M_0}{e^2}\frac{1}{t_{max}^{(0)}}\frac{d^3\rho_0}{d\epsilon_F^3}\xi^3(T)\sigma_{xx}^{1.758}, \tag{6.72}$$

and

$$\{\sigma_{xy}^{AH}\}_{max} \simeq 0.002L\sigma_0^{0.621}(T)\frac{M_0}{e^2}\frac{1}{t_{max}^{(0)}}\frac{d^3\rho_0}{d\epsilon_F^3}\xi^3(T)\sigma_{xx}^{1.379}. \tag{6.73}$$

6.5 Efros-shklovskii hopping conduction regime

In the strong coulomb interaction case, the DOS may be greatly reduced around the Fermi energy [67, 75]. In this case the assumption in previous section that the DOS has a small variation relative to ρ_0 is not valid. The limit situation is that

both the DOS and the first derivative at Fermi level varnish (i.e. the E-S hopping regime), which corresponds to the appearance of a gap due to coulomb interaction. In this case $\rho_0 = 0$ and $d\rho/d\epsilon_F = 0$, and thus

$$\rho(\epsilon) \simeq \frac{1}{2}\frac{d^2\rho_0}{d\epsilon^2}\epsilon^2 + \frac{1}{6}\frac{d^3\rho_0}{d\epsilon^3}\epsilon^3. \tag{6.74}$$

This situation is different from the cases discussed in the previous section, since around the Fermi energy DOS is not dominated by a constant but by a parabolic function of on-site energy. This may lead to a quantitative variation of the probability function in then configuration averaging, and finally affect the quantitative result of the scaling relation. The formula of the connectivity $n(\epsilon_i, \xi)$ is now given by

$$\begin{aligned} n(\epsilon_i,\xi) &= \frac{1}{(2ak_BT)^3}\frac{4\pi}{3}\Big[\int_0^{\epsilon_i} d\epsilon_j\rho(\epsilon_j)(\xi-\epsilon_i)^3 + \int_{\epsilon_i}^{\xi} d\epsilon_j\rho(\epsilon_j)(\xi-\epsilon_j)^3 \\ &\quad + \int_{-(\xi-|\epsilon_i|)}^{0} \rho(\epsilon_j)(\xi-|\epsilon_i|-|\epsilon_j|)^3\Big] \\ &= \frac{1}{(2ak_BT)^3}\frac{2\pi}{3}\frac{d^2\rho_0}{d\epsilon^2}\big(\frac{1}{30}\xi^6 - \frac{1}{10}\xi^5|\epsilon_i| + \frac{1}{4}\xi^4|\epsilon_i|^2 - \\ &\quad -\frac{1}{3}|\epsilon_i|^3\xi^3 + \frac{3}{10}|\epsilon_i|^5\xi - \frac{3}{20}|\epsilon_i|^6\big). \end{aligned} \tag{6.75}$$

The configuration averaging of AH conductivity can be calculated in the similar way as before. Specifically, we can again separate the calculation of $\langle R_{ijk}^{max\,min}\rangle_c$ into two steps, with the first step to do the configuration integral with respect to position and the second step with respect to onsite energies. It is straightforward to know the first step yields the same result and the difference of the DOS affects only the result in the second step. For the lower limit we get

$$\begin{aligned} \langle R_1 + R_2 - R_3\rangle_c|_{R_1,R_2<R_3} &\simeq 0.33\frac{\beta}{2a}\frac{\int_{-\xi}^{\xi} d\epsilon_i[n(\epsilon_i)]^3\rho(\epsilon_i)(\xi-|\epsilon_i|)^7}{\int_{-\xi}^{\xi} d\epsilon_i[n(\epsilon_i)]^3\rho(\epsilon_i)(\xi-|\epsilon_i|)^6} \\ &\simeq 0.092\beta\xi/a. \end{aligned} \tag{6.76}$$

The new forms of the DOS (6.74) and connectivity (6.75) have been considered. The average of on-site energy can be calculated by

$$
\begin{aligned}
\tfrac{1}{2k_BT}\quad & \langle|\epsilon_i|+|\epsilon_j|+|\epsilon_j-\epsilon_k|-|\epsilon_i-\epsilon_k|\rangle_c|_{|\epsilon_i|<|\epsilon_j|<|\epsilon_k|}= \\
= \quad & \frac{1}{2k_BT}\frac{\int d\epsilon_i \frac{d^2\rho_0}{d\epsilon_F^2}\epsilon_i^2[n(\epsilon_i)]^3|\epsilon_i|}{\int d\epsilon_i\rho(\epsilon_i)[n(\epsilon_i)]^3}+\frac{1}{2k_BT}\frac{\int d\epsilon_j \frac{d^2\rho_0}{d\epsilon_F^2}\epsilon_j^2[n(\epsilon_j)]^3|\epsilon_j|}{\int d\epsilon_j\rho(\epsilon_j)[n(\epsilon_j)]^3}- \\
& -\frac{1}{2}\frac{1}{2k_BT}\frac{\int d\epsilon_i\int d\epsilon_j \frac{d^2\rho_0}{d\epsilon_F^2}\epsilon_i^2[n(\epsilon_i)]^3\rho(\epsilon_j)[n(\epsilon_j)]^3|\epsilon_i-\epsilon_j|}{\int d\epsilon_i\int d\epsilon_j \frac{d^2\rho_0}{d\epsilon_F^2}\epsilon_j^2[n(\epsilon_i)]^3\rho(\epsilon_j)[n(\epsilon_j)]^3} \\
= \quad & \frac{1}{2k_BT}\frac{\int_0^\xi d\epsilon_i\left(\frac{1}{30}\xi^6-\frac{1}{10}\xi^5|\epsilon_i|+\frac{1}{4}\xi^4|\epsilon_i|^2-\frac{1}{3}|\epsilon_i|^3\xi^3+\frac{3}{10}|\epsilon_i|^5\xi-\frac{3}{20}|\epsilon_i|^6\right)^3\epsilon_i^3}{\int_0^\xi d\epsilon_i\left(\frac{1}{30}\xi^6-\frac{1}{10}\xi^5|\epsilon_i|+\frac{1}{4}\xi^4|\epsilon_i|^2-\frac{1}{3}|\epsilon_i|^3\xi^3+\frac{3}{10}|\epsilon_i|^5\xi-\frac{3}{20}|\epsilon_i|^6\right)^3\epsilon_i^2}- \\
& -\frac{1}{8k_BT}\frac{\int_0^\xi d\epsilon_i\int_0^\xi d\epsilon_j\left(\frac{1}{30}\xi^6-\frac{1}{10}\xi^5|\epsilon_i|+\frac{1}{4}\xi^4|\epsilon_i|^2-\frac{1}{3}|\epsilon_i|^3\xi^3+\frac{3}{10}|\epsilon_i|^5\xi-\frac{3}{20}|\epsilon_i|^6\right)^3\times}{\int d\epsilon_i\int d\epsilon_j\left(\frac{1}{30}\xi^6-\frac{1}{10}\xi^5|\epsilon_i|+\frac{1}{4}\xi^4|\epsilon_i|^2-\frac{1}{3}|\epsilon_i|^3\xi^3+\frac{3}{10}|\epsilon_i|^5\xi-\frac{3}{20}|\epsilon_i|^6\right)^3\times} \\
& \frac{\left(\frac{1}{30}\xi^6-\frac{1}{10}\xi^5|\epsilon_j|+\frac{1}{4}\xi^4|\epsilon_j|^2-\frac{1}{3}|\epsilon_j|^3\xi^3+\frac{3}{10}|\epsilon_j|^5\xi-\frac{3}{20}|\epsilon_j|^6\right)^3|\epsilon_i-\epsilon_j|\epsilon_i^2\epsilon_j^2}{\left(\frac{1}{30}\xi^6-\frac{1}{10}\xi^5|\epsilon_j|+\frac{1}{4}\xi^4|\epsilon_j|^2-\frac{1}{3}|\epsilon_j|^3\xi^3+\frac{3}{10}|\epsilon_j|^5\xi-\frac{3}{20}|\epsilon_j|^6\right)^3|\epsilon_i^2\epsilon_j^2} \\
\simeq \quad & 0.29\xi\beta. \qquad (6.77)
\end{aligned}
$$

From above two equations we can see, comparing with the results with constant DOS, the magnitude of energy averaging in the present case increases, while the magnitude of position averaging decreases. This is reasonable since the DOS varies as a function of ϵ^2, which increases the contribution to the Hall effect from the impurity states with energies far away from the Fermi energy and accordingly, decreases the contribution from hopping between impurity sites with large distances.

Together with the results in Eqs. (6.76) and (6.77) we find

$$\langle R_{ijk}^{min}\rangle_c\langle\epsilon_{ijk}^{min}\rangle_c \simeq e^{0.38\beta\xi}. \qquad (6.78)$$

The lower limit of the AHC is then obtained by

$$\{\sigma_{xy}^{AH}\}_{min} \simeq 0.059L\sigma_0^{0.38}(T)\frac{M_0}{e^2}\frac{1}{t_{max}^{(0)}}\frac{d^3\rho_0}{d\epsilon_F^3}\xi^3(T)\sigma_{xx}^{1.62}. \qquad (6.79)$$

Similarly, for the upper limit of AH conductivity, we have

$$\begin{aligned}\langle R_1+R_2-R_3\rangle_c|_{R_1,R_2>R_3} &\simeq 1.03\frac{\beta}{2a}\frac{\int_{-\xi}^{\xi}d\epsilon_i[n(\epsilon_i)]^3\rho(\epsilon_i)(\xi-|\epsilon_i|)^7}{\int_{-\xi}^{\xi}d\epsilon_i[n(\epsilon_i)]^3\rho(\epsilon_i)(\xi-|\epsilon_i|)^6}\\ &\simeq 0.29\beta\xi/a. \end{aligned} \tag{6.80}$$

The average of on-site energy can be calculated by

$$\begin{aligned}\tfrac{1}{2k_BT}\quad &\langle|\epsilon_i|+|\epsilon_j|+|\epsilon_i-\epsilon_k|-|\epsilon_j-\epsilon_k|\rangle_c|_{|\epsilon_i|>|\epsilon_j|>|\epsilon_k|}=\\ =\quad &\frac{1}{2k_BT}\frac{\int d\epsilon_i\frac{d^2\rho_0}{d\epsilon_F^2}\epsilon_i^2[n(\epsilon_i)]^3|\epsilon_i|}{\int d\epsilon_i\rho(\epsilon_i)[n(\epsilon_i)]^3}+\frac{1}{2k_BT}\frac{\int d\epsilon_j\frac{d^2\rho_0}{d\epsilon_F^2}\epsilon_j^2[n(\epsilon_j)]^3|\epsilon_j|}{\int d\epsilon_j\rho(\epsilon_j)[n(\epsilon_j)]^3}+\\ &+\frac{1}{2}\frac{1}{2k_BT}\frac{\int d\epsilon_i\int d\epsilon_j\frac{d^2\rho_0}{d\epsilon_F^2}\epsilon_i^2[n(\epsilon_i)]^3\rho(\epsilon_j)[n(\epsilon_j)]^3|\epsilon_i-\epsilon_j|}{\int d\epsilon_i\int d\epsilon_j\frac{d^2\rho_0}{d\epsilon_F^2}\epsilon_j^2[n(\epsilon_i)]^3\rho(\epsilon_j)[n(\epsilon_j)]^3}\\ =\quad &\frac{1}{2k_BT}\frac{\int_0^{\xi}d\epsilon_i\left(\frac{1}{30}\xi^6-\frac{1}{10}\xi^5|\epsilon_i|+\frac{1}{4}\xi^4|\epsilon_i|^2-\frac{1}{3}|\epsilon_i|^3\xi^3+\frac{3}{10}|\epsilon_i|^5\xi-\frac{3}{20}|\epsilon_i|^6\right)^3\epsilon_i^3}{\int_0^{\xi}d\epsilon_i\left(\frac{1}{30}\xi^6-\frac{1}{10}\xi^5|\epsilon_i|+\frac{1}{4}\xi^4|\epsilon_i|^2-\frac{1}{3}|\epsilon_i|^3\xi^3+\frac{3}{10}|\epsilon_i|^5\xi-\frac{3}{20}|\epsilon_i|^6\right)^3\epsilon_i^2}+\\ &+\frac{1}{8k_BT}\frac{\int_0^{\xi}d\epsilon_i\int_0^{\xi}d\epsilon_j\left(\frac{1}{30}\xi^6-\frac{1}{10}\xi^5|\epsilon_i|+\frac{1}{4}\xi^4|\epsilon_i|^2-\frac{1}{3}|\epsilon_i|^3\xi^3+\frac{3}{10}|\epsilon_i|^5\xi-\frac{3}{20}|\epsilon_i|^6\right)^3\times}{\int d\epsilon_i\int d\epsilon_j\left(\frac{1}{30}\xi^6-\frac{1}{10}\xi^5|\epsilon_i|+\frac{1}{4}\xi^4|\epsilon_i|^2-\frac{1}{3}|\epsilon_i|^3\xi^3+\frac{3}{10}|\epsilon_i|^5\xi-\frac{3}{20}|\epsilon_i|^6\right)^3\times}\\ &\frac{\left(\frac{1}{30}\xi^6-\frac{1}{10}\xi^5|\epsilon_j|+\frac{1}{4}\xi^4|\epsilon_j|^2-\frac{1}{3}|\epsilon_j|^3\xi^3+\frac{3}{10}|\epsilon_j|^5\xi-\frac{3}{20}|\epsilon_j|^6\right)^3|\epsilon_i-\epsilon_j|\epsilon_i^2\epsilon_j^2}{\left(\frac{1}{30}\xi^6-\frac{1}{10}\xi^5|\epsilon_j|+\frac{1}{4}\xi^4|\epsilon_j|^2-\frac{1}{3}|\epsilon_j|^3\xi^3+\frac{3}{10}|\epsilon_j|^5\xi-\frac{3}{20}|\epsilon_j|^6\right)^3|\epsilon_i^2\epsilon_j^2}\\ \simeq\quad &0.38\xi\beta. \end{aligned} \tag{6.81}$$

Thus we have

$$\langle R_{ijk}^{min}\rangle_c\langle\epsilon_{ijk}^{min}\rangle_c\simeq e^{0.67\beta\xi}. \tag{6.82}$$

This leads to the scaling relation between the lower limit of the AHC and the longitudinal conductivity in the following form

$$\{\sigma_{xy}^{AH}\}_{max}\simeq 0.026L\sigma_0^{0.67}(T)\frac{M_0}{e^2}\frac{1}{t_{min}^{(0)}}\frac{d^3\rho_0}{d\epsilon_F^3}\xi^3(T)\sigma_{xx}^{1.33}. \tag{6.83}$$

Therefore in the E-S hopping regime the scaling relation between anomalous Hall and longitudinal conductivities becomes $\sigma_{xy}^{AH} \propto \sigma_{xx}^{\gamma}$ with $1.33 \leq \gamma \leq 1.62$, which is only a small quantitative shift relative to the scaling obtained in the case with a constant DOS. This result is consistent with the observations in the experiments by Aronzon et al [35], and by Allen et al [39], who found the scaling relation as $1.4 \leq \gamma \leq 1.6$ for the E-S hopping conduction regime. Furthermore, the result that the AHC σ_{xy}^{AH} proportional to $d\rho_0/d\epsilon_F$ (when the DOS varies monotonically with respect to energy around Fermi energy) or $d^3\rho_0/d\epsilon_F^3$ (when the DOS has a local minimum at Fermi level) indicates an interesting property that the AHC may change sign when the first or third order derivative of DOS with respect to energy changes sign. This result is consistent with the observation by Allen et al [39]. Finally, it can be expected that the general situation with a reduced DOS (not necessarily zero) at Fermi level will be associated with a scaling falling in between the E-S hopping regime and the case with a constant DOS. This confirms that the scaling relation between σ_{xy}^{AH} and σ_{xx} is insensitive to what types of hopping conduction the material belongs to, and is therefore generic for the disordered insulating regime.

6.6 Activation E_3 hopping regime

Finally, we present a brief study on the AHE in the activation E_3 hopping regime, which dominates the charge transport in the disordered insulating system when the temperature $T > T_0$. In the activation E_3 hopping regime, the hopping between nearest neighbor impurity sites dominates the charge transport. In this case the hopping configuration in the position space is not affected by temperature. Thus the configuration averaging over position space is independent of temperature. The temperature dependence of the conductivities is solely determined by the energy configuration integral. Again we consider that the impurity sites are homogeneously

distributed in position space. Then connectivity $n(\epsilon_i)$ for a specific impurity site with on-site energy ϵ_i is given by

$$n(\epsilon_i) = \frac{4}{3}\pi R_c^3 \int d\epsilon_j \rho(\epsilon_j) \Theta\big[E_3 - \frac{1}{2}(|\epsilon_i| + |\epsilon_j| + |\epsilon_i - \epsilon_j|)\big], \tag{6.84}$$

where E_3 is the cut-off for on-site energy and R_c represents the typical distance between the neighbor impurity sites. For a constant DOS, one has

$$n(\epsilon_i) = \frac{4}{3}\pi R_c^3 \rho_0 (2E_3 - |\epsilon_i|), \tag{6.85}$$

with $|\epsilon| \leq E_3$. It can be seen that for the present regime, $n(E_3) = \frac{4}{3}\pi R_c^3 \rho_0 E_3 > 0$. This is different from the situation in the VRH regime discussed in previous sections. Substituting the above formula into Eq. (5.12) one calculate the relation between the cut-off E_3 and $\bar{n}$ straightforwardly, with which one can verify that E_3 is a constant independent of temperature and $E_3 \propto (\rho_0 R_c^3)^{-1}$ [75]. The longitudinal conductivity is then given by

$$\sigma_{xx} = \sigma_0 e^{-E_3/k_B T}. \tag{6.86}$$

The AHC is given by Eq. (5.33) with the difference that the function of $n(\epsilon_i)$ is different and the configuration integral over position is unrelated to that over on-site energies and does not affect the temperature dependence of σ_{xy}^{AH}. For this we obtain the upper and lower limits of the AHC that

$$\{\sigma_{xy}^{AH}\}_{\substack{min \\ max}} \simeq 3L\sigma_{xx}^2 \frac{k_B T e^{aR_c}}{e^2 t_{max/min}^{(0)}} \langle \epsilon_{ijk}^{\substack{min \\ max}} \rangle_c. \tag{6.87}$$

By a similar procedure we obtain that $\langle \epsilon_{ijk}^{\max} \rangle_c \approx e^{0.61\beta E_3}$, $\langle \epsilon_{ijk}^{min} \rangle_c \approx e^{0.34\beta E_3}$. With these we obtain the scaling relation $\sigma_{xy}^{AH} \propto \sigma_{xx}^{\gamma}$ with $1.39 \leq \gamma \leq 1.66$. With this result

we can see the scaling in the activation E_3 hopping regime has only a quantitative small shift relative to the scaling in the VRH hopping regimes.

7. CONCLUSIONS AND DISCUSSIONS

To sum up, we have developed a theory based on the phonon-assisted hopping mechanism and percolation theory to study the anomalous Hall effect (AHE) in the disordered insulating regime. A general formula for the anomalous Hall conductivity (AHC) has been derived for the hopping conduction regime, with the key physics that the Hall currents are averaged over percolation cluster being completely considered. We calculated the lower and upper limits of the AHC, and show it scales with the longitudinal conductivity as $\sigma_{xy}^{AH} \sim \sigma_{xx}^{\gamma}$ with γ predicted to be $1.33 \leq \gamma \leq 1.76$. The predicted scaling only slightly dependents on the specific hopping types, and is quantitatively in agreement with the experimental observations.

From our theory the scaling relation in the insulating AHE is fully determined by the microscopic origin: phonon-assisted hopping conduction mechanism, and by the procedure that the macroscopic AHC is obtained through a configuration integral over the percolation cluster. It is clear such two aspects are generic for the hopping regime in disordered insulators, and therefore the obtained scaling in this regime is qualitatively generic in the disordered insulating regime. We have shown that this scaling remains similar regardless of whether the hopping process is Mott-variable-range-hopping, influenced by interactions, or activation E_3 hopping (nearest neighbor hopping) regime. Our theory explains naturally how the scaling between the two quantities remain true even when the diagonal conductivity crosses regimes and why this type of scaling is so prevalent in the insulating regime. Our theory completes the understanding of the AHE phase diagram in the insulating regime.

While the present theory has resolved the most challenging issue of the AHE in the insulating regime, there are several interesting issues deserving further efforts following this study. For example, in this work only the electron-phonon coupling is considered. Generally, the electron-magnon scattering may also contribute to the charge transport, especially when the temperature is close to Curie temperature T_c. A

qualitative difference from the electron-phonon coupling is that the electron-magnon scattering flips spin. The longitudinal conductivity around $T = T_c$ exhibits a local hump in both the metallic and insulating regime [89], although in the later regime it is less obvious. This phenomenon is believed to be a consequence of electron-magnon scattering [90]. For the insulating regime, it is therefore expected that the electon-magnon scattering and the random distribution of local magnetic moments will play important roles for the hopping conduction besides the thermal effect. Another important issue is the transition of the AHE from insulating to metallic regime. When the impurity doping increases, the coupling between impurity states strengthens and the metal insulator transition will finally take place. A systematic study of the AHE in both the insulating side and metallic side will be helpful to reveal the mechanism of the transition from insulating AHE to metallic regime. Furthermore, as a comparison, it is also interesting to study the spin Hall effect in the insulating regime. A similar behavior of the spin Hall conductivity (SHC) is expected to result. However, another important thing that needs to be made clear is that one need to relate the spin accumulation to the SHC in this regime.

REFERENCES

[1] E. Hall, Philos. Mag. **12**, 157 (1881).

[2] N. Nagaosa, J. Sinova, S. Onoda, A. H. MacDonald, and P. Ong, Rev. Mod. Phys. **82**, 1539 (2010).

[3] R. Karplus and J. M. Luttinger, Phys. Rev. **95**, 1154 (1954).

[4] J. Smit, Physica (Amsterdam) **21**, 877 (1955).

[5] J. Smit, Physica (Amsterdam) **24** 39 (1958).

[6] J. M. Luttinger, Phys. Rev. **112** 739 (1958).

[7] L. Berger, Phys. Rev. B **2**, 4559 (1970).

[8] L. Berger, Phys. Rev. B **5**, 1862 (1972).

[9] M. V. Berry, Proc. R. Soc. London **392**, 45 (1984).

[10] D. J. Thouless, M. Kohmoto, M. P. Nightingale, and M. den Nijs, Phys. Rev. Lett. **49**, 405 (1982).

[11] M. Chang and Q. Niu, Phys. Rev. B **53**, 7010 (1996).

[12] G. Sundaram and Q. Niu, Phys. Rev. B **59**, 14915 (1999).

[13] T. Jungwirth, Q. Niu, and A. H. MacDonald, Phys. Rev. Lett. **88**, 207208 (2002).

[14] M. Onoda and N. Nagaosa, J. Phys. Soc. Jpn. **71**, 19 (2002).

[15] F. D. M. Haldane, Phys. Rev. Lett. **61**, 2015 (1988).

[16] X. L. Qi, Y. S. Wu, and S.C. Zhang, Phys. Rev. B **74**, 045125 (2006).

[17] Chao-Xing Liu, Xiao-Liang Qi, Xi Dai, Zhong Fang and Shou-Cheng Zhang, Phys. Rev. Lett. **101**, 146802 (2008).

[18] Congjun Wu, Phys. Rev. Lett. **101**, 186807 (2008).

[19] L. B. Shao, Shi-Liang Zhu, L. Sheng, D.Y. Xing and Z. D. Wang, Phys. Rev. Lett. **101**, 246810 (2008).

[20] X.-J. Liu, X. Liu, C. Wu, and J. Sinova, Phys. Rev. A **81**, 033622 (2010).

[21] Rui Yu, Wei Zhang, Hai-Jun Zhang, Shou-Cheng Zhang, Xi Dai1, and Zhong Fang, Science **329** , 61 (2010).

[22] M. Z. Hasan and C. L. Kane, Rev. Mod. Phys. **82**, 3045 (2010).

[23] T. Miyasato, N. Abe, T. Fujii, A. Asamitsu, S. Onoda, Y. Onose, N. Nagaosa, and Y. Tokura, Phys. Rev. Lett. **99**, 086602 (2007).

[24] Y. Shiomi, Y. Onose, and Y. Tokura, Phys. Rev. B **79**, 100404 (2009).

[25] N. A. Sinitsyn, Q. Niu, J. Sinova, and K. Nomura, Phys. Rev. B **72**, 045346 (2005).

[26] N. A. Sinitsyn, Q. Niu, and A. H. MacDonald, Phys. Rev. B **73**, 075318 (2006).

[27] S. Onoda, N. Sugimoto, and N. Nagaosa, Prog. Theor. Phys. **116**, 61 (2006).

[28] M. Borunda, T. Nunner, T. Luck, N. Sinitsyn, C. Timm, J. Wunderlich, T. Jungwirth, A. H. MacDonald, and J. Sinova, Phys. Rev. Lett. **99**, 066604 (2007).

[29] N. A. Sinitsyn, A. H. MacDonald, T. Jungwirth, V. K. Dugaev, and J. Sinova, Phys. Rev. B **75**, 045315 (2007).

[30] T. S. Nunner, N. A. Sinitsyn, M. F. Borunda, V. K. Dugaev, A. A. Kovalev, A. Abanov, C. Timm, T. Jungwirth, J. ichiro Inoue, A. H. MacDonald, and J. Sinova, Phys. Rev., B **76**, 235312 (2007).

[31] N. A. Sinitsyn, J. Phys.: Condens. Matter **20**, 023201 (2008).

[32] A. A. Kovalev, K. Výborný, and J. Sinova, Phys. Rev. B **78**, 041305 (R) (2008).

[33] S. Onoda, N. Sugimoto, and N. Nagaosa, Phys. Rev. B **77**, 165103 (2008).

[34] J. S.-Y. Feng, R. D. Pashleyz and M.-A. Nicolet, J. Phys. C: Solid State Phys. **8**, 1010 (1975)

[35] B. A. Aronzon, D. Yu. Kovalev, A. N. Lagar'kov, E. Z. Meilikhov, V. V. Ryl'kov, M. A. Sedova, N. Negre, M. Goiran, and J. Leotin, JETP, **70** 90 (1999).

[36] B. A. Aronzon, V. V. Rylkov, D. Yu. Kovalev, E. Z. Meilikhov, A. N. Lagarkov, M. A. Sedova, M. Goiran, N. Negre, B. Raquet, and J. Leotin, Phys. Stat. Sol. (B) **218**, 169 (2000).

[37] A. V. Samoilov, G. Beach, C. C. Fu, N.-C. Yeh, and R. P. Vasquez, Phys. Rev. B **57**, 14032(R) (1998).

[38] H. Toyosaki, T. Fukumura, Y. Yamada, K. Nakajima, T. Chikyow, T. Hasegawa, H. Koinuma and M. Kawasaki, Nat. Mater. **3**, 221 (2004).

[39] W. Allen, E. G. Gwinn, T. C.Kreutz, and A. C. Gossard, Phys. Rev. B **70**, 125320 (2004).

[40] Sh. U. Yuldashev, H. C. Jeon, H. S. Im, T. W. Kang, S. H. Lee, and J. K. Furdyna, Phys. Rev. B **70**, 193203 (2004).

[41] K. Ueno, T. Fukumura, H. Toyosaki, M. Nakano, and M. Kawasaki, Appl. Phys. Lett. **90**, 072103 (2007).

[42] S. Shen, X. Liu, Z. Ge, J. K. Furdyna, M. Dobrowolska, and J. Jaroszynski, J. Appl. Phys. **103**, 07D134 (2008).

[43] A. Fernández-Pacheco, J. M. De Teresa, J. Orna, L. Morellon, P. A. Algarabe, J. A. Pardo, and M. R. Ibarra, Phys. Rev. B **77**, 100403(R) (2008).

[44] D. Venkateshvaran, W. Kaiser, A. Boger, M. Althammer, M. S. Ramachandra Rao, Sebastian T. B. Goennenwein, M. Ope, and R. Gross, Phys. Rev. B **78**, 092405 (2008).

[45] M. Glunk, J. Daeubler, W. Schoch, R. Sauer, and W. Limmer, Phys. Rev. B **80**, 125204 (2009).

[46] D. Chiba, A. Werpachowska, M. Endo, Y. Nishitani, F. Matsukura,1 T. Dietl, and H. Ohno, Phys. Rev. Lett. **104**, 106601 (2010).

[47] S. Onoda, N. Sugimoto, and N. Nagaosa, Phys. Rev. Lett. **97**, 126602 (2006).

[48] S. H. Chun, M. B. Salamon, Y. Lyanda-Geller, P. M. Goldbart, and P. D. Han, Phys. Rev. Lett. **84**, 757 (2000).

[49] Y. Lyanda-Geller, S. Chun, M. Salamon, P. Goldbart, P. Han, Y. Tomioka, A. Asamitsu, and Y. Tokura, Phys. Rev. B **63**, 184426 (2001).

[50] A. A. Burkov and L. Balents, Phys. Rev. Lett. **91**, 057202 (2003).

[51] W. Zawadzki, in Optical Properties of Solids, E. D. Haidemenakis (ed.), Gordon and Breach, New York, 1970.

[52] R. Winkler, Spin-orbit coupling effects in two-dimensional electron and hole systems, Spinger-Verlag, New York (2003).

[53] Neil W. Ashcroft and N. David Mermin, Solid State Physics, Harcourt: Orlando, (1976).

[54] J. Sinova and A.H. MacDonald, Semicond. and Semimetals, **2**, 45 (2008).

[55] G. Dresselhaus, Phys. Rev. **100**, 580 (1955).

[56] E.I. Rashba, Sov. Phys. - Solid State **2**, 1109 (1960).

[57] J. Sinova, D. Culcer, Q. Niu, N. A. Sinitsyn, T. Jungwirth and A.H. MacDonald, Phys. Rev. Lett. **92**, 126603 (2004).

[58] J. M. Luttinger, Phys. Rev. **102**, 1030 (1956).

[59] S. Murakami, N. Nagaosa, S.-C. Zhang, Science **301**, 1348 (2003).

[60] Xiong-Jun Liu, Xin Liu, Leong-Chuan Kwek, and Choo-Hiap Oh, Front. Phys. China, **3**, 113 (2008).

[61] K. G. Wilson, Phys. Rev. D, **10**, 2445 (1974).

[62] C. P. Sun, M. L. Ge, Phys. Rev. D **41**, 1349 (1990).

[63] E. J. W. Verwey, P. W. Haayman and F. C. Romeijn, J. Chem. Phys. **15**, 181 (1947).

[64] A. L. Efros and B. I. Shklovskii, Phys. Stat. Sol. B **50**, 45 (1972).

[65] B. I. Shklovskii, A. L. Efros, and L. Y. Yanchev, Sov. Phys. -JETP Lett. **14**, 233 (1971).

[66] N. F. Mott, Phil. Mag. **19**, 835 (1969).

[67] A. L. Efros and B. I. Shklovskii, J. Phys. C **8**, L49 (1975).

[68] J. M. Ziman, Principles of the Theory of Solids, Cambridge University Press, Cambridge (1972).

[69] M. P. Marder, Condensed Matter Physics, Wiley, New York (2000).

[70] J. Schliemann and D. Loss, Phys. Rev. B **68**, 165311 (2003)

[71] A. Miller and E. Abrahams, Phys. Rev. **120**, 745 (1960).

[72] W. Kohn, Solid St. Phys., **5**, 257 (1957).

[73] F. Bassani, G. Iadonisi, and B. Preziosi, Rep. Prog. Phys. **37**, 1099 (1974).

[74] G. L. Bir and G. E. Pikus, Symmetry and Deformation Effects in Semiconductors, Nauka, Moscow (1972).

[75] B. I. Shklovskii and A. L. Efros, Electronic Properties of Doped Semiconductors, Springer-Verlag, Berlin (1984).

[76] B. V. Shanabrook, O. J. Glembocki, D. A. Broido, and W. I. Wang, Phys. Rev. B **39**, 3411 (1989).

[77] L. D. Landau and E. M. Lifshitz, Quantum Mechanics, Non-relativistic Theory, Third Edition: Vol. 3, Butterworth-Heinemann, Burlington (1981).

[78] Gel'mont and D'yakonov, Sov. Phys. -Semicond, **5**, 1905 (1971).

[79] A. Baldereschi and Nunzio O. Lipari, Phys. Rev. B **8**, 2697 (1973).

[80] Philip W. Phillips, Advanced Solid State Physics, Westview Press, Cambridge (2003).

[81] E. Abrahams, P. W. Anderson, D. C. Licciardello, and T. V. Ramakrishnan, Phys. Rev. Lett. **42**, 673 (1979).

[82] T. Holstein, Phys. Rev. **1**, 1329 (1961).

[83] G. A. Fiete, G. Zaránd, and K. Damle, Phys. Rev. Lett. **91**, 097202 (2003).

[84] M. Pollak, J. Non-Cryst. Solids **11**, 1 (1972).

[85] V. Ambegaokar, B. I. Halperin, and J. S. Langer, Phys. Rev. B **4**, 2612 (1971).

[86] G. E. Pike and C. H. Seager, Phys. Rev. B **10**, 1421 (1974).

[87] H. Overhof, Phys. Stat. Sol. (b) **67**, 709 (1975).

[88] H. Böttger and V. V. Bryksin., Phys. Stat. Sol. (b) **81**, 433 (1977).

[89] F. Matsukura, H. Ohno, A. Shen, and Y. Sugawara, Phys. Rew. B, **57**, 2038(R) (1998).

[90] E.L. Nagaev, Phys. Rep. **346**, 387 (2001).

VITA

Name: Xiongjun Liu

Address: Department of Physics
Texas A&M University
4242 TAMU
College Station, TX 77843-4242

Email Address: xiongjunliu@yahoo.com.cn

Education: B.S., Physics, Nankai University, 2002
M.S., Physics, Nankai University, 2005

Publications: 25 publications, including 2 Phys. Rev. Lett.;
13 Phys. Rev. B and A; 1 Europhys. Lett;
1 Review article; 1 Book Chapter; and others.